**MATHEWS DE OLIVEIRA KRAMBECK FRANCO**

# DETERMINAÇÃO DE COMPONENTES E CONTAMINANTES EM CACHAÇA EMPREGANDO MÉTODOS BASEADOS EM ANÁLISE DE IMAGEM DIGITAL

Tese apresentada à Universidade Federal de Viçosa, como parte das exigências do Programa de Pós-Graduação em Agroquímica, para obtenção de título de *Doctor Scientiae.*

Orientador: Willian Toito Suarez

**VIÇOSA - MINAS GERAIS**
**2022**

**Ficha catalográfica elaborada pela Biblioteca Central da Universidade Federal de Viçosa - Campus Viçosa**

T

F825d
2022

Franco, Mathews de Oliveira Krambeck, 1993-

Determinação de componentes e contaminantes em cachaça empregando métodos baseados em análise de imagem digital / Mathews de Oliveira Krambeck Franco. – Viçosa, MG, 2022.

1 tese eletrônica (162 f.): il.

Orientador: Willian Toito Suarez.

Tese (doutorado) - Universidade Federal de Viçosa, Departamento de Química, 2022.

Referências bibliográficas: f. 75-87.

DOI: https://doi.org/10.47328/ufvbbt.2023.067

Modo de acesso: World Wide Web.

1. Cachaça - Contaminação - Análise. 2. Imagens digitais - Análise. 3. Smartphones. I. Suarez, Willian Toito, 1976-. II. Universidade Federal de Viçosa. Departamento de Química. Programa de Pós-Graduação em Agroquímica. III. Título.

CDD 22. ed. 663.5

Bibliotecário(a) responsável: Alice Regina Pinto Pires CRB-6/2523

**MATHEWS DE OLIVEIRA KRAMBECK FRANCO**

# DETERMINAÇÃO DE COMPONENTES E CONTAMINANTES EM CACHAÇA EMPREGANDO MÉTODOS BASEADOS EM ANÁLISE DE IMAGEM DIGITAL

Tese apresentada à Universidade Federal de Viçosa, como parte das exigências do Programa de Pós-Graduação em Agroquímica, para obtenção do título de *Doctor Scientiae*.

APROVADA: 31 de agosto de 2022.

Assentimento:

Documento assinado digitalmente
gov.br
MATHEWS DE OLIVEIRA KRAMBECK FRANCO
Data: 01/03/2023 22:52:20-0300
Verifique em https://verificador.iti.br

_____

Mathews de Oliveira Krambeck Franco
Autor

Documento assinado digitalmente
gov.br
WILLIAN TOITO SUAREZ
Data: 02/03/2023 11:03:00-0300
Verifique em https://verificador.iti.br

_____

Willian Toito Suarez
Orientador

Dedico esse trabalho aos meus pais, Mônica e Ronaldo, minhas irmãs Rayana e Amanda, meu amigo e orientador Willian.

## AGRADECIMENTOS

Incumbe a mim o compromisso de reconhecer aqueles que contribuíram, direta ou indiretamente, para a concretização deste sonho. Logo, dirijo sinceros agradecimentos, primeiramente, à toda minha família que sempre me apoiaram nos âmbitos pessoal e profissional, incluindo minha esposa Thaís, por todo apoio e suporte.

Gratulo e expresso o meu carinho infindável pelo meu orientador, Willian, que, de tão importante em minha trajetória acadêmica, tornou-se também um grande amigo. Reconheço que, acima de tudo, acreditou no meu potencial desde o dia em que cheguei ao laboratório, não apenas depositando confiança no meu trabalho, mas, inclusive, conferindo-me a autonomia para desenvolver os nossos projetos com criatividade e altivez.

Agradeço, profundamente, aos amigos conquistados no decorrer da trajetória que trilhei até o presente momento, permitindo-me desfrutar de momentos inesquecíveis, os quais guardarei nas lembranças mais prazerosas deste sonho.

Sou grato profundamente aos amigos e colegas de trabalho Castelo, Gabriel Abranches e Gustavo Rodrigues que me acompanharam durante a realização de todos os experimentos, muitas vezes trabalhando comigo até tarde da noite para que esse trabalho fosse possível, e também aos Professores: Sergio Antônio Fernandes, por toda atenção e disponibilidade na colaboração deste trabalho; Vagner Dos Santos Bezerra, pela parceria de anos com nosso grupo de pesquisa, sempre solicito e com boas ideias e por fim, Alexandre Fontes, por todo conhecimento e boa vontade em nos ofertar amostras de bebidas para fazer análise.

Ao Conselho Nacional de Desenvolvimento Científico e Tecnológico (CNPq), pela concessão da bolsa de estudos.

O presente trabalho foi realizado com apoio da Coordenação de Aperfeiçoamento de Pessoal de Nível Superior – Brasil (CAPES) – Código de Financiamento 001.

“Na vida, não vale tanto o que temos, nem tanto importa o que somos. Vale o que realizamos com aquilo que possuímos e, acima de tudo, importa o que fazemos de nós”.

CHICO XAVIER

## RESUMO

FRANCO, Mathews de Oliveira Krambeck, D.Sc., Universidade Federal de Viçosa, agosto de 2022. **Determinação de componentes e contaminantes em cachaça empregando métodos baseados em análise de imagem digital.** Orientador: Willian Toito Suarez.

Por meio desse trabalho, propõe-se o desenvolvimento e aplicação de quatro métodos analíticos simples, rápidos e de baixo custo. Foi empregado um smartphone como instrumento analítico para determinação de componentes e contaminantes em amostras de cachaças. Os métodos baseiam-se na decomposição das imagens em modelos algébricos, sendo o RGB, o modelo empregado. Desta feita, foi proposto uma metodologia analítica para determinação do teor de acidez volátil nas bebidas empregando o alaranjado de metila e sua propriedade halocrômica. A faixa dinâmica linear para determinação da acidez volátil foi linear de 25 a 275 mg/100 mL de álcool anidro com $R^2$=0,99 e com limites de detecção e quantificação de 6,70 e 22,33 mg/100 mL, respectivamente. Além disso, validou-se uma metodologia analítica para determinação de açúcares em cachaça, baseado na redução do $Cu^{2+}$ à $Cu^{+}$ pelos açúcares redutores (sacarose e frutose) e formação do complexo colorido entre Neocuproína e $Cu^{1+}$ em meio alcalino. A curva analítica foi linear de 0,1 a 15 g $L^{-1}$ para glicose e frutose com limites de detecção de 0,012 g $L^{-1}$ e 0,010 g $L^{-1}$, respectivamente. Ademais, foi proposto um método para determinação de $Cu^{2+}$ empregando uma tiocarbazona como reagente complexante. Esta reação é inédita na literatura, e foi possível obter uma reação altamente sensível e mais seletiva que outros complexantes, como por exemplo, a cuprizona. Após otimizar a reação, obteve-se uma curva analítica para determinar $Cu^{2+}$ entre 0,25 e 6,75 mg $L^{-1}$ com um desvio padrão relativo (n = 5) de 3,2%, bem como um limite de detecção de 0,18 mg $L^{-1}$ usando um volume de amostra de 400 µL . Por fim, foi proposto um método para determinação simultânea de $Cu^{2+}$ e furfural em amostras de cachaças usando um sistema bifásico e ferramentas quimiométricas. O furfural reage com a anilina em meio ácido formando furfulidenanelina, que apresenta coloração rósea. Por outro lado, $Cu^{2+}$ reage com Cuprizona em meio básico para formar um complexo azul. A regressão por mínimos quadrados parciais (PLS) foi utilizada para construir os modelos de predição dos teores de $Cu^{2+}$ e furfural em amostras de cachaças. O método desenvolvido foi eficaz para estimar os valores de ambos analitos em cachaças, com erro absoluto médio de 0,2 mg/L para

o modelo $Cu^{2+}$, e 0,3 mg/100 mL de álcool anidro para o modelo furfural. Todos os métodos analíticos demonstraram alta exatidão e precisão em relação aos valores encontrados pelos métodos de referência. Não obstante, apresentaram faixas de recuperação adequadas, demonstrando ausência de efeitos de matriz significativos nas amostras estudadas. Sendo assim, as metodologias propostas apresentam como uma alternativa altamente promissora para análises dos analitos *in situ* e pode auxiliar os produtores na fabricação de um produto seguro para consumo e com propriedades sensoriais superiores.

Palavras-chave: Análise de imagem digital. Cachaça. Smartphone.

## ABSTRACT

FRANCO, Mathews de Oliveira Krambeck, D.Sc., Universidade Federal de Viçosa, August 2022. **Determination of components and contaminants in cachaça using methods based on digital image analysis**. Advisor: Willian Toito Suarez.

Through this work, we propose the development and application of four simple, fast and low-cost analytical methods using a smartphone as an analytical instrument for the determination of components and contaminants in samples of cachaça. The methods are based on the decomposition of images into algebraic models, with RGB being the model used. The methods are based on the decomposition of images into algebraic models, with RGB being the model used. This time, an analytical methodology was proposed to determine the volatile acidity content in beverages using methyl orange and its halochromic property. The linear dynamic range for determination of volatile acidity was linear from 25 to 275 mg/100 mL of anhydrous alcohol with $R^2$=0.99 and detection and quantification limits of 6.70 and 22.33 mg/100 mL, respectively. Furthermore, an analytical methodology was validated for the determination of sugars in cachaça, based on the reduction of $Cu^{2+}$ to $Cu^{+}$ by reducing sugars (sucrose and fructose) and formation of the colored complex between Neocuproine and $Cu^{1+}$ in alkaline medium. The calibration curve was linear from 0.1 to 15 g $L^{-1}$ for glucose and fructose with detection limits of 0.012 g $L^{-1}$ and 0.010 g $L^{-1}$, respectively. Furthermore, a method for $Cu^{2+}$ determination was proposed using a thiocarbazone as a complexing reagent. This reaction is unprecedented in the literature, and it was possible to obtain a highly sensitive and more selective reaction than other complexing agents, such as cuprizone. After optimizing the reaction, an analytical curve was obtained to determine $Cu^{2+}$ between 0.25 and 6.75 mg $L^{-1}$ with a relative standard deviation (n = 5) of 3.2%, as well as a detection limit of 0.18 mg $L^{-1}$ using a sample volume of 400 µL. Finally, a method was proposed for the simultaneous determination of $Cu^{2+}$ and furfural in cachaça samples using a two-phase system and chemometric tools. Furfural reacts with aniline in an acidic medium to form furfulidenanelin, which is pink in color. On the other hand, $Cu^{2+}$ reacts with cuprizone in basic medium to form a blue complex. Partial least squares regression (PLS) was used to build prediction models for $Cu^{2+}$ and furfural in cachaça samples. The method developed was effective to estimate the values of both analytes in cachaças, with a mean absolute error of 0.2 mg/L for the $Cu^{2+}$ model, and

0.3 mg/100 mL of anhydrous alcohol for the furfural model. All analytical methods demonstrated high accuracy and precision in relation to the values found by the reference methods. Nevertheless, they showed adequate recovery ranges, demonstrating the absence of significant matrix effects in the samples studied. Therefore, the proposed methodologies present a highly promising alternative for in situ analyte analysis and can help producers in the manufacture of a safe product for consumption and with superior sensory properties.

Keywords: Digital image analysis. Cachaça. Smartphone.

## LISTA DE SIGLAS

1A - 1-(4-methoxybenzaldehyde)thiocarbazone;

1B- 1-(4-nitrobenzaldehyde)thiocarbazone;

1C - 1-(4-(dimethylamino)benzaldehyde)thiocarbazone;

1D – 1-(4-aminobenzaldehyde)thiocarbazone;

1E - 1-(2-nitrobenzaldehyde)thiocarbazone;

AAS – Atomic absorption spectrometry;

ANOVA - Analysis of variance;

AOAC - Association of Official Analytical Chemists;

CCD – Charge Coupled Device;

CMOS – Complementary Metal Oxide Semicondutor;

DIB – Digital Image-based;

CMY – Cyan, Magenta e Yellow;

FTIR - Fourier transform infrared spectrometry;

IR - Infrared spectroscopy;

GC-FID - Gas Chromatography-Flame Ionization detector;

HPLC - High performance liquid chromatography;

HSL - hue, saturation, lightness;

HSV - hue, saturation, value;

ICP-OES- Inductively coupled plasma-atomic emission spectroscopy

LC-UV - Liquid chromatography with ultraviolet detection;

LOD – Limit of Detection;

LEDs – Light Emitting Diodes;

LQ – Limit of Quantification;

MAPA – Ministry of Agriculture, Livestock and Supply;

NMR - Nuclear magnetic resonance spectroscopy;

NC – Neocuproine;

RGB – Red, Green and Blue;

RSD – Relative Standard Deviation;

RSM - Response surface methodology;

SD - Standard Deviation;

UV - Ultraviolet

**SUMÁRIO**

# CAPÍTULO 1 - INTRODUÇÃO

## 1.1. Cachaça

Segundo a legislação brasileira, cachaça é a denominação típica e exclusiva da aguardente de cana-de-açúcar produzida no Brasil, com graduação alcóolica de 38% a 48% em volume a 20ºC, obtida pela destilação do mosto fermentado do caldo de cana-de-açúcar com características sensoriais peculiares, podendo ser adicionada até 6 g $L^{-1}$ de açucares, expressos em sacarose (MAPA, 2015a).

Ao longo dos anos, as técnicas de produção de cachaça se beneficiaram com os avanços tecnológicos, expungindo a ideia equivocada que essa bebida é pouco nobre. Segundo dados da Associação Brasileira de Bebidas (ABRABE), no ano de 1970 a média anual de consumo de cachaça por habitante, no Brasil, era de 4,4 litros. Em 1995, já eram consumidos, em média 8,7 litros e, em 2013 o consumo foi próximo de 11 litros por habitante (SOUZA et al., 2013).

O setor produtivo da cachaça desempenha importante papel na economia nacional e, segundo dados do IBRAC, o Brasil possui capacidade instalada de produção na ordem de 1,2 bilhão de litros e gera mais de 600 mil empregos diretos e indiretos. Atualmente são cerca de 40.000 produtores em todo o Brasil - dos quais 99% são micro e pequenas empresas - e estima-se que existam cerca de 4.000 marcas no mercado (“IBRAC”, 2017). O faturamento anual do setor é de mais de R$ 2 bilhões, sendo apreciada pelos consumidores que requerem um maior controle de qualidade por parte dos pequenos produtores (LABANCA et al., 2006). Praticamente toda a produção de cachaça é consumida internamente no Brasil, sendo exportado menos de 1,0% do total produzido (SOUZA et al., 2013).

No que tange às propriedades químicas, constitui-se de elementos primários, etanol e água, de compostos secundários, álcoois superiores, ácidos, ésteres, fenóis, compostos nitrogenados e sulfurados, aldeídos e açúcares (ODELLO *et al*., 2009). Além de compostos orgânicos, a cachaça apresenta também compostos inorgânicos, tais como íons metálicos de alumínio, cádmio, cálcio, chumbo, cobalto, cobre, crómio, ferro, zinco e outros que, em conjunto, são responsáveis pela caracterização e qualidade da bebida (LUNA *et al*., 2002).

Isto posto, a Instrução Normativa número 13, de 29 de junho de 2005, do Ministério da Agricultura, Pecuária e Abastecimento (MAPA, 2005a), designa os padrões basilares do processo de fabricação da cachaça (Tabela 1), a fim de garantir, atendendo aos parâmetros estabelecidos, a identidade e qualidade do produto final.

**Tabela 1:** Graduação alcoólica e teores de componentes secundários e de contaminantes estabelecidos para a cachaça (MAPA, 2005a).

| Componente | Unidade | Limite | |
|---|---|---|---|
| | | Mínimo | Máximo |
| Graduação alcoólica | % v/v* a 20ºC | 38,00 | 48,00 |
| Açúcares | g $L^{-1}$ | 6,00 | 30,00 |
| Acidez volátil, em ácido acético | mg/100 mL* | - | 150,00 |
| Ésteres, em acetato de etila | mg/100 mL* | - | 200,00 |
| Aldeídos, em acetaldeído | mg/100 mL* | - | 30,00 |
| Furfural + hidroximetilfurfural | mg/100 mL* | - | 5,00 |
| Álcoois superiores** | mg/100 mL* | - | 360,00 |
| Congêneres*** | mg/100 mL* | 200,00 | 650,00 |
| Álcool metílico | mg/100 mL* | - | 20,00 |
| Álcool sec-butílico (2-butanol) | mg/100 mL* | - | 10,00 |
| Álcool n-butílico (1-butanol) | mg/100 mL* | - | 3,00 |
| Acroleína (propenal) | mg/100 mL | - | 5,00 |
| Carbamato de etila | µg $L^{-1}$ | - | 150,00 |
| Cobre | mg $L^{-1}$ | - | 5,00 |
| Arsênio | µg $L^{-1}$ | - | 100,00 |
| Chumbo | µg $L^{-1}$ | - | 200,00 |
| Extrato seco | g $L^{-1}$ | - | 6,00 |

* de álcool anidro ** Álcoois superiores: isobutílico + isoamílico + propílico *** Congêneres: acidez volátil + ésteres + aldeídos + furfural + hidroximetilfurfural + álcoois superiores

Em síntese, a cachaça apresenta propriedades sensoriais peculiares e custo relativamente baixo. Estes aspectos permitem, além da consolidação no mercado

interno e externo, tornando-a a segunda bebida mais consumida no Brasil e o terceiro destilado mais consumido no mundo (LIMA *et al*., 2009).

Portanto, considerando a sua relevância no âmbito econômico, social e cultural, surge a necessidade de garantir padrões rígidos de qualidade que, por sua vez, atrelam-se à aptidão de atender a critérios internacionais de exportação, bem como assegurar que a bebida esteja em conformidade com as exigências estipuladas para a produção.

## 2. Métodos Digitais de análise empregando *spot tests*

A fim de melhor compreender, na Química Analítica, o funcionamento dos métodos digitais envolvendo *spot tests* como ferramenta de detecção de analitos, é imprescindível assimilar o respectivo processo sob dois aspectos relevantes.

O primeiro, como transcorre o processo de formação das cores e a sua intrínseca relação com a radiação incidente, absorvida e refletida. O segundo, por outro lado, como a radiação eletromagnética resultante (refletida) chega ao detector da câmera digital para gerar a resposta analítica, na qual utiliza-se um ou mais modelos de decomposição de cores, especialmente o RGB.

Desta feita, para fins analíticos, as imagens adquiridas a partir da reação colorimétrica podem ser decompostas de duas formas: a primeira, empregando-se um software externo, como por exemplo, o software livre *Image J*. Neste procedimento, as imagens precisam ser transferidas para um computador para depois serem decompostas em um modelo algébrico, através do software em questão.

Após a obtenção do sinal analítico, os dados são analisados e obtém-se os parâmetros analíticos desejados. Este é um método que tem perdido adesão, e foi muito empregado durante o período de 2005 à 2017 em diversos trabalhos publicados (BENEDETTI et al., 2015a, 2015b; FRANCO et al., 2017; FRANCO; SUAREZ; SANTOS, 2017; PESSOA et al., 2017a; RAVAZZI et al., 2018). Os métodos analíticos baseados em análise imagens digitais, atualmente, empregam principalmente aplicativos de smartphones, que tornam a obtenção de dados muito mais rápida e permite a análise em tempo real, podendo ser usada, por exemplo, em titulações ou em sistema de análise por injeção em fluxo (BUSCHER, 2022; FANG

*et al*., 2022; HONORATO SANTOS NETO *et al*., 2022; RUTTANAKORN *et al*., 2021).

Além disso, por meio deste método, não é necessário, a transferência de imagens para o computador, uma vez que as imagens podem ser decompostas automaticamente em um modelo matemático previamente selecionado pelo usuário dentro do próprio aplicativo do celular. Dentre os aplicativos mais usados para este fim, destaca-se o Photometrix (HELFER *et al*., 2017), que tem sido empregado em diversos trabalhos publicados recentemente (BÖCK *et al*., 2022; COSTA *et al*., 2020; HOLKEM *et al*., 2021; SCHLESNER *et al*., 2022).

Este aplicativo, emprega as técnicas de correlação linear simples para análise univariada e análise de componentes principais (PCA) para análise exploratória multivariada. Os dados da imagem são capturados pela câmera principal do dispositivo e convertidos em histogramas vermelho, verde e azul (RGB). Além disso, o módulo de análise univariada permite ao usuário realizar a calibração, amostragem e previsão da concentração de amostras reais. O módulo de análise multivariada permite amostragem, reprocessar uma análise anterior (por exemplo, usando diferentes configurações de variáveis ou canais de cores). Todos estes fatores, tornam as análises muito mais rápidas e dinâmicas, e por isso, aplicativos como este tem sido cada vez mais explorados nos últimos anos (HELFER *et al*., 2017).

Portanto, seja por meio de um software externo ou aplicativo de celular, as imagens digitais são decompostas em um modelo matemático, que será usado como resposta analítica relacionada aos canais do sistema de cores. Para a resposta analítica, a equação $-\log (I/I_0)$ normalmente é usada, onde I é o valor médio do canal medido por amostra ou solução padrão e $I_0$ é o valor médio adquirido do canal analítico em branco.

Assim, a curva analítica é normalmente é apresentada como $-\log (I/I_0)$ vs. concentração. (FRANCO et al., 2017, 2021a; FRANCO; SUAREZ; SANTOS, 2017; LUIZ et al., 2019). Este tipo de tratamento dos dados é comumente usado por ser linearmente correlacionado com a concentração sendo muito empregado para colorimetria e espectrofotometria (BYRNE et al., 2000; CANTRELL et al., 2010; KOHL; LANDMARK; STICKLE, 2006). Usando este cálculo, é possível usar um valor de referência (Branco) e realizar a subtração do sinal analítico, sendo semelhante à

lei de Lambert-Beer para colorimetria. O sinal capturado de uma câmera digital é devido a reflexão, no entanto, este sinal está correlacionado com o sinal absorvido, e assim, o sinal logarítmico pode ser usado sem perda de desempenho analítico.

Além disso, existem trabalhos que não empregam a linearização, uma vez que dependendo da faixa analítica trabalhada o próprio canal escolhido responde de forma linear (DE TARSO GARCIA *et al*., 2014; SARRAFZADEH *et al*., 2015). Ademais, em trabalhos, nos quais há uma contribuição efetiva de mais de um canal, um cálculo vetorial (v) baseado na distância euclidiana usando todos os canais, pode ser empregado, como por exemplo, na equação 1 usada aplicada para o modelo RGB;

$$v=\sqrt{\left(R-R_0\right)^2+\left(G-G_0\right)^2+\left(B-B_0\right)^2} \quad (1)$$

Onde R, G e B são os valores obtidos pelos canais RGB, e $R_0$, $G_0$ e $B_0$ são os sinais provenientes do branco analítico.

Este tipo de tratamento dos dados dos canais, muitas vezes resulta em uma diminuição do limite de detecção, bem como uma melhora na linearidade do método (DA SILVA *et al*., 2020).

### 2.1. Teoria das cores

A cor de uma imagem pode ser definida como a percepção humana da combinação de comprimentos de onda do espectro eletromagnético na região visível que reflete sobre uma superfície (DAMASCENO *et al*., 2015). Portanto, a cor pode ser entendida como a aparência subjetiva da luz, sendo detectada pelo olho após interação da radiação com a matéria. A faixa do espectro eletromagnético à qual o sistema visual humano é sensível se estende aproximadamente de 400 a 700 nm, sendo denominada região visível (TILLEY, 2011), conforme mostrado na Figura 1.

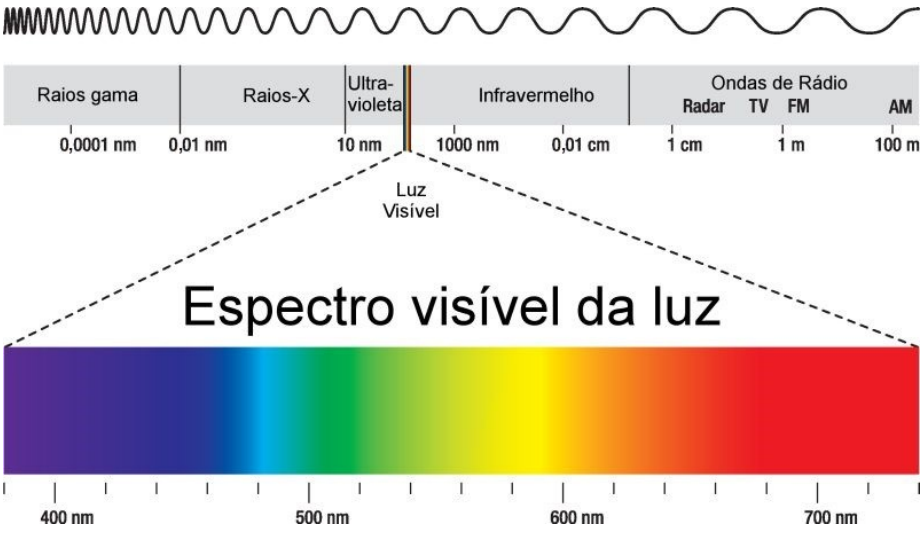


**Figura 1**: Espectro eletromagnético destacando a região da radiação visível.

Uma substância colorida absorve seletivamente comprimentos de onda da região visível do espectro eletromagnético e a coloração resultante, a qual é conhecida como cor complementar, é composta pelos comprimentos de ondas restantes, ou seja, pelos comprimentos de onda que são refletidos pela substância (GOMES *et al*, 2008). De fato, se a cor exibida por uma determinada solução é vermelha, por exemplo, o comprimento de onda que tem a maior absorção é o verde (cor complementar). Neste caso a cor verde é absorvida pela solução e a cor vermelha refletida até os olhos ou detector digital. A Figura 2 demonstra um diagrama de cores complementares.

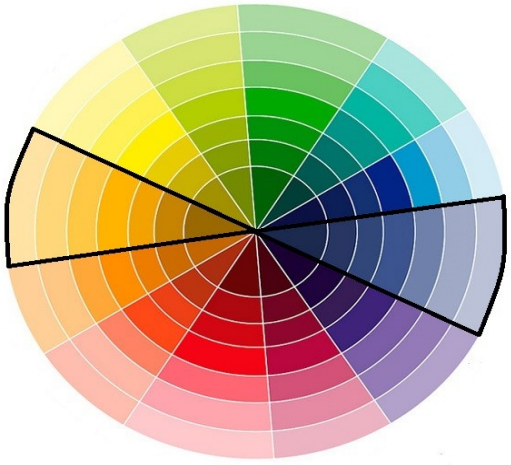

**Figura 2:** Diagrama esquemático que elucida as cores primárias e complementares no espectro eletromagnético do visível.

O diagrama esquemático acima, ilustra de forma clara, a relação entre as regiões de comprimento de onda absorvido e os comprimentos de onda que são refletidos pela substância. Por exemplo, a parte destacada em preto ilustra, em questão, que se um objeto absorver radiação eletromagnética na região do azul selecionado, consequentemente irá refletir radiação na região do laranja, conforme destacado.

## 2.2. Modelo de cor RGB em imagens digitais

As imagens digitais coloridas, podem ser representadas por diferentes modelos matemáticos para elaboração de uma imagem, tais como RGB (do inglês red, green e blue), CMY (do inglês cyan, magenta e yellow) HLS (do inglês hue, lightness e saturation), HSV ( do inglês hue, saturation, value), HSI (do inglês hue, saturation, intensity) (PACIORNIK *et al*., 2006) os quais foram criados para permitir a especificação das cores em um formato padronizado (GONZALEZ; WOODS, 2008).

O modelo RGB é reconhecido como o sistema de cor mais amplo e mais aceito (LOPEZ-MOLINERO *et al*., 2010). Neste modelo, são empregadas as cores primárias vermelha, verde e azul, sendo utilizada a luz transmitida para exibição das cores (YAM; PAPADAKIS, 2004), e as demais cores são geradas pela combinação linear destas três cores, motivo pelo qual o modelo é dito aditivo.

É sabido ainda, que as intensidades das cores geradas são armazenadas em 256 níveis, adotando, para isso, uma escala de 0 a 255. Nesse sentido, a cor preta pura representa o valor de 0 para todos os canais, enquanto, por outro lado, o valor de RGB igual a 255 é representada pela cor branca pura (PACIORNIK *et al*., 2006). O modelo RGB, por sua vez, pode ser representado em um espaço tridimensional cúbico, conforme demonstrado na Figura 3.

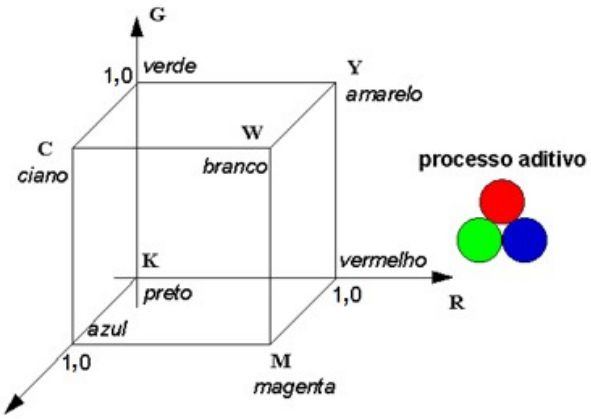


**Figura 3:** Representação geométrica do modelo de cores RGB.

Ao analisar a figura 3, temos um cubo representando o modelo RGB, nas arestas em R ou G ou B têm-se as cores primárias (vermelha, verde e azul) e as faces nos planos GB, BR, RG tem-se as secundarias (ciano, magenta e amarelo), formadas da combinação de duas cores primárias. Na origem do cubo, tem-se o preto e o vértice mais afastado da origem corresponde à cor branca. Na diagonal entre esses dois pontos, tem-se a escala de cinza (PACIORNIK *et al*., 2006). Neste modelo cada canal R, G ou B de cor é formado por 8 bits resultando em uma imagem de 24 bits. Como temos 256 níveis para cada canal, e três canais, temos $256^3$ ou 16,7 milhões de cores possíveis empregando esse modelo.

## 2.3. Métodos analíticos baseados em imagens digitais

A Química Analítica demanda gradativamente avanços significativos nos métodos de análise, a fim de que alcancem não apenas resultados satisfatórios, mas que sejam acessíveis e práticos. Desse modo, nos últimos anos a busca por métodos simples, precisos, exatos e de baixo custo têm sido um dos grandes desafios para esse campo de pesquisa (FRANCO *et al*., 2021b).

Perante os investimentos no respectivo ramo da ciência, a descoberta e os avanços nos métodos de análise de custo reduzido e de fácil manuseio, propiciam uma forte interação entre a área da pesquisa com a comunidade e, consequentemente, com as suas múltiplas ramificações (BENEDETTI *et al*., 2015b).

Nesse sentido, é notório que o desenvolvimento da tecnologia em dispositivos digitais têm se aperfeiçoado consideravelmente nos últimos anos, como em câmeras

fotográficas (BENEDETTI *et al*., 2015a; BYRNE *et al*., 2000; DAKASHEV; PAVLOV; STANCHEVA, 2013; DEBUS *et al*., 2015; FRANCO; SUAREZ; SANTOS, 2017; LEY *et al*., 2013; LI *et al*., 2016), smartphones (PATEL *et al*., 2022; SÁEZ-HERNÁNDEZ *et al*., 2022; SCHLESNER *et al*., 2022; SHAHVALINIA; LARKI; GHANEMI, 2022), webcams (DANCHANA *et al*., 2020; DANTAS *et al*., 2017a; PORTO *et al*., 2019a) e scanners (BOTELHO; DE ASSIS; SENA, 2014b; KIM; HONG; CHANG, 2017; SANTOS; WENTZELL; PEREIRA-FILHO, 2012), de forma que mesmo os aparelhos de menor valor exercem, hoje, as funções necessárias para a realização de um procedimento de análise (PACIORNIK *et al*., 2006).

Existem diversas vantagens e desvantagens ao se empregar diferentes tipos de dispositivos eletrônicos para obtenção dos dados em pesquisas envolvendo análise de imagem digitais. Inicialmente, a maioria dos trabalhos foram feitos empregando câmeras fotográficas. Este tipo recurso atualmente tem sido cada vez menos usado, devido principalmente ao pouco dinamismo do processo, que demanda a transferência das fotografias para computador, para posterior análise por um aplicativo externo, e não obstante, é muito mais difícil acoplar uma câmera digital a um sistema de análise devido ao tamanho, do que um smartphone.

Benedetti *et al* (2015b). desenvolveram um procedimento analítico simples e de baixo custo para determinação de sulfito em amostras de bebidas. A abordagem proposta consistiu na captura de imagens a partir de uma câmera digital de uma reação colorimétrica de sulfito utilizando um sistema construído com materiais de baixo custo para controle de luminosidade e decomposição digital de imagens nas cores primárias vermelho (R), verde (G) e azul (B). A reação colorimétrica é baseada na redução de $Fe^{3+}$ a $Fe^{2+}$ na presença de sulfito e posterior reação com o-fenantrolina para formar um complexo vermelho. Sob condições otimizadas de reação e sistema, a curva analítica foi linear em uma faixa de concentração de sulfito de 8,0 a 140 mg $L^{-1}$, com limites de detecção e quantificação de 2,6 mg $L^{-1}$ e 8,0 mg $L^{-1}$, respectivamente.

O método analítico foi aplicado à quantificação de sulfito em diferentes amostras de bebidas como vinho branco, vinagre, vinho, suco de caju e água de coco. Os resultados adquiridos estavam de acordo com aqueles obtidos usando titulação iodométrica como método comparativo, com nível de confiança de 95%.

Além disso, o método pode ser útil no que diz respeito aos impactos sociais e ambientais, devido ao baixo resíduos gerados (800 µL por *spot test*) e emprega instrumentação facilmente disponível com o potencial para determinação in situ durante a aplicação de sulfito como aditivos durante a bebida produção e controle de qualidade (BENEDETTI *et al*., 2015b). A figura 4 ilustra o equipamento empregado pelos pesquisadores.

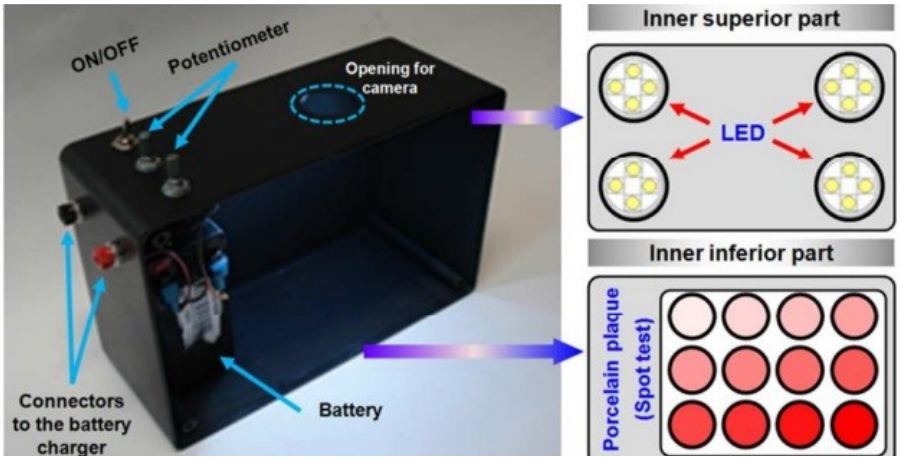


Fonte: Benedetti *et al.* (2015b)

**Figura 4:** Ilustração do sistema construído para a captura de imagens digitais de Benedetti *et al.*, indicando seus componentes. No sistema, a parte superior é utilizada para a fixação dos quatro LEDs, e a placa de porcelana (suporte reacional) é colocada na parte inferior.

O mesmo grupo de pesquisa, também empregou o sistema construído para captura de imagens para quantificação de etanol em bebidas, baseado na combinação de um teste colorimétrico e um método baseado em imagem digital (DIB). O canal R apresentou a melhor linearidade, com duas faixas lineares de concentração de etanol: de 1,0% a 20,0% v/v (r = 0,999) e de 25,0% a 50,0% v/v (r = 0,980), com limites de detecção e quantificação de 0,25% e 0,85% v/v, respectivamente, para a primeira curva analítica.

O método desenvolvido foi aplicado à quantificação de etanol em amostras de bebida alcoólica com resultados próximos aos obtidos pelo método espectrofotométrico com nível de confiança de 95% e com baixa geração de resíduos (835 µL/spot-test). Um ponto interessante deste trabalho, foi que os

pesquisadores testaram várias câmeras com diferentes resoluções para perceber se havia alguma diferença em termos de sensibilidade analítica.

Por fim, os pesquisadores concluíram que a resolução não é um parâmetro essencial na obtenção de resultados exatos e precisos, os quais sofreram pouca influência quando diferentes câmeras foram utilizadas, mesmo quando confrontadas as câmeras com 12.0MP e 0.3MP. Dessa forma, os resultados foram similares, indicando a não necessidade de uma máquina com alta resolução (e, consequentemente, com alto valor comercial) para realizar a captura das imagens (BENEDETTI et al., 2015a).

Vale ressaltar que existe um certo impacto em relação ao uso de câmeras com diferentes resoluções, mas não na sensibilidade e sim, na precisão, pois as imagens com menor resolução têm maior dispersão dos valores de RGB, e assim, apresentam mais ruído, e maiores desvios padrões que, por consequência, diminuem a precisão.

Em relação às webcams, assim como as câmeras digitais, foram usadas principalmente no início dos trabalhos envolvendo análise de imagens digitais, antes da disseminação de smartphones. A principal desvantagem das webcams é sem dúvidas a pouca portabilidade do equipamento, uma vez que a webcam tem que estar conectada diretamente ao computador na maioria dos casos, problema esse, que as câmeras digitais não apresentam esse probema, uma vez que elas podem ser conduzidas para análises em campo devido sua fácil portabilidade.

Por outro lado, as webcams apresentam algumas vantagens consideráveis em relação às câmeras digitais, como por exemplo, as imagens ou vídeos podem ser alocados diretamente ao computador. Isso permitem as análises em tempo real, podendo ser adequadamente empregadas para análises em fluxo ou até mesmo titulações (LIMA *et al*., 2016).

Danchana *et al.*(2020), desenvolveram um sistema espectrofotométrico simples e econômico baseado no uso de um dispositivo criado por impressão 3D e uma webcam de baixo custo. Neste caso, todo o sistema é alimentado apenas pelas saídas USB de um computador, o que torna o sistema portátil e realmente prático para as medições em campo.

Este método foi aplicado para a determinação de ferro (II) em águas usando o-fenantrolina como reagente cromogênico dando um complexo vermelho, e para a determinação de hipoclorito usando tetrametilbenzidina como reagente gerando uma cor amarela. Para confirmar a exatidão e precisão deste método, um espectrofotômetro tradicional foi utilizado para validação, indicando que não existiu diferenças entre ambos métodos (DANCHANA *et al*., 2020).

Neste trabalho os autores afirmaram que não existe problemas de portabilidade com a presença das webcams pelo fato de o sistema ser conectado com saídas USB. De fato, o sistema webcam-cubeta-LEDs (figura 5) são portáteis, entretanto, como o sistema tem que ser conectado diretamente a um computador, não o torna perfeitamente adequado para análises em campo, que seria muito mais facilitado com o emprego de um smartphone como ferramenta para análise das imagens.

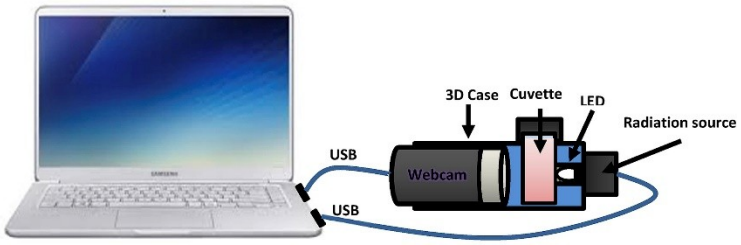


Fonte: Dachana *et al.* (2020)

**Figura 5:** Representação esquemática do sistema espectrofotométrico desenvolvido por Danchana *et al*.

Assim como as câmeras digitais, webcams, os scanners também foram usados no início dos trabalhados envolvendo análise de imagem digital. Estes equipamentos, possuem algumas vantagens consideráveis, por exemplo, dispensa a necessidade da presença de um sistema de iluminação externo controlado, bem como o desenvolvimento de um aparato para análise de imagens digitais, uma vez que o scanner já consegue promover um sistema de análise baseado em ambiente controlado com excelente precisão (PACIORNIK *et al*., 2006). Por outro lado, a principal desvantagem do emprego de scanners é pouca portabilidade que dificulta o

emprego de análises em campo, neste ponto, é o menos adequado entre os equipamentos mencionados, como câmeras digitais e webcams.

Paciornik *et al*. (2006) em trabalho pioneiro, desenvolveram um procedimento de análise digital de imagem para a quantificação de mercúrio, baseado no desenvolvimento de uma cor derivada de uma reação, utilizando-se um scanner comercial.

A análise digital de imagem da cor desenvolvida foi usada para estabelecer uma relação quantitativa entre os componentes da cor e a concentração de mercúrio, sendo a sua intensidade relacionada à concentração na amostra original. O procedimento, quando aplicado a amostras de peixes, apresentou boa correspondência entre os valores encontrados e aqueles relatados, deixando claro que, a estabilidade do scanner deve ser verificada regularmente usando soluções de calibração novas (PACIORNIK *et al*., 2006).

Em um trabalho mais recente, Passaretti Filho *et al*(2015) empregando um scanner como instrumento para captura de fotos desenvolveram um método para detectar a presença de  dióxido de nitrogênio ($NO_2$). Esse gás é um importante indicador de poluição atmosférica, derivado principalmente de processos de combustão. Sendo assim o dióxido de nitrogênio está frequentemente presente em níveis indesejáveis em ambientes abertos e fechados em todo o mundo, exigindo monitoramento sob uma variedade de condições diferentes.

O método foi baseado no processamento de imagens digitais do produto da reação. O $NO_2$ foi coletado e pré-concentrado usando cartuchos C-18 impregnados com trietanolamina, seguido de eluição com solução de metanol a 5%. A reação para formação do produto colorido exigiu apenas 300 µL de volumes de amostra contendo reagente, minimizando a geração de resíduos químicos. Calibrações usando atmosferas padrão mostraram que é possível medir $NO_2$ em uma faixa de concentração de 5,1 a 100,0 ppb, usando uma vazão de amostragem de 0,50 L $min^{-1}$ e um tempo de coleta de 60 min.

O limite de detecção alcançado com um volume de solução de 300 µL foi de 5,0 ppb, com erro relativo de 2% e coeficiente de variação de 1,6%. Os próprios autores, entretanto,  citam que para aumentar a portabilidade do método deveria ser apropriado desenvolver um software adequado para uso com diferentes plataformas

de medição, incluindo celulares e tablets (PASSARETTI FILHO; DA SILVEIRA PETRUCI; CARDOSO, 2015). A figura 6 ilustra o procedimento descrito para determinação de $NO_2$.

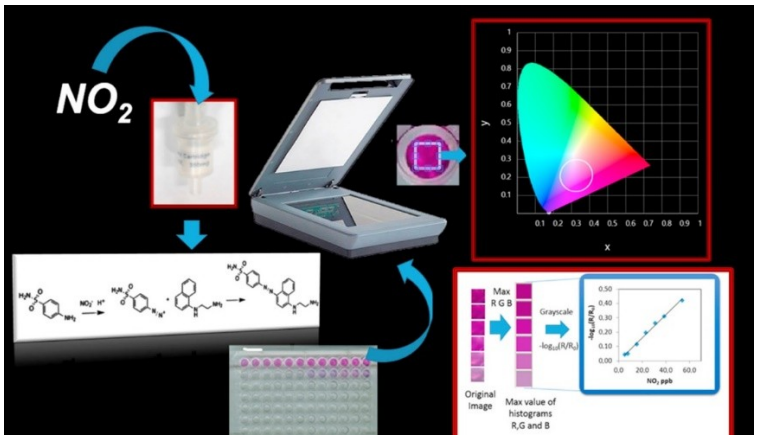


Fonte: Passaretti Filho *et al*. (2015)

**Figura 6:** Representação do procedimento desenvolvido para determinação de $NO_2$ de Passaretti Filho *et al*.

A inserção de smartphones na Química Analítica como ferramentas de captura e análise de imagens, tem se tornado cada vez mais frequente, e atualmente é a principal ferramenta empregada para análises de imagens digitais. Isso se deve a vários fatores, como por exemplo, alta disponibilidade, baixo preço, capacidade de se fazer análises em tempo real, processamento automático de dados via aplicativos, alta portabilidade, além da possibilidade de usar o *flesh* do smartphone como fonte de iluminação (REZAZADEH *et al*., 2019).

Schlesner *et al.*, desenvolveram recentemente um procedimento para determinação do teor de açúcar total dos refrigerantes empregando uma câmara impressa em 3D. O sistema é equipado com uma câmera USB acoplada ao smartphone para tirar fotos diretamente dos vasos usados para a reação dos monossacarídeos com o íon cúprico do reagente de Benedict.

O aplicativo *PhotoMetrix* UVC disponível gratuitamente foi usado para controlar o dispositivo e processar as imagens e o procedimento de análise está sintetizado na figura 7. A regressão PLS foi viável para análise e obteve concordância de (95,3 a 108,7%) com o método oficial de referencia (AOAC 923.09-Lane-Eynon Method)(LATIMER JR, 2012). O método obteve alta frequência analítica de até 444 leituras/hora.

Além disso, pode ser destacado uma significativa redução no gasto de energia em 5,5 vezes, bem como 78 vezes menos volume de resíduos do que o método AOAC. Por fim, as características de segurança devem ser enfatizadas devido à redução da quantidade de reagentes e ao uso de recipientes fechados para reação (SCHLESNER *et al*., 2022).

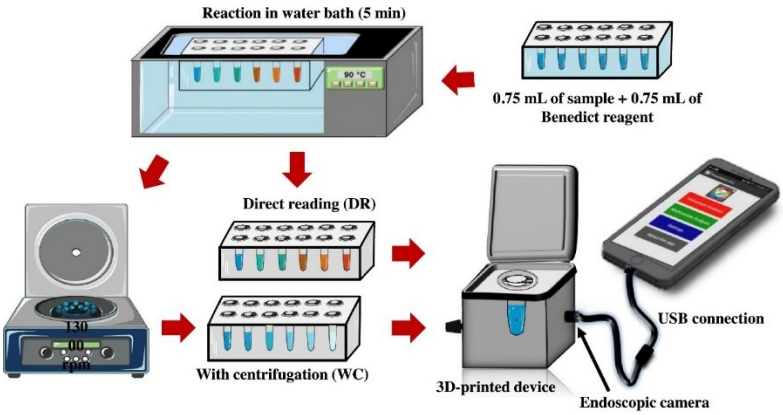


Fonte: Schlesner *et al*. (2022)

**Figura 7:** Procedimentos utilizados para determinação do teor de açúcar de refrigerantes de Schlesner *et al*.

Isto posto, a Química Analítica tem introduzido, em virtude da rápida captura de imagens e estabilidade de fundo, o uso de câmeras e smartphones com sensores CCD (Charge Coupled Device) ou CMOS (Complementary Metal Oxide Semicondutor), visto que propiciam o desenvolvimento de novos métodos analíticos com alta sensibilidade, robustez, rapidez e baixo custo de implementação (SENA *et al*., 2011).

Estes sensores são capazes de converter a intensidade da luz incidente em valores digitais armazenáveis, os bits, e a resposta analítica gera uma imagem baseada em um modelo de decomposição de cor, no qual são utilizadas matrizes para armazenar as informações contidas em uma imagem (FRANCO et al., 2017).

O uso de imagens digitais representa uma oportunidade atual para o desenvolvimento rápido e direto de determinações quantitativas, particularmente quando combinadas com métodos colorimétricos ou cromogênicos que podem ser analisados a partir de dados do modelo de cores RGB, HSV, HSY entre otros (LOPEZ-MOLINERO *et al*., 2010).

Dessa forma, portanto, a química analítica têm empregado amplamente as imagens digitais para quantificação dos mais diversos analitos, dentre os quais se incluem diversas áreas da Ciência, como: alimentícia (ALÇIÇEK; BALABAN, 2015; CRUZ-FERNÁNDEZ *et al*., 2017; KUCHERYAVSKIY; MELENTEVA; BOGOMOLOV, 2014); farmacêutica (SIMA; CASONI; SÂRBU, 2013; SOUZA *et al*., 2014); forense (CHOODUM *et al*., 2014), bioquímica (MATHAWEESANSURN; MANEERAT; CHOENGCHAN, 2017), agricultura e ciência do solo (CHOODUM *et al*., 2013; RIBEIRO *et al*., 2011), análises biológicas (SUMRIDDETCHKAJORN; CHAITAVON; INTARAVANNE, 2014) análises clínicas (LI; BUI; PANTANOWITZ, 2022; POMPONIO *et al*., 2022; SHAFI *et al*., 2022), análises físicas (JESUS *et al*., 2022; KIBITKIN *et al*., 2022), médicas (ADENIYI; MASHAZI, 2022; FAN *et al*., 2022) e etc.

### 2.4. Métodos digitais aplicados à análise de bebidas

Os métodos digitais, devido suas inúmeras vantagens, tem despertado interesse da comunidade científica principalmente na identificação e quantificação de componentes importantes em bebidas. A necessidade de se realizar análises simples, rápidas e principalmente *in situ*, tem sido fatores preponderantes para o desenvolvimento de metodologias analíticas que contemplem estas características. Além disso, produtores de bebidas deparam-se com um custo extremamente elevado exigido por laboratórios certificados para as análises que garantam a qualidade química dos produtos.

O MAPA regulamenta os padrões basilares da cachaça brasileira, referenciando as concentrações máximas permitidas. Sendo assim, se um produtor envelhece uma cachaça em 4 tonéis de madeira diferentes, como: grápia, carvalho, bálsamo e jatobá ele deverá fazer análise de todas as quatro amostras, trazendo grandes custos para cadeia produtiva.

Além da questão financeira, a maioria dos métodos do MAPA para análise de bebidas demandam uma grande quantidade de volume de reagentes, o que não corrobora com os princípios da Química verde, além de serem métodos normalmente morosos.

Desta feita, surge a necessidade do desenvolvimento de metodologias analíticas que tenham baixo custo, que possam ser empregadas pelos próprios

produtores para análise das cachaças fabricadas nos próprios alambiques, de tal modo que, os procedimentos sejam portáteis, simples, empreguem baixa quantidade de reagentes e consigam realizar análises precisas e exatas.

Nesse sentido, surgem as os métodos baseados na análise de imagem digital que cumprem todas estas exigências. Com isso a combinação de smartphones com testes colorimétricos, oferece uma alternativa promissora para aquisição de dados qualitativos e quantitativos em determinações analíticas.

Alguns trabalhos são descritos na literatura envolvendo análise de bebidas empregando imagens digitais como ferramenta analítica. Franco *et al*. desenvolveram um procedimento analítico simples, preciso e de baixo custo para a determinação de metanol em cachaça utilizando análise de imagens digitais. Foi construído um sistema portátil com iluminação empregando materiais baratos para a construção de um aparato para a captura das imagens que foram obtidas com um smartphone (Franco et al.,2007)

A reação química foi feita em uma placa de porcelana, que foi acomodada em câmara plástica preta com dimensões aproximadas de 20 × 12 × 18 cm. A reação para a determinação do metanol em bebidas consistiu na oxidação de metanol em metanal e consequente formação de um cromóforo violeta na presença de ácido cromotrópico na temperatura de 80 °C. A partir da otimização do sistema, foram construídas curvas analíticas que apresentaram boa linearidade para o canal verde (G), com coeficiente de regressão ($R^2$) de 0,998.

O spot test desenvolvido apresentou-se como um método econômico e ambientalmente correto, uma vez que apresentou baixo consumo químico e geração de resíduos com apenas 800 µL/spot. O método foi adequado para determinar metanol em amostra de aguardente de açúcar com porcentagem de recuperação variando de 83 a 110% e os resultados foram compatíveis com o método espectrofotométrico com nível de confiança de 95%. Em comparação com os métodos descritos na literatura, oferece maior frequência de amostragem, maior versatilidade e menor consumo de reagentes.

Além disso, o método apresentou uma alta frequência analítica 1,7 min/spot, baixo custo e de fácil manuseio são muito atrativos para pequenos produtores e indústrias na produção de aguardente de cana. De fato, devido à rápida resposta

fornecida pelo método é possível tomar decisões sobre a continuidade do processo de produção para evitar problemas futuros. (FRANCO et al., 2017)

O mesmo grupo de pesquisa desenvolveu a partir do equipamento supracitado um procedimento para determinação de furfural em cachaça empregando um smartphone. O método proposto baseou-se na reação do furfural com anilina em meio ácido gerando um cromóforo vermelho.

O método foi desenvolvido e aplicado para a determinação de furfural em amostras de cachaça não envolvidas com resultados satisfatórios. A recuperação de furfural variou de 85,7 a 106%, apresentando-se como uma alternativa viável e importante para determinar alguns analitos como o furfural durante a produção de bebidas alcoólicas. De fato, o método demonstrou ser preciso, rápido e reprodutivo com baixa geração de resíduos (600 µL/cavidade) (FRANCO; SUAREZ; SANTOS, 2017).

Um trabalho recente de Fernandes *et al.* (2018), foi proposto para a identificação simultânea de diferentes tipos de madeira em cachaças envelhecidas e suas adulterações com extratos de madeira usando uma metodologia baseada em imagem digital empregando histogramas de cores obtidos a partir de imagens digitais associadas a métodos de reconhecimento de padrões, sem qualquer passo de preparação de amostra.

O método atingiu precisão, exatidão e taxas de especificidade superiores a 90,0% no conjunto de teste. Esta pode ser uma ferramenta rápida e confiável para evitar a rotulagem fraudulenta; garantindo que a informação que está no rótulo reflete a qualidade das cachaças envelhecidas, certificando segurança aos consumidores e às agências reguladoras (FERNANDES *et al*., 2018).

Outro trabalho importante, para o desenvolvimento de metodologias analíticas baseadas em análise de imagens digitais para controle de qualidade de bebidas, é o de Lapresta-Fernández e Capitán-Vallvey. Os autores desenvolveram um método para determinar potássio usando um scanner de mesa trabalhando no modo de reflexão para obter informações quantitativas.

O método foi aplicado em amostras de água e bebidas diversas. Os autores compararam os resultados obtidos pelo método proposto com o espectrofotométrico, e não tiveram diferenças estatisticamente significativas. O método proposto pode ser

uma alternativa atraente para instrumentação mais sofisticada e cara, permitindo monitorar muitas amostras dependendo das dimensões da superfície do scanner (LAPRESTA-FERNÁNDEZ; CAPITÁN-VALLVEY, 2011).

Em outro trabalho do grupo citado, foi proposta uma metodologia para a quantificação de um corante artificial, amarelo crepúsculo em bebidas, usando análise de imagem (histogramas RGB) e regressão de mínimos quadrados parciais.

O método desenvolvido, apresentou muitas vantagens se comparado com metodologias alternativas, como a HPLC e a espectrofotometria UV/VIS, visto que foi mais rápido, não exigiu etapas de pré-tratamento de amostras ou qualquer tipo de solventes e reagentes, e usou um equipamento de baixo custo, um scanner de mesa comercial (LAPRESTA-FERNÁNDEZ; CAPITÁN-VALLVEY, 2011).

Casos como este que não são necessários de pré-tratamento das amostras, de fato, metodologias baseadas em análise de imagem digitais são bem vantajosas, mas há de se ressaltar para análises mais complexas, nas quais há necessidade de um tratamento de amostra, bem como há substâncias potencialmente interferentes, instrumentos como HPLC tem vantagens consideráveis.

Em outro trabalho pioneiro, Benedetti *et al*, desenvolveram um método baseado na análise de imagens digitais para quantificação de etanol em bebidas como cerveja, vinho, vodka e cachaça. As imagens digitais das reações de *spot tests* foram capturadas usando uma câmera digital em uma câmara plástica portátil projetada com controle de iluminação interna (BENEDETTI *et al*., 2015a).

A estratégia proposta pode ser empregada para análise de bebida *in situ*, por exemplo, indústria e pequenas propriedades, devido à facilidade de manuseio e baixo custo dos materiais e instrumentação portátil utilizados. Adicionalmente, uma curva de calibração foi obtida utilizando apenas uma imagem digital em um curto tempo de 12 minutos, indicando a possibilidade de obter resultados rápidos de análise com baixa geração de resíduos (835 mL/spot-test).

Assim, o método proposto se apresentou como uma ferramenta útil no que diz respeito aos impactos ambientais e sociais, devido à sua baixa geração de resíduos, e utiliza um dispositivo de fácil acesso com potencial para determinação *in situ* e/ou controle de qualidade de bebidas alcoólicas. (BENEDETTI *et al*., 2015a).

**Referências**

ADENIYI, O.; MASHAZI, P. Kirigami paper-based colorimetric immunosensor integrating smartphone readout for determination of humoral autoantibody immune response. **Microchemical Journal**, v. 178, p. 107427, 1 jul. 2022.

ALÇIÇEK, Z.; BALABAN, M. Ö. Characterization of Green Lipped Mussel Meat. Part II: Changes in Physical Characteristics as a Result of Brining and Liquid Smoke Application. **Journal of Aquatic Food Product Technology**, v. 24, p. 15–30, 2015.

BENEDETTI, L. P. D. S.; SANTOS, V. B. DOS; SILVA, T. A.; FILHO, E. B.; MARTINS, V. L.; FATIBELLO-FILHO, O. A digital image-based method employing a spot-test for quantification of ethanol in drinks. **Anal. Methods**, v. 7, n. 10, p. 4138–4144, 2015a.

BENEDETTI, L. P. DOS S.; SANTOS, V. B. DOS; SILVA, T. A.; FILHO, E. B.; MARTINS, V. L.; FATIBELLO-FILHO, O. A digital image analysis method for quantification of sulfite in beverages. **Anal. Methods**, v. 7, n. 18, p. 7568–7573, 2015b.

BÖCK, F. C.; HELFER, G. A.; DA COSTA, A. B.; DESSUY, M. B.; FERRÃO, M. F. Low cost method for copper determination in sugarcane spirits using Photometrix UVC® embedded in smartphone. **Food Chemistry**, v. 367, p. 130669, 15 jan. 2022.

BOTELHO, B. G.; DE ASSIS, L. P.; SENA, M. M. Development and analytical validation of a simple multivariate calibration method using digital scanner images for sunset yellow determination in soft beverages. **Food Chemistry**, v. 159, p. 175–180, 15 set. 2014.

BUSCHER, S. Digital image analysis of gas-liquid flow in a cross-corrugated plate heat exchanger channel: A feature-based approach on various two-phase flow patterns. **International Journal of Multiphase Flow**, v. 154, p. 104149, 1 set. 2022.

BYRNE, L.; BARKER, J.; PENNARUN-THOMAS, G.; DIAMOND, D.; EDWARDS, S. Digital imaging as a detector for generic analytical measurements. **TrAC - Trends in Analytical Chemistry**, v. 19, n. 8, p. 517–522, 2000.

CANTRELL, K.; ERENAS, M. M.; DE ORBE-PAYÁ, I.; CAPITÁN-VALLVEY, L. F. Use of the hue parameter of the hue, saturation, value color space as a quantitative analytical parameter for bitonal optical sensors. **Analytical chemistry**, v. 82, n. 2, p.

531–42, 15 jan. 2010.

CHOODUM, A.; KANATHARANA, P.; WONGNIRAMAIKUL, W.; NIC DAEID, N. Using the iPhone as a device for a rapid quantitative analysis of trinitrotoluene in soil. **Talanta**, v. 115, p. 143–149, 2013.

CHOODUM, A.; PARABUN, K.; KLAWACH, N.; DAEID, N. N.; KANATHARANA, P.; WONGNIRAMAIKUL, W. Real time quantitative colourimetric test for methamphetamine detection using digital and mobile phone technology. **Forensic Science International**, v. 235, p. 8–13, 2014.

COSTA, R. A.; MORAIS, C. L. M.; ROSA, T. R.; FILGUEIRAS, P. R.; MENDONÇA, M. S.; PEREIRA, I. E. S.; VITTORAZZI, B. V.; LYRA, M. B.; LIMA, K. M. G.; ROMÃO, W. Quantification of milk adulterants (starch, $H_2O_2$, and NaClO) using colorimetric assays coupled to smartphone image analysis. **Microchemical Journal**, v. 156, p. 104968, 1 jul. 2020.

CRUZ-FERNÁNDEZ, M.; LUQUE-COBIJA, M. J.; CERVERA, M. L.; MORALES-RUBIO, A.; DE LA GUARDIA, M. Smartphone determination of fat in cured meat products. **Microchemical Journal**, v. 132, p. 8–14, 2017.

DA SILVA, E. K. N.; DOS SANTOS, V. B.; RESQUE, I. S.; NEVES, C. A.; MOREIRA, S. G. C.; FRANCO, M. DE O. K.; SUAREZ, W. T. A fluorescence digital image-based method using a 3D-printed platform and a UV-LED chamber made of polyacid lactic for quinine quantification in beverages. **Microchemical Journal**, v. 157, p. 104986, 1 set. 2020.

DAKASHEV, A.; PAVLOV, S.; STANCHEVA, K. Application of Digital Camera and Digital Image Processing Techmique for Molecular Absorption Analysis in the Visible Spectrum. **Universal Journal of Chemistry**, v. 1, n. 4, p. 129–134, 2013.

DAMASCENO, D.; TOLEDO, T. G.; GODINHO, M. S.; DA SILVA, C. P.; DE OLIVEIRA, S. B.; DE OLIVEIRA, A. E. Análise multivariada de imagens na química: um experimento para determinação do pH de águas potáveis. **Quim. Nova**, v. 38, n. 6, p. 836–841, 2015.

DANCHANA, K.; PHANSI, P.; T. DE SOUZA, C.; L.C. FERREIRA, S.; CERDÀ, V. Spectrophotometric system based on a device created by 3D printing for the accommodation of a webcam chamber as a detection system. **Talanta**, v. 206, p. 120250, 1 jan. 2020.

DANTAS, H. V.; BARBOSA, M. F.; PEREIRA, A.; PONTES, M. J. C.; MOREIRA, P. N. T.; ARAÚJO, M. C. U. An inexpensive NIR LED Webcam photometer for detection of adulterations in hydrated ethyl alcohol fuel. **Microchemical Journal**, v. 135, p. 148–152, 1 nov. 2017.

DE TARSO GARCIA, P.; GARCIA CARDOSO, T. M.; GARCIA, C. D.; CARRILHO, E.; TOMAZELLI COLTRO, W. K. A handheld stamping process to fabricate microfluidic paper-based analytical devices with chemically modified surface for clinical assays. **RSC Adv.**, v. 4, n. 71, p. 37637–37644, 2014.

DEBUS, B.; KIRSANOV, D.; YAROSHENKO, I.; SIDOROVA, A.; PIVEN, A.; LEGIN, A. Two low-cost digital camera-based platforms for quantitative creatinine analysis in urine. **Analytica Chimica Acta**, v. 895, p. 71–79, 2015.

FAN, Y.; SHI, S.; MA, J.; GUO, Y. Smartphone-based electrochemical system with multi-walled carbon nanotubes/thionine/gold nanoparticles modified screen-printed immunosensor for cancer antigen 125 detection. **Microchemical Journal**, v. 174, p. 107044, 1 mar. 2022.

FANG, X.; LI, W.; GAO, T.; AIN ZAHRA, Q. U.; LUO, Z.; PEI, R. Rapid screening of aptamers for fluorescent targets by integrated digital PCR and flow cytometry. **Talanta**, v. 242, p. 123302, 15 maio 2022.

FERNANDES, D. D. DE S.; ALMEIDA, E. DE V.; FONTES, M. M.; DE ARAÚJO, M. C. U.; VÉRAS, G.; DINIZ, P. H. G. D. Simultaneous identification of the wood types in aged cachaças and their adulterations with wood extracts using digital images and SPA-LDA. **Food Chemistry**, 2018.

FRANCO, M. DE O. K.; SUAREZ, W. T.; DOS SANTOS, V. B.; RESQUE, I. S. A novel digital image method for determination of reducing sugars in aged and non-aged cachaças employing a smartphone. **Food Chemistry**, v. 338, p. 127800, 15 fev. 2021a.

FRANCO, M. DE O. K.; SUAREZ, W. T.; DOS SANTOS, V. B.; RESQUE, I. S.; DOS SANTOS, M. H.; CAPITÁN-VALLVEY, L. F. Microanalysis based on paper device functionalized with cuprizone to determine $Cu^{2+}$ in sugar cane spirits using a smartphone. **Spectrochimica Acta - Part A: Molecular and Biomolecular Spectroscopy**, v. 253, p. 119580, 2021b.

FRANCO, M. DE O. K.; SUAREZ, W. T.; MAIA, M. V.; DOS SANTOS, V. B.

Smartphone Application for Methanol Determination in Sugar Cane Spirits Employing Digital Image-Based Method. **Food Analytical Methods**, v. 10, n. 6, p. 2102–2109, 29 dez. 2017.

FRANCO, M. DE O. K.; SUAREZ, W. T.; SANTOS, V. B. DOS. Digital Image Method Smartphone-Based for Furfural Determination in Sugarcane Spirits. **Food Analytical Methods**, v. 10, n. 2, p. 508–515, 19 jul. 2017.

GONZALEZ, R. C.; WOODS, R. E. **Digital Image Processing**. [s.l: s.n.].

HELFER, G. A.; MAGNUS, V. S.; BÖCK, F. C.; TEICHMANN, A.; FERRÃO, M. F.; DA COSTA, A. B. PhotoMetrix: An Application for Univariate Calibration and Principal Components Analysis Using Colorimetry on Mobile Devices. **Journal of the Brazilian Chemical Society**, v. 28, n. 2, p. 328–335, 1 fev. 2017.

HOLKEM, A. P.; VOSS, M.; SCHLESNER, S. K.; HELFER, G. A.; COSTA, A. B.; BARIN, J. S.; MÜLLER, E. I.; MELLO, P. A. A green and high throughput method for salt determination in crude oil using digital image-based colorimetry in a portable device. **Fuel**, v. 289, p. 119941, 1 abr. 2021.

HONORATO SANTOS NETO, J.; DOS SANTOS, L. O.; DOS SANTOS, A. M. P.; GALVÃO NOVAES, C.; LUIS COSTA FERREIRA, S. A new and accessible instrumentation to determine urea in UHT milk using digital image analysis. **Food Chemistry**, v. 381, p. 132221, 1 jul. 2022.

**IBRAC**. Disponível em: <https://ibrac.net/cachaca-na-midia/9/13-de-setembro-fatores-culturais-e-economicos-justificam-o-dia-nacional-da-cachaca->. Acesso em: 7 ago. 2022.

JESUS, L. C. C.; OLIVEIRA, J. M.; LEÃO, R. M.; BELTRAMI, L. R.; ZATTERA, A. J.; ANFLOR, C. T. M.; DOCA, T. C. R.; LUZ, S. M. Tensile behavior analysis combined with digital image correlation and mechanical and thermal properties of microfibrillated cellulose fiber/ polylactic acid composites. **Polymer Testing**, v. 113, p. 107665, 1 set. 2022.

KIBITKIN, V.; GRIGORIEV, M.; SOLODUSHKIN, A.; SAVCHENKO, N. Failure analysis of porous segmented alumina by digital image correlation method. **Procedia Structural Integrity**, v. 40, n. C, p. 223–230, 1 jan. 2022.

KIM, D. BIN; HONG, J. M.; CHANG, S. K. Colorimetric determination of $Cu^{2+}$ ions with a desktop scanner using silica nanoparticles via formation of a quinonediimine

dye. **Sensors and Actuators B: Chemical**, v. 252, p. 537–543, 1 nov. 2017.

KOHL, S. K.; LANDMARK, J. D.; STICKLE, D. F. Demonstration of Absorbance Using Digital Color Image Analysis and Colored Solutions. **Journal of Chemical Education**, v. 83, n. 4, p. 644, abr. 2006.

KUCHERYAVSKIY, S.; MELENTEVA, A.; BOGOMOLOV, A. Determination of fat and total protein content in milk using conventional digital imaging. **Talanta**, v. 121, p. 144–152, 2014.

LAPRESTA-FERNÁNDEZ, A.; CAPITÁN-VALLVEY, L. F. Evaluation of analytical reflection scanometry as an analytical tool. **Analytical Methods**, v. 3, n. 11, p. 2644, 1 nov. 2011.

LATIMER JR, G. W. **The Official Methods of Analysis of AOAC International**. 19th Editi ed. Rockville, USA.: [s.n.].

LEY, S. V; INGHAM, R. J.; O'BRIEN, M.; BROWNE, D. L. Camera-enabled techniques for organic synthesis. **Beilstein Journal of Organic Chemistry**, v. 9, n. 1, p. 1051–1072, 31 maio 2013.

LI, W.; ZHANG, R.; WANG, H.; JIANG, W.; WANG, L.; LI, H.; WU, T.; DU, Y. Digital image colorimetry coupled with a multichannel membrane filtration-enrichment technique to detect low concentration dyes. **Analytical Methods**, v. 8, n. 14, p. 2855–2980, 2016.

LI, Z.; BUI, M. M.; PANTANOWITZ, L. Clinical tissue biomarker digital image analysis: A review of current applications. **Human Pathology Reports**, v. 28, p. 300633, 1 jun. 2022.

LIMA, R. A. C.; ALMEIDA, L. F.; LYRA, W. S.; SIQUEIRA, L. A.; GAIÃO, E. N.; PAIVA JUNIOR, S. S. L.; LIMA, R. L. F. C. Digital movie-based on automatic titrations. **Talanta**, v. 147, p. 226–232, 2016.

LOPEZ-MOLINERO, A.; LIÑAN, D.; SIPIERA, D.; FALCON, R. Chemometric interpretation of digital image colorimetry. Application for titanium determination in plastics. **Microchemical Journal**, v. 96, n. 2, p. 380–385, 2010.

LUIZ, V. H. M.; LIMA, L. S.; ROSSINI, E. L.; PEZZA, L.; PEZZA, H. R. Paper platform for determination of bumetanide in human urine samples to detect doping in sports using digital image analysis. **Microchemical Journal**, v. 147, p. 43–48, 1 jun. 2019.

LUNA, H. G. S.; CANUTO, M. H.; LIMA, G. M. DE; SILVA, J. B. B. DA. Cachaça

Artesanal de Minas. **Informe Agropecuário**, v. 23, n. 217, p. 59–62, 2002.

MATHAWEESANSURN, A.; MANEERAT, N.; CHOENGCHAN, N. A mobile phone-based analyzer for quantitative determination of urinary albumin using self-calibration approach. **Sensors and Actuators B: Chemical**, v. 242, p. 476–483, 2017.

ODELLO, L.; BRACESCHI, G. P.; SEIXAS, F. R. F.; SILVA, A. A. DA; GALINARO, C. A.; FRANCO, D. W. **Avaliação sensorial de cachaça**.

PACIORNIK, S.; YALLOUZ, A. V.; CAMPOS, R. C.; GANNERMAN, D. Scanner image analysis in the quantification of mercury using spot-tests. **Journal of the Brazilian Chemical Society**, v. 17, n. 1, p. 156–161, 2006.

PASSARETTI FILHO, J.; DA SILVEIRA PETRUCI, J. F.; CARDOSO, A. A. Development of a simple method for determination of NO2 in air using digital scanner images. **Talanta**, v. 140, p. 73–80, 1 maio 2015.

PATEL, S.; SHRIVAS, K.; SINHA, D.; MONISHA; KUMAR PATLE, T.; YADAV, S.; THAKUR, S. S.; DEB, M. K.; PERVEZ, S. Smartphone-integrated printed-paper sensor designed for on-site determination of dimethoate pesticide in food samples. **Food Chemistry**, v. 383, p. 132449, 30 jul. 2022.

PESSOA, K. D.; SUAREZ, W. T.; DOS REIS, M. F.; DE OLIVEIRA KRAMBECK FRANCO, M.; MOREIRA, R. P. L.; DOS SANTOS, V. B. A digital image method of spot tests for determination of copper in sugar cane spirits. **Spectrochimica Acta - Part A: Molecular and Biomolecular Spectroscopy**, v. 185, p. 310–316, 2017.

POMPONIO, R.; TANG, Q.; MEI, A.; CARON, A.; COULIBALY, B.; THEILHABER, J.; ROGERS-GRAZADO, M.; SANICOLA-NADEL, M.; NAIMI, S.; OLFATI-SABER, R.; COMBEAU, C.; POLLARD, J.; LIN, T. T.; WANG, R. An integrative approach of digital image analysis and transcriptome profiling to explore potential predictive biomarkers for TGFβ blockade therapy. **Acta Pharmaceutica Sinica B**, 25 mar. 2022.

PORTO, I. S. A.; SANTOS NETO, J. H.; DOS SANTOS, L. O.; GOMES, A. A.; FERREIRA, S. L. C. Determination of ascorbic acid in natural fruit juices using digital image colorimetry. **Microchemical Journal**, v. 149, p. 104031, 1 set. 2019.

RAVAZZI, C. G.; KRAMBECK FRANCO, M. DE O.; VIEIRA, M. C. R.; SUAREZ, W. T. Smartphone application for captopril determination in dosage forms and synthetic urine employing digital imaging. **Talanta**, v. 189, p. 339–344, nov. 2018.

REZAZADEH, M.; SEIDI, S.; LID, M.; PEDERSEN-BJERGAARD, S.; YAMINI, Y. The modern role of smartphones in analytical chemistry. **TrAC Trends in Analytical Chemistry**, v. 118, p. 548–555, 1 set. 2019.

RIBEIRO, A.; RANZ, J.; BURGOS-ARTIZZU, X. P.; PAJARES, G.; SANCHEZ, M. J.; ARCO, D.; NAVARRETE, L. An Image Segmentation Based on a Genetic Algorithm for Determining Soil Coverage by Crop Residues. **Sensors**, v. 11, p. 6480–6492, 2011.

RUTTANAKORN, K.; PHADUNGCHAROEN, N.; LAIWATTANAPAISAL, W.; CHINSRIWONGKUL, A.; ROJANARATA, T. Smartphone-based technique for the determination of a titration equivalence point from an RGB linear-segment curve with an example application to miniaturized titration of sodium chloride injections. **Talanta**, v. 233, p. 122602, 1 out. 2021.

SÁEZ-HERNÁNDEZ, R.; RUIZ, P.; MAURI-AUCEJO, A. R.; YUSA, V.; CERVERA, M. L. Determination of acrylamide in toasts using digital image colorimetry by smartphone. **Food Control**, v. 141, p. 109163, 1 nov. 2022.

SANTOS, P. M.; WENTZELL, P. D.; PEREIRA-FILHO, E. R. Scanner Digital Images Combined with Color Parameters: A Case Study to Detect Adulterations in Liquid Cow's Milk. **Food Analytical Methods**, v. 5, n. 1, p. 89–95, 2012.

SARRAFZADEH, M. H.; LA, H.-J.; LEE, J.-Y.; CHO, D.-H.; SHIN, S.-Y.; KIM, W.-J.; OH, H.-M. Microalgae biomass quantification by digital image processing and RGB color analysis. **Journal of Applied Phycology**, v. 27, n. 1, p. 205–209, 24 fev. 2015.

SCHLESNER, S. K.; VOSS, M.; HELFER, G. A.; COSTA, A. B.; CICHOSKI, A. J.; WAGNER, R.; BARIN, J. S. Smartphone-based miniaturized, green and rapid methods for the colorimetric determination of sugar in soft drinks. **Green Analytical Chemistry**, v. 1, p. 100003, 1 abr. 2022.

SENA, R. C. DE; SOARES, M.; PEREIRA, M. L. O.; CRUZ DOMINGUES DA SILVA, R.; FERREIRA DO ROSÁRIO, F.; CAJAIBA DA SILVA, J. F. A Simple Method Based on the Application of a CCD Camera as a Sensor to Detect Low Concentrations of Barium Sulfate in Suspension. **Sensors**, v. 11, n. 12, p. 864–875, 13 jan. 2011.

SHAFI, S.; KELLOUGH, D. A.; LUJAN, G.; SATTURWAR, S.; PARWANI, A. V.; LI, Z. Integrating and validating automated digital imaging analysis of estrogen receptor immunohistochemistry in a fully digital workflow for clinical use. **Journal of**

**Pathology Informatics**, v. 13, p. 100122, 1 jan. 2022.

SHAHVALINIA, M.; LARKI, A.; GHANEMI, K. Smartphone-based colorimetric determination of triclosan in aqueous samples after ultrasound assisted-dispersive liquid–liquid microextraction under optimized response surface method conditions. **Spectrochimica Acta Part A: Molecular and Biomolecular Spectroscopy**, v. 278, p. 121323, 5 out. 2022.

SIMA, I. A.; CASONI, D.; SÂRBU, C. High sensitive and selective HPTLC method assisted by digital image processing for simultaneous determination of catecholamines and related drugs. **Talanta**, v. 114, p. 117–123, 2013.

SOUZA, F. R. DE; DUARTE JUNIOR, G. F.; GARCIA, P. DE T.; COLTRO, W. K. T. Evaluation of digital image capture devices for colorimetric detection on printed microzones. **Química Nova**, v. 37, n. 7, p. 1171–1176, 2014.

SOUZA, L. M. DE; ALCARDE, A. R.; LIMA, F. V. DE; BORTOLETTO, A. M. **Produção de Cachaça de Qualidade**. ESALQ, Piracicaba: [s.n.].

SUMRIDDETCHKAJORN, S.; CHAITAVON, K.; INTARAVANNE, Y. Mobile-platform based colorimeter for monitoring chlorine concentration in water. **Sensors and Actuators B: Chemical**, v. 191, p. 561–566, 2014.

TILLEY, R. J. D. **Colour and the Optical Properties of Materials – An Exploration of the Relationship Between Light, the Optical Properties of Materials and Colour.** 2. ed. Wes Sussex, United Kingdom: John Wiley & Sons, Ltd, 2011.

YAM, K. L.; PAPADAKIS, S. E. A simple digital imaging method for measuring and analyzing color of food surfaces. **Journal of Food Engineering**, v. 61, n. 1 SPEC., p. 137–142, 2004.

# CAPÍTULO 2:

## Um novo método de imagem digital para determinação de açúcares redutores em cachaças envelhecidas e não envelhecidas utilizando um smartphone

Food Chemistry 338 (2021) 12780

Food Chemistry

journal homepage: www.elsevier.com/locate/foodche

Analytical Methods

# A novel digital image method for determination of reducing sugars in aged and non-aged cachaças employing a smartphone

Mathews de O.K. Franco[a], Willian T. Suarez[a,*], Vagner B. dos Santos[b], Ian S. Resque[b]

[a] Department of Chemistry, Federal University of Viçosa, Center for Exact Sciences and Technology, Viçosa, MG 36570-900, Brazil [b] Fundamental Chemistry Department, Federal University of Pernambuco, Recife, PE 50670-901, Brazil

ARTICLE INFO

Keywords:
Reducing sugars
Cachaça
Adulteration
Digital image
RGB
Smartphone

ABSTRACT

For the first time, a method is proposed for colorimetric determination of reducing sugars in cachaça employing digital image and a smartphone as detector. The method was based on the reduction of Cu(II) to Cu(I) by sugars and followed by the formation of a colored Cu(I)-Neocuproine complex. A calibration curve was linear from 0.1 to 15 g $L^{-1}$ for glucose and fructose with limits of detection of 0.012 g $L^{-1}$ and 0.010 g $L^{-1}$, respectively. It was observed that the non-aged cachaças, known for having inferior flavors and aromas, had a reducing sugar content three times higher than the aged cachaças, once a common practice among producers is to add sugar to adjust sensory deficits in the final product. Furthermore, the method is simple, does not require complex technical knowledge and it could be used as a tool to check possible fraud, adulteration or non-compliance to the law.

## 1. Introduction

Sugar cane spirits (*Cachaça*) is a Brazilian alcoholic beverage with an alcoholic graduation from 38 to 48% by volume at 20 °C. It is obtained from the distillation of the fermented mash of sugarcane juice (MAPA, 2011). *Cachaça* is exclusively produced in Brazil and, after beer, it is the most consumed alcoholic beverage in the country occupying the fourth position worldwide (GRANATO *et al*., 2014; SOUZA *et al*., 2013). Besides its economic factor, the beverage has important social, cultural and historical significance being consumed and produced in all states of the country.

The determination of sugars is an important factor to evaluate the quality of the fermentation process in the production of *cachaça*, since high concentrations of sugar can promote a slow and incomplete fermentation, leading to loss of quality in the final product. Likewise, the control of these analytes is important to verify the presence of adulterations, since high sugar content may be improperly added, and in this case, *cachaça* should be labeled as sugary *cachaça* (*cachaça adocicada),* with sugar concentrations higher than 6 and less than 30 g $L^{-1}$. Usually up to 6 g $L^{-1}$ of sugars expressed as sucrose can be add (MAPA, 2005a, 2011). The official method described by the Ministry of Agriculture and Livestock for determination of sugars in *cachaça* is titration, using the Lane-Eynon method with Fehling's reagent (MAPA-MINISTRY OF AGRICULTURE LIVESTOCK AND SUPPLY, 2013).

As far as we know, there is only one published method for determining reducing sugars in cachaças, which is the official method, there are no alternatives to make this analysis, which is very important to guarantee the quality of the manufactured spirits. The determination of reducing sugars is widely discussed in the literature for analysis of soft beverages, fruit juices and alcoholic beverages (ANDRÉS; TENORIO; VILLANUEVA, 2015; BAŞKAN *et al*., 2016; GREENWAY; KOMETA, 1995; KULIGOWSKI *et al*., 2008; MAQUIEIRA; LUQUE DE CASTRO; VALCARCEL, 1987; NEGRULESCU *et al*., 2012). However, few studies report the determination of sugars in the sugar cane spirits, being employed the official method in these works (LUIZ; BISPO, 2011; MIRANDA *et al*., 2007).

There are some sugars that have free carbonyl and ketone groups, which are oxidized in the presence of oxidizing agents in alkaline solutions. These are reducing

sugars, which are monosaccharides, namely glucose and fructose, and some disaccharides, such as maltose (formed by glucose) and lactose (formed by galactose and glucose). The free ketone and aldehyde functions enable the reduction of cationic ions, such as copper and iron (DEMIATE *et al*., 2002). Non-reducing sugars must undergo the hydrolysis of the glycosidic bond in order to be oxidized. An example is sucrose, which is formed by the link between the aldehydic functional group of a glucose molecule and the ketone functional group of a fructose molecule.

Hydrolysis of non-reducing sugars is usually done with strong acid, for instance hydrochloric acid or with the use of enzymes (such as invertase, in the case of sucrose). The official method for determination of sugars in *cachaça* is titration. This method is time-consuming, once it employs high reagent consumption and requires heating equipment, considering the point of equivalence difficult to be visualized. Furthermore, the titration cannot last more than 3 min due to the degradation of sugars when exposed to high temperatures. All these adversities inappropriate the method for analysts with few analytical skills, making it impossible the analysis *in situ*. Considering these issues, the digital method of analysis is an extremely useful alternative to determine the sugar content in the stills where they are produced.

The use of cameras with charge-coupled device (CCD) sensor and complementary metal oxide semiconductor (CMOS) has been introduced in analytical chemistry for different reasons, such as fast signal acquisition, low background stability and good linearity. In this way, it proves appropriate for the development of new analytical methods with high sensitivity and robustness with a quick, low-cost implementation. The digital image based method was recently employed in quality control for a variety of beverages, such as wine, vinegar, rosé wine, cashew juice, coconut water, teas and sugar cane spirits (Benedetti *et al*., 2015; Botelho, de Assis, & Sena, 2014; Fernandes *et al*., 2018; Franco, Suarez, Maia, & dos Santos, 2017; Lima, Andrade, Barreto, Almeida, & Araújo, 2013).

Therefore, it is necessary to develop analytical methods that ensure the proper physical-chemical quality of the beverage, improving its sensorial quality and assuring that the beverage meets the standards adopted by the national legislation.

In this sense, it is extremely important to control the sugar levels in the sugar cane spirits, since the sugar content directly affects the flavor and aroma of the beverage.

In the present work, it is proposed an analytical method which is simple and relies on low consumption of reagents and samples, using the cell phone's own packaging as analysis equipment, allowing any producer of *cachaça* to determine the sugar content in the stills. Thereby, the developed method was optimized in order to obtain a more efficient fermentation process, which will directly influence the overall organoleptic qualities of the distillate, meeting the criteria required by law. In this sense, controlling the content of sugars present in cachaças becomes essential for producers to obtain a quality product.

## 2. Materials and methods

### 2.1. Chemicals and samples

The solutions were prepared with ultrapure water (resistivity > 18.0 MΩ cm) obtained from a Millipore Milli-Q system (USA) and all chemical reagents were of analytical grade. The solutions of D-(+)-glucose, D-(-)-fructose, sucrose 20 g $L^{-1}$ were prepared from commercial reagents (Sigma–Aldrich). Sodium hydroxide solution 1.0 mol $L^{-1}$ was prepared from commercial NaOH (Merck). The stock solution of Cu(II) 0.02 mol $L^{-1}$ was prepared by dissolving $CuSO_4 \cdot 5H_2O$ (Merck) in distilled water. The solution of 2,9-dimethyl-1,10-phenanthroline (Neocuproine: NC) 0.02 mol $L^{-1}$ was prepared dissolving the commercial reagent (Sigma–Aldrich) in 40% (ethanol/water) and then stored in a suitable storage flask, which was kept away from direct sunlight and heat. All samples of *cachaça* used for our studies were obtained from supermarkets in the city of Viçosa-MG-Brazil.

Sugars having acetyl or ketal linkages are not reducing sugars. Because of the free aldehyde chains, they do not react with any of the reducing-sugar test reagents, and therefore, non-reducing sugar need to be hydrolyzed. In this way Hydrolysis process was performed on 2 mL of cachaça, using 0.06 mL concentrated HCl for 10 min at 60 °C.

## 2.2. Apparatus and Instrumentation

The apparatus developed for digital image analysis (**Fig. 1**) was proposed in order to simplify the construction and operation of the equipment, so that it could be easily produced and used by the *cachaça* producers themselves. In this sense, a box with dimensions of 20 x 10 x 6 cm was used as an apparatus of image capture. On the top of the box was made an opening for dispose an Asus ZenFone 3 smartphone, which was used to capture the digital image. The most of the equipment developed for digital image analysis involves an external lighting system with LED lamps and a coupled electrical circuit. However, to simplify the cell phone's own LED flashlight function was used to illuminate colorimetric reaction. Lids of glass vials of 2 cm in diameter were employed as solution support and to accommodate the lids in the box, a foam was duly cut into a circular shape to avoid movements of solution support in the apparatus.

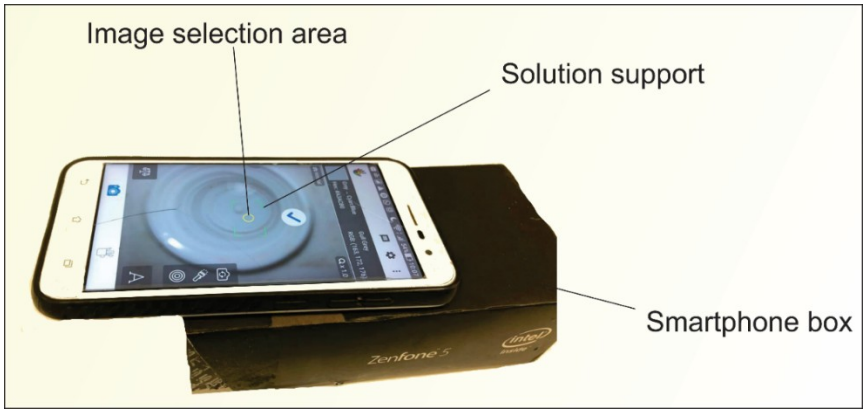


**Fig. 1.** Apparatus developed for the determination of reducing sugars in cachaças

After construction of the equipment, it was necessary to optimize it in order to obtain satisfactory responses from the RGB channels. All analysis performed in the present work were performed using an open access application Color Grab (version 3.6.1, Loomatix ©) (LOOMATIX, 2017). This application allows to obtain responses from the RGB channels in real time, in addition to providing the color name that corresponds instantly, which makes it easier for the analyst to control and interpret the responses obtained in every procedure.

In this regard, the detection selection area was analyzed, corresponding to the region that the application establishes for the RGB reading. Circular areas were tested on 4 pixels offered by the application in order to verify that the container to accommodate the solutions was receiving light in a homogeneously. In addition, the appropriate volume of solution was also evaluated, which permits an adequate RGB response and consumes a low volume of reagents, minimizing costs and collaborating with Green Chemistry. Volumes at nine levels ranging from 200 to 1000 µL were evaluated. All of the above tests were performed with a glucose concentration equivalent to 3 g $L^{-1}$.

The analytical response was obtained by a simple logarithmic equation and was employed similarly to the transmittance calculation used for colorimetric reactions described by Lambert-Beer's law. As the R, G, and B signals from the reactions ($I$) were lower than the analytical background ($I_0$), the equation $-\log (I/I_0)$ was used to construct the analytical curve (KOHL; LANDMARK; STICKLE, 2006). For this, a single channel, the one which exhibited the best analytical sensitivity, was used in all experiments. Thus, it was noticed that channel B supplied a more sensitivity analytical signal, as expected, since the color developed by the complex is yellow (color complementary to blue) (PESSOA *et al*., 2017a).

### 2.3. Optimization of the Cu(I)-NC charge-transfer complex

To determine the reducing sugars, a colorimetric method based on the reduction of Cu(II) to Cu(I) by reducing sugars was used and followed by the formation of a colored Cu(I)-NC charge-transfer complex in alkaline medium. In this sense, the concentration of all reagents was duly optimized using a univariate method. Thus, the optimal concentration of Cu(II) was evaluated at a concentration ranged from the 1.0 x $10^{-5}$ to 1.0 x $10^{-2}$ mol $L^{-1}$ subjected to concentrations of 1.0 x $10^{-3}$ and 1.0 x $10^{-2}$ mol $L^{-1}$ of NC. After verifying which optimal concentration of Cu(II), it was evaluated which concentration of the complexing agent was adequate to obtain a maximum analytical signal. Therefore, the NC concentration was evaluated at seven levels ranging from 5 x $10^{-4}$ to 1 x $10^{-2}$ mol $L^{-1}$. The concentration of NaOH was

also assessed at five levels in the range of 0.025 to 0.125 mol $L^{-1}$. All tests were performed using glucose solution 3 g $L^{-1}$ at room temperature for 60 min.

Previous studies have reported the influence of temperature on the formation of the charge-transfer complex. The reactions were subjected to room temperature (25º C) and heating in an oven at temperatures of 40, 50, 60 and 70 ºC. Additionally, to check the influence of the heating time, the response of the RGB channels was evaluated in the range of 5 to 60 min. These tests were performed using glucose concentrations equivalent to 3 and 10 g $L^{-1}$, using the reagent concentrations optimized in previous studies. All tests were performed in triplicate (*n = 3*).

Some potential interferents for the determination of glucose in *cachaça* were evaluated, such as methanol, isopropanol, ethyl acetate, propanol, butanol, furfural and acetic acid. All potential interferences in *cachaça* were evaluated in a glucose solution at 3 g $L^{-1}$, with the following proportions of analyte/interfering agent: 1:1, 1:10 and 1:100.

### 2.4. Statistical validation of the data

Statistical tests to evaluate some parameters of the proposed method were used. The precision and accuracy of the method were assessed by analyzing the variances by the F test and by verifying whether the differences are significant by the paired T test, respectively. All tests were performed with 95% confidence levels.

## 3. Results and discussion

### 3.1. Optimization of system parameters

For the capture of digital images, the built system was submitted to precision assays based on the obtained RGB data. At first, it was observed that all areas selected to capture the images obtained satisfactory responses with standard deviation less than 2%. It shows that que apparatus developed to obtain the digital image was adequate allowing to acquire a homogeneous illumination. Thus, the largest area of image selection was applied to ensure greater sampling of solutions. In the study of the volume, it was observed that the volume used is directly correlated with the optical path, and consequently, the analytical response, once it causes

variations in the absorbed radiation which was subsequentially reflected towards the smartphone camera's detector. The analytical signal increases linearly up to a volume of 400 µL (**Fig. S1**). After the analytical increasing is lower, thus, in order to reduce the consumption of reagents/sample, the volume of 400 µL was considered the most suitable for all experiments.

### 3.2. Reaction optimization

Firstly, we sought to identify the most ideal concentration of Cu(II) which would provide the best analytical signal. The test was performed under two different concentrations of the complexing agent. The best concentration of Cu(II) that allowed to reach a high analytical response was 4.0 x $10^{-4}$ mol $L^{-1}$ or 25.4 mg $L^{-1}$ (**Fig. S2**) and it was chosen for further analysis. However, most Brazilian *cachaças* are made in copper stills, since the beverages produced in this equipment acquire some organoleptic properties which are considered superior to *cachaças* made from other materials such as porcelain and stainless steel. The maximum Cu(II) allowed by legislation for this metal is 5 mg $L^{-1}$. In this sense, if the beverage contains the maximum allowed concentration for this metal, the error caused by the sum of Cu(II) present in the beverage is 1.25% in the analytical response, considering a sample with a concentration of Cu(II) equivalent to 5 mg $L^{-1}$.

We found that the concentration of 1 x $10^{-3}$ mol $L^{-1}$ of NC promoted a higher analytical signal. In this sense, a more detailed study was perfomed in order to obtain the optimal concentration of NC. The analytical signal increased until to a concentration of 1 x $10^{-3}$ mol $L^{-1}$, after this concentration the signal remains relatively constant until the concentration of 8 x $10^{-3}$ mol $L^{-1}$, and after it decreasing (Fig. S3). Therefore, the concentration of 1 x $10^{-3}$ mol $L^{-1}$ was used in further studies.

Regarding the optimal concentration of NaOH, an increase in the signal was observed when the reaction was subjected to a concentration of sodium hydroxide equivalent to 0.75 mol $L^{-1}$, with a decrease in the signal at concentrations above and below this (**Fig. S4**). So, this concentration was chosen for further studies.

Following the optimization steps of the proposed analytical method. The temperature and time of reaction were evaluated. In this sense, the graphs of this

study referring to the two glucose concentrations tested; 3 and 10 mg $L^{-1}$ are shown in **Fig. 2(a)** and **Fig. 2(b)**, respectively.

As can be seen in **Fig. 2**, the temperature of 70 °C was the one that obtained the greatest analytical responses, mainly for a time of reaction of 50-60 min, where the analytical response reaches the appropriate working region (>1). The temperatures of 40 and 50 °C demonstrated satisfactory results for both concentrations tested, generating relatively stable analytical signals after 20 min of reaction. When the reactions were subjected to heating under a temperature of 60 °C, intense analytical responses were acquired after only 10 min. When the samples were subjected to heating at room temperature, lower analytical signals were obtained, indicating that the temperature and the heating times are important factors for the chemical reaction in question.

However, three factors were taken into account when choosing the best temperature and heating times: 1) To obtain a high and stable analytical signal; 2) Construction of a model that presents a wide linear working range; 3) To obtain a simple, fast, and precision method that can be applied to the *in situ* quality control of *cachaças*. Thus, in order to obtain a satisfactory response in a short period of time, a temperature of 60 °C and a time of 10 min was used for other studies.

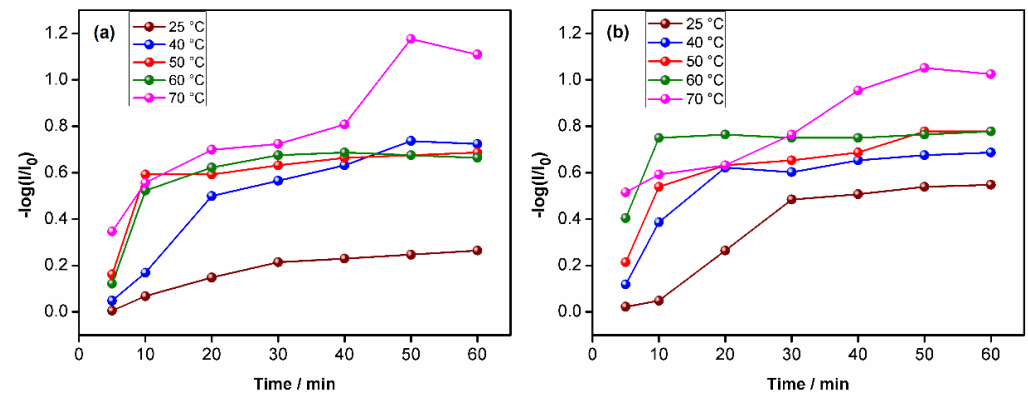


**Fig. 2.** Study of the appropriate temperature to perform the chemical reaction to determine reducing sugars using two glucose solutions: a) 3 and b) 10 mg $L^{-1}$.

However, if the method is used by a beverage producer who does not have heating equipment, such as an electric oven, the reaction can still be attained at room temperature. In these circumstances, the reaction could be performed in about

30 min. Considering that a higher detection limit can be expected, however, this is not a factor that will limit the application of the method under these conditions.

### 3.3. Analytical features

The linearity of the developed method was verified through the analysis of the calibration curve using the method of least squares methods (LSM). In the Fig. S5, it is shown that two analytical curves with a linear range ranging from 0.1 to 15 g $L^{-1}$ were constructed using the two reducing sugars mostly present in *cachaças* (glucose and fructose). For glucose, the regression equation obtained was: $-\log (I/I_0) = 0.049 + 0.509\times$ [glucose], where [glucose] is g $L^{-1}$ with $R^2$ equal to 0.992. For fructose, the following regression equation was obtained: $-\log (I/I_0) = 0.048 + 0.550 \times$ [fructose] where [fructose] is g $L^{-1}$ with $R^2$ equal to 0.996. The limits of detection (LOD) and quantification (LOQ) were calculated using the relations $3 \times \sigma/m$ and $10 \times \sigma/m$, respectively, where σ is the standard deviation of ten times the analytical blank and m is the slope of the analytical curve. Thus, the LOD and LOQ were 0.010 and 0.035 g $L^{-1}$ for fructose and 0.012 and 0.039 g $L^{-1}$ for glucose, respectively. These values were obtained using the optimized reaction conditions and heating the solution at a temperature of 60 °C for 10 min.

However, analytical curves for glucose and fructose without employing heating in the oven have also been constructed, if producers do not have appropriate heating equipment. Thus, a narrower linear range was obtained with sugar concentration ranging from 1 to 10 g $L^{-1}$. For glucose, the regression equation obtained was: $-\log (I/I_0) = 0.23 + 0.075 \times$ [glucose], where [glucose] is g $L^{-1}$ with $R^2$ equal to 0.993. For fructose, the following regression equation was obtained: $-\log (I/I_0) = 0.24 + 0.068 \times$ [fructose] where [fructose] is g $L^{-1}$ with $R^2$ equal to 0.995. Thus, the LOD and LOQ were 0.025 and 0.085 g $L^{-1}$ for glucose and 0.024 and 0.081 for fructose, respectively.

Therefore, any of the analytical curves could be used in the determination of reducing sugars in *cachaças*. In addition, even at room temperature, the reaction processes properly, although the reaction time increases by 20 min. For the other studies, the curve containing glucose was used at a temperature of 60 °C for 10 minute to reach a faster analytical method.

Besides this, the developed method demonstrated a reliable precision with an RSD of 2.8 % for a glucose solution with a concentration of 3 g $L^{-1}$ (*n = 10*).

Some potential interferents for determination of glucose in *cachaça* were evaluated in the following proportion of analyte/interfering agent: 1:1, 1:10, and 1:100. Interfering potential were tested in a glucose solution of 3 g $L^{-1}$. None of the analytes promoted relative errors higher than 2.5 %, even at high concentrations of interfering agents, highlighting the selectivity of the proposed method. The results for the selectivity study are described in **Table 1.**

**Table 1.** Selectivity study for determination of reducing sugars in *Cachaça* (*n=3*), the response is relative errors.

| | Potential interferents | | | | | | |
|---|---|---|---|---|---|---|---|
| Ratio: Analyte/ Interferent | Methanol/ % | Isopranol/ % | Ethyl acetate / % | Propanol/ % | Butanol / % | Furfural/ % | Acetic Acid/ % |
| 1:1 | 0.50 | 0.36 | 0.45 | 1.26 | 1.25 | 1.35 | 1.54 |
| 1:10 | 0.54 | 1.44 | 1.57 | 2.43 | 1.11 | 2.54 | 1.98 |
| 1:100 | 0.35 | 1.12 | 2.5 | 0.56 | 1.57 | 2.33 | 2.36 |

### 3.4. Hydrolysis of sucrose

In this sense, two sucrose solutions containing 3 g $L^{-1}$ and 10 g $L^{-1}$ were subjected to hydrolysis before to be analyzed using the proposed method to check the accuracy of this procedure regards to the direct method to determine monosaccharides glucose and fructose. In fact, only polysaccharides need to be hydrolyzed before reaction. Thus, two solutions containing 50% glucose and 50% fructose at concentrations of 3 g $L^{-1}$ and 10 g $L^{-1}$ were evaluate. The results found are shown in **Table 2**. The analytical curve used in this experiment was obtained by averaging the values obtained for the glucose and fructose curve (**Fig. S5**).

**Table 2.** Responses obtained for solutions containing glucose + fructose and sucrose hydrolyzed in concentrations of 3 and 10 g $L^{-1}$.

| Sample | Proposed method / g $L^{-1}$ | Relative error/ % |
|---|---|---|
| Sucrose hydrolyzate 3 g $L^{-1}$ | 2.96 ± 0.6 | -1.34 |
| Glucose+Fructose 3 g $L^{-1}$ | 2.80 ± 0.5 | -6.67 |
| Sucrose hydrolyzate 10 g $L^{-1}$ | 9.85 ± 0.4 | -1.50 |
| Glucose+Fructose 10 g $L^{-1}$ | 9.79 ± 0.3 | -2.10 |

The findings of the proposed method were found very close to the expected with relative errors varying from -1.34 to 6.67%. These results demonstrate that the present method can be used accurately for the determination of total reducing sugars in spirits containing sucrose hydrolyzed or equivalent sugars.

### 3.5. Analysis of cachaça samples

After the method was properly optimized, some samples of *cachaça* were subjected to analysis to determine reducing sugar content. Samples of aged and non-aged *cachaça* were analyzed because of the their different chemical compositions and which, consequently, could provide different matrix effects.

Recovery assessments for the digital image method were performed by spiking the samples with two known amounts of glucose (2 and 5 g $L^{-1}$), where glucose standard solutions were added directly to the spirits, without any dilution. The total sugar contents were determined using the calibration curve of the glucose standard solution. **Table 3** shows that the glucose recovery percentage in the samples ranged from 84.2 to 113 %, with a mean value of 99.45 %; these values indicate that the matrix effect is not significant for the determination of total reducing sugars by the developed digital image method.

However, aged *cachaças* exhibited recoveries slightly higher than non-aged *cachaças*. The habit of aging the beverage is becoming a common practice among producers, who seek to add value to their product, making it more competitive in the market. During this stage, important changes occur, the complexity of the aroma is increased due to the extraction of some compounds present in the wood; phenolic

compounds that are solubilized to improve taste; and a mild oxidation of some phenolic compounds occur, reducing the astringency and altering the color.

In this perspective, it can be seen that each wood contributes differently to the composition of aged cane spirit, predominantly with specific phenolic compounds in the beverage: in the case of oak (*Quercus sp*), the ellagic and vanillic acids; in amburana (*Amburana cearensis*), vanillic acid and synapaldehyde; in the balm (*Myroxylon balsamum*), vanillin and ellagic acid; in white *jequitibájequitibá*. (*Carinana estrellensis*), gallic acid; in the *jatobá* (*Hymenaea courbaril*). These phenolic compounds that are present in low concentrations in aged *cachaças*, in the order of a few mg $L^{-1}$, can change the color of beverages. Therefore, this factor may have influenced a more pronounced matrix effect in relation to non-aged *cachaças*. According to the capacity of phenols as reducing agents is not efficient here, since the concentration of reducing sugars is expressly higher than that of phenols in *cachaça*, which can be observed according to the good recovery values for beverage samples.

After analyzing the spirits using the proposed method based on the analysis of digital images, we observed that only one *cachaça* had a concentration above the allowed (6 g $L^{-1}$). One *cachaça* had a concentration of reducing sugars of 25.23 g $L^{-1}$, according to the proposed method. However, this sample's label characterized the product as sugary *cachaça*, so the sugar levels were within those allowed by law.This sample needed to be properly diluted before being analyzed

In addition, it was observed that the non-aged *cachaças* had a reducing sugar content three times higher than the aged *cachaças*. A common practice among producers is to add sugar to adjust sensory deficits in the drink, which are known to have inferior flavors and aromas to aged *cachaças*.

For purposes of method comparison, all *cachaças* analyzed in the present study were also analyzed using the official method for determining reducing sugars which is currently recommended by the Ministry of Agriculture, Livestock and Supply (MAPA) of Brazil. As can be seen in Table 3, the results are close, with relative errors ranging from -6.55 to 10.17% in relation to both methods.

Furthermore, the results obtained through both methods were statistically comparable using the paired *t* test with 95% confidence in a bilateral test.

The *t* value (2.35) calculated was lower than the critical *t* (2.59). In that sense, no statistically significant differences in the results were generate by either method. Also, the accuracy of the proposed method was compared with the reference method considering the *F* test with 95%. Table 3 shows the calculated *F* value of each sample, which are below the critical *F* (19.0), so the accuracy of both methods are statistically similar.

**Table 3.** Analysis of cachaças using the proposed method and the reference method, as well as a recovery study for the analyzed beverages**.**

| Samples | DIB method / g $L^{-1}$ | Reference method / g $L^{-1}$ | R.E./ % | F value | Added / g $L^{-1}$ | Found / g $L^{-1}$ | Recovery / % |
|---|---|---|---|---|---|---|---|
| A1 | 1.25 ± 0.10 | 1.32 ± 0.05 | -5.30 | 4.00 | 2.00 | 3.29 ± 0.07 | 102 |
| | | | | | 5.00 | 6.00 ± 0.20 | 95.0 |
| A2 | 2.56 ± 0.15 | 2.36 ± 0.12 | 8.47 | 1.56 | 2.00 | 4.31 ± 0.14 | 87.0 |
| | | | | | 5.00 | 7.90± 0.15 | 107 |
| A3 | 8.57 ± 0.30 | 8.98 ± 0.35 | -4.57 | 1.17 | 2.00 | 10.55 ± 0.22 | 99.0 |
| | | | | | 5.00 | 13.23 ± 0.33 | 94.3 |
| A4 | 3.54 ± 0.12 | 3.55 ± 0.13 | -0.28 | 1.17 | 2.00 | 5.32 ± 0.14 | 89.0 |
| | | | | | 5.00 | 8.87 ± 0.21 | 107 |
| A5 | 2.36 ± 0.25 | 2.27 ± 0.15 | 3.96 | 2.78 | 2.00 | 4.21 ± 0.15 | 92.5 |
| | | | | | 5.00 | 7.87 ± 0.33 | 110 |
| A6 | 25.23 ± 1.12 | 24.36 ±1.36 | 3.57 | 1.47 | 2.00 | 27.20 ± 0.98 | 98.5 |
| | | | | | 5.00 | 29.45 ± 0.89 | 84.4 |
| B1 | 1.57 ± 0.12 | 1.68 ± 0.05 | -6.55 | 5.76 | 2.00 | 3.65 ± 0.12 | 104 |
| | | | | | 5.00 | 5.89 ± 0.17 | 86.4 |
| B2 | 0.56± 0.07 | 0.54 ± 0.03 | 3.70 | 5.44 | 2.00 | 2.83 ± 0.11 | 113 |
| | | | | | 5.00 | 5.99 ± 0.23 | 109 |
| B3 | 0.98 ± 0.10 | 1.00± 0.10 | -2.00 | 1.00 | 2.00 | 3.10 ± 0.08 | 106 |
| | | | | | 5.00 | 5.60 ± 0.21 | 92.4 |
| B4 | 0.68 ± 0.05 | 0.72 ± 0.04 | -5.55 | 1.56 | 2.00 | 2.95 ± 0.12 | 113 |
| | | | | | 5.00 | 5.89 ± 0.28 | 106 |
| B5 | 1.69 ± 0.25 | 1.58 ± 0.20 | 6.96 | 1.56 | 2.00 | 3.71 ± 0.09 | 101 |
| | | | | | 5.00 | 6.55 ± 0.24 | 97.2 |
| B6 | 0.65 ± 0.05 | 0.59 ± 0.07 | 10.17 | 1.96 | 2.00 | 2.89 ± 0.11 | 112 |
| | | | | | 5.00 | 6.23 ± 0.35 | 112 |

Finally, a brief comparison was made of the studies previously reported in the literature related to the determination of reducing sugars using the Cu(I)-NC reaction. In all studies, a spectrophotometer was used, which is a much more expensive and sophisticated instrument than a popular smartphone.

As can be seen in **Table 4**, the present method presented a broader linear range than practically all the other methods mentioned, as well as one of the lowers detection limits. The accuracy is compatible with those of the methods used. The difference between the results are attributed to the use of simpler instrumentation. Regarding the consumption of reagents (NaOH, NC, $CuSO_4 \cdot 5H_2O$), the present method consumed significantly less than the other reported methods, indicating that it generates a much smaller amount of waste, being it considered an environmentally friendly method.

Relying on the use of a digital image based (DIB) method for analytical purposes, a spot test can provide information on the presence of a chemical component in the sample analyzed generating small amount of waste. Besides, it contributes to new knowledge due to its characteristics, highlighting the possibility to use a simple, portable, fast and low-cost device that does not require sophisticated equipment for the analyst operation. In addition, it is the first time that an alternative method has been proposed for the determination of sugars in cachaça in relation to the official method (titration).

The cachaça producers do not carry out analyzes of the sugar content present in the drinks in the stills themselves. This fact is due to their lack of knowledge of this need and also to the lack of simplicity that the official method presents.

Thus, through the proposed method, producers with the help of their own smartphone will be able to perform daily analysis of the sugar content in the drinks. This analysis can benefit them from having an effective control of the fermentation process, and consequently, obtaining a final product with superior sensory qualities. Obtaining a product with superior quality, means having greater acceptance of the product in the market, resulting this way, improving the business economy.

**Table 4.** Comparison of some parameters of the present method with some spectrophotometric methods described involving the Cu(I)-NC reaction to determine reducing sugars**.**

| **Parameters** | AOAC (LATIMER JR, 2012) | (MAQUIEIRA; DE DOLORES LUQUE CASTRO; VALCARCEL, 1987) | (PERIS-TORTAJADA; PUCHADES; MAQUIEIRA, 1992) | (ARAÚJO *et al*., 2000) | (DA SILVA *et al*., 2018) | **Proposed Method** |
|---|---|---|---|---|---|---|
| **Linear Range / (g $L^{-1}$)** | - | 0.05 - 1.0 | 1.2 - 7.2 | 2 - 25 or 20 - 140 | 0.25 - 4.0 | 0.1 - 15 |
| **Detection limit / (g $L^{-1}$)** | - | | 0.143 | 1.2 or 11.2 | 0.03 | 0.01 |
| **R.S.D./ %** | - | 1.61 | - | 2.1 or 1.7 | 2.6 | 2.8 |
| **Sample volume / mL** | 50 | 0.0453 | - | 0.120 or 0.340 | 0.160 | 0.400 |
| **NaOH consumption/ mg** | 1000 | 40.32 | 34.50 | 4.95 | 0.160 | 0.012 |
| **NC consumption / mg** | - | 0.672 | 0.690 | 0.054 | 0.330 | 0.083 |
| **$CuSO_4$/ mg** | 692.78 | 0.336 | 0.345 | 0.027 | 0.128 | 0.00002 |

## 4. Conclusion

To the best of our knowledge, it is the first time that a method based on the use of digital images is proposed for the determination of reducing sugars in *cachaça*. Based on the need to control the levels of these sugars, the present method proved to be extremely effective and accurate. The method uses a low amount of reagents, and therefore corroborates the precepts of Green Chemistry. In addition, it can be easily used by producers of *cachaça* with reduced access to

infrastructure in order to assess the fermentative quality, as well as to verify if the sugar contents are within the acceptable limits as per Brazilian legislation, allowing more room for the producers to make adjustments in their production system with low cost and high portability.

Twelve *cachaças* were analyzed, and only one sample contained values of reducing sugars above that permitted by law, which suggests a potential use as a forensic tool to check fraud or non-compliance. In fact, it has been observed that non-aged *cachaças* have sugar content on average three times higher than aged *cachaças*, which may be associated with adjustments made by producers to mask negative sensorial properties.

**Acknowledgments**

The authors acknowledge the Foundation for Supporting Research in the State of Minas Gerais (Fapemig) (CEX-APQ02436-15).

## Appendix A. Supplementary data

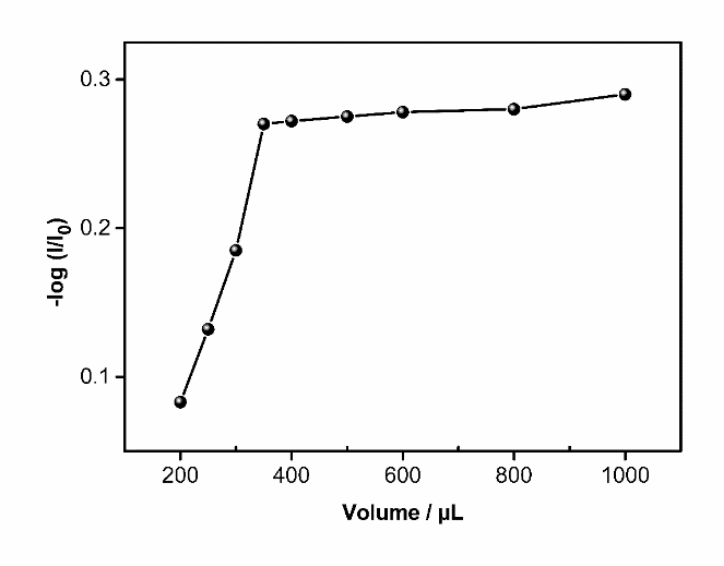


**Fig. S1.** Study of the total volume variation in the solution support.

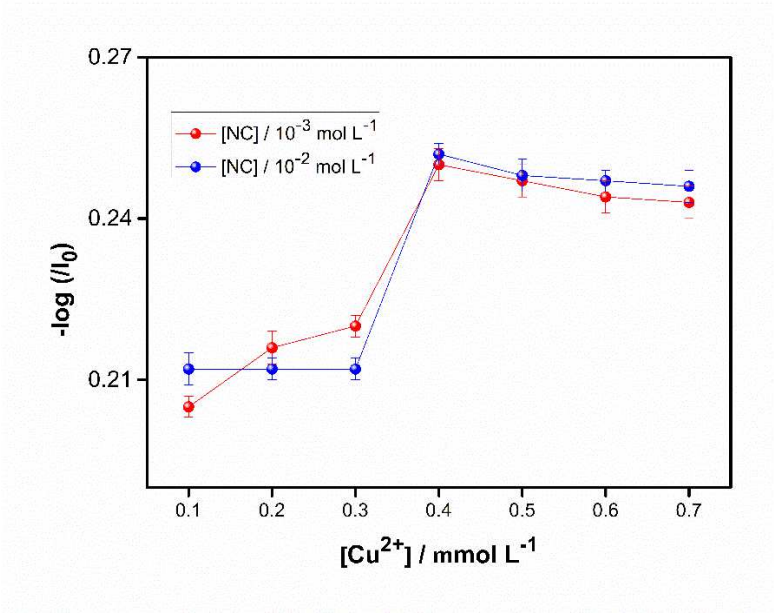


**Fig. S2.** Variation of the concentration of the $Cu^{2+}$ in the analytical signal using two levels of NC.

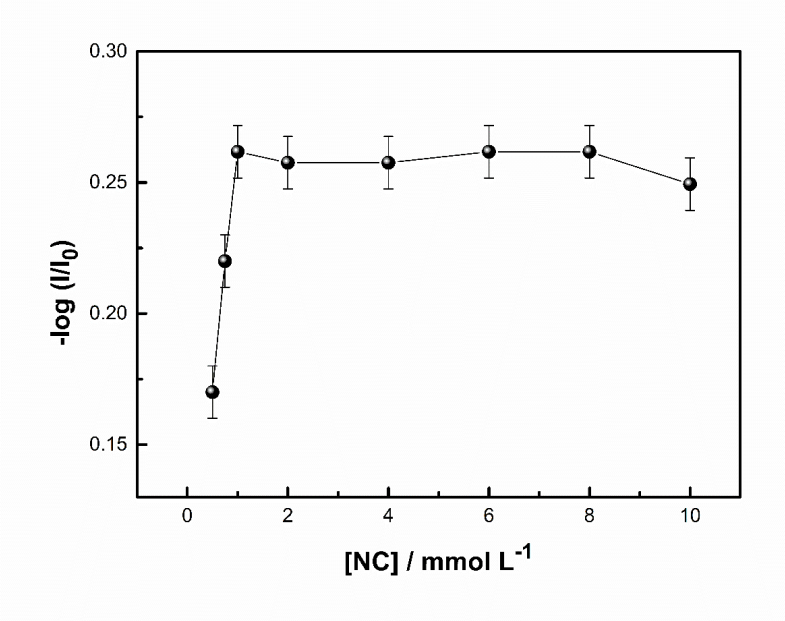


**Fig. S3.** Variation of the concentration of the Neocuproine in the analytical signal.

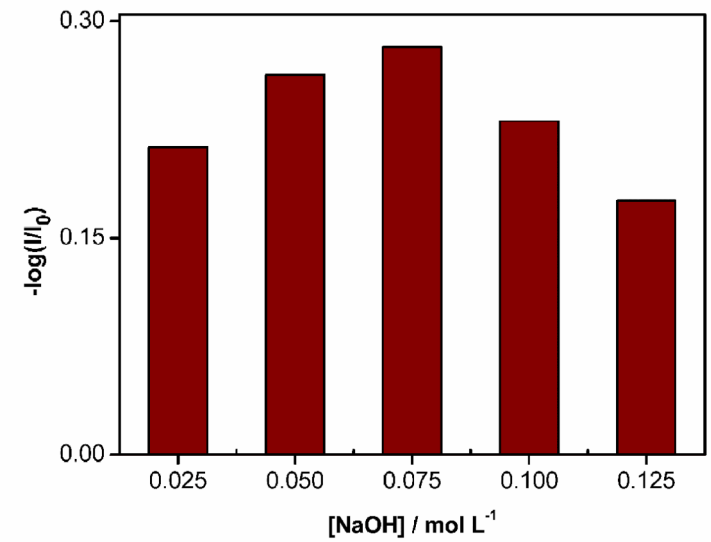


**Fig. S4.** Variation of the concentration of the sodium hydroxide in the analytical signal.

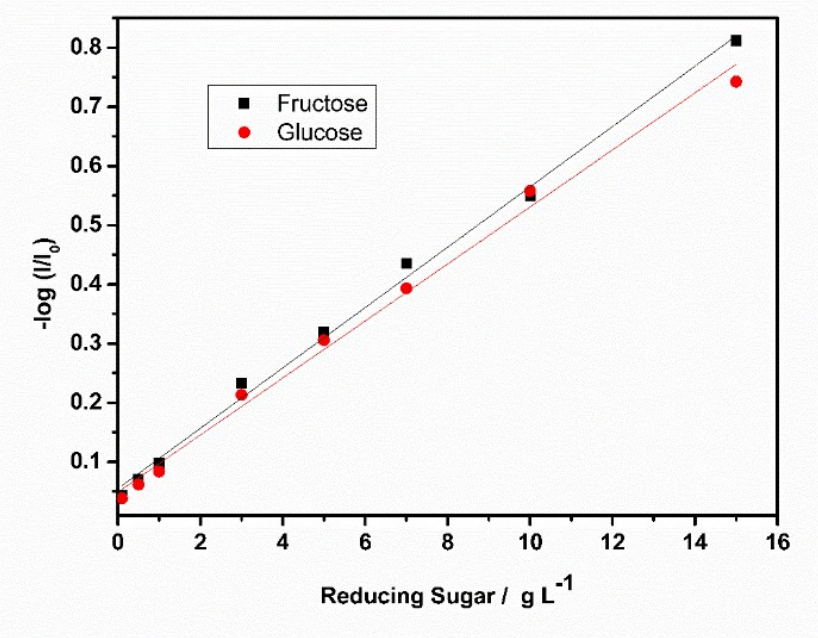


**Fig.S5.** Calibration curve using the method of least squares methods (LSM) for determination of glucose and fructose in cachaças.

## References

Andrés, V., Tenorio, M. D., & Villanueva, M. J. (2015). Sensory profile, soluble sugars, organic acids, and mineral content in milk- and soy-juice based beverages. *Food Chemistry*, *173*, 1100–1106. https://doi.org/10.1016/J.FOODCHEM.2014.10.136

Araújo, A. N., Lima, J. L. F. C., Rangel, A. O. S. S., & Segundo, M. A. (2000). Sequential injection system for the spectrophotometric determination of reducing sugars in wines. *Talanta*, *52*(1), 59–66. https://doi.org/10.1016/S0039-9140(99)00338-0

Başkan, K. S., Tütem, E., Akyüz, E., Özen, S., & Apak, R. (2016). Spectrophotometric total reducing sugars assay based on cupric reduction. *Talanta*, *147*, 162–168. https://doi.org/10.1016/J.TALANTA.2015.09.049

Benedetti, L. P. dos S., Santos, V. B. dos, Silva, T. A., Filho, E. B., Martins, V. L., & Fatibello-Filho, O. (2015). A digital image analysis method for quantification of sulfite in beverages. *Anal. Methods*, *7*(18), 7568–7573. https://doi.org/10.1039/C5AY01372K

Botelho, B. G., de Assis, L. P., & Sena, M. M. (2014). Development and analytical validation of a simple multivariate calibration method using digital scanner images for sunset yellow determination in soft beverages. *Food Chemistry*, *159*, 175–180. https://doi.org/10.1016/J.FOODCHEM.2014.03.048

Da Silva, P. A. B., De Souza, G. C. S., Paim, A. P. S., & Lavorante, A. F. (2018). Spectrophotometric determination of reducing sugar in wines employing in-line dialysis and a multicommuted flow analysis approach. *Journal of the Chilean Chemical Society*, *63*(2), 3994–4000. https://doi.org/10.4067/s0717-97072018000203994

Demiate, I., Wosiacki, G., Czelusniak, & Nogueira, C. (2002). Analysis of total and reducing sugar in foods. A comparative study between colorimetric and titration technique. *Exact and Soil Sciences, Agrariam S and Engineering*, *8*, 65–78.

Franco, M. de O. K., Suarez, W. T., Maia, M. V., & dos Santos, V. B. (2017). Smartphone Application for Methanol Determination in Sugar Cane Spirits Employing Digital Image-Based Method. *Food Analytical Methods*, *10*(6), 2102–2109. https://doi.org/10.1007/s12161-016-0777-y

Granato, D., de Oliveira, C. C., Caruso, M. S. F., Nagato, L. A. F., & Alaburda, J. (2014). Feasibility of different chemometric techniques to differentiate commercial Brazilian sugarcane spirits based on chemical markers. *Food Research International*, *60*, 212–217.

https://doi.org/10.1016/j.foodres.2013.09.044

Greenway, G. M., & Kometa, N. (1995). The determination of sugars in beverages and medicines using on-line dialysis for sample preparation. *Food Chemistry*, *53*(1), 105–110. https://doi.org/10.1016/0308-8146(95)95795-8

Kohl, S. K., Landmark, J. D., & Stickle, D. F. (2006). Demonstration of Absorbance Using Digital Color Image Analysis and Colored Solutions. *Journal of Chemical Education*, *83*(4), 644. https://doi.org/10.1021/ed083p644

Kuligowski, J., Quintás, G., Garrigues, S., & de la Guardia, M. (2008). On-line gradient liquid chromatography–Fourier transform infrared spectrometry determination of sugars in beverages using chemometric background correction. *Talanta*, *77*(2), 779–785. https://doi.org/10.1016/J.TALANTA.2008.07.036

Latimer Jr, G. W. (2012). *The Official Methods of Analysis of AOAC International* (19th Editi). Rockville, USA.

Lima, M. B., Andrade, S. I. E., Barreto, I. S., Almeida, L. F., & Araújo, M. C. U. (2013). A digital image-based micro-flow-batch analyzer. *Microchemical Journal*, *106*, 238–243. https://doi.org/10.1016/j.microc.2012.07.010

Loomatix. (2017). *Color Grab*. Retrieved from https://play.google.com/store/apps/details?id=com.loomatix.colorgrab&hl=pt_BR

Luiz, J., & Bispo, P. (2011). *Características Físico-Químicas De Cachaças Artesanais Envelhecidas E Não Envelhecidas Produzidas E Comercializadas Na Bahia Lavras - Mg*. 173–180. Retrieved from http://repositorio.ufla.br/bitstream/1/4762/1/DISSERTAÇÃO_Características físico-químicas de cachaças artesanais envelhecidas e não envelhecidas produzidas e comercializadas na Bahia.pdf

MAPA- Ministry of Agriculture Livestock and Supply. (2013). Intrução de trabalho - Determinação de Açúcares por Titulometria. Retrieved September 25, 2018, from http://www.agricultura.gov.br/assuntos/laboratorios/legislacoes-e-metodos/arquivos-metodos-da-area-bev-iqa/it-labv-026-rev02-determinacao-de-acucares-por-titulometria.pdf

MAPA. (2005a). *Instrução Normativa no. 13, de 30 de junho de 2005. Aprova o Regulamento Técnico para Fixação dos Padrões de Identidade e Qualidade para Aguardente de Cana e para Cachaça*. Brasília: Diário oficial da União.

MAPA. (2005b). *Instrução normativa nº 24, de 08 de setembro de 2005. Manual operacional de bebidas e vinagres. Diário Oficial da União, Brasília*.

Maquieira, A, Luque de Castro, M. D., & Valcarcel, M. (1987). Determination of reducing sugars in wine by flow injection analysis. *The Analyst*, *112*(11), 1569–1572. Retrieved from http://www.ncbi.nlm.nih.gov/pubmed/3439606

Maquieira, Angel, De Dolores Luque Castro, M., & Valcarcel, M. (1987). Determination of reducing sugars in wine by flow injection analysis. *The Analyst*, *112*(11), 1569–1572. https://doi.org/10.1039/an9871201569

Miranda, M. B. de, Martins, N. G. S., Belluco, A. E. de S., Horii, J., & Alcarde, A. R. (2007). Qualidade química de cachaças e de aguardentes brasileiras. *Ciência e Tecnologia de Alimentos*, *27*(4), 897–901. https://doi.org/10.1590/S0101-20612007000400034

Negrulescu, A., Patrulea, V., Mincea, M. M., Ionascu, C., Vlad-Oros, B. A., & Ostafe, V. (2012). Adapting the reducing sugars method with dinitrosalicylic acid to microtiter plates and microwave heating. *Journal of the Brazilian Chemical Society*, *23*(12), 2176–2182. https://doi.org/10.1590/S0103-50532013005000003

Peris-Tortajada, M., Puchades, R., & Maquieira, A. (1992). Determination of reducing sugars by the neocuproine method using flow injection analysis. *Food Chemistry*, *43*(1), 65–69. https://doi.org/10.1016/0308-8146(92)90243-U

Pessoa, K. D., Suarez, W. T., dos Reis, M. F., de Oliveira Krambeck Franco, M., Moreira, R. P. L., & dos Santos, V. B. (2017). A digital image method of spot tests for determination of copper in sugar cane spirits. *Spectrochimica Acta - Part A: Molecular and Biomolecular Spectroscopy*, *185*, 310–316. https://doi.org/10.1016/j.saa.2017.05.072

Souza, L. M. De, Alcarde, A. R., Lima, F. V. De, & Bortoletto, A. M. (2013). *Produção de Cachaça de Qualidade*. ESALQ, Piracicaba.

# CAPÍTULO 3

## Emprego de um teste colorimétrico e análise de imagem digital para determinação de acidez volátil em cachaça com o auxílio de um smartphone

Microchemical Journal 187 (2023) 108416

Microchemical Journal

# Using colorimetric spot test and digital imaging-based technique for volatile acidity determination in *cachaça* with the aid of a smartphone

Mathews de Oliveira Krambeck Franco [a], Willian Toito Suarez [a,*], Gustavo Rodrigues Penha Pereira [a], Castelo Bandane Vilanculo [a], Maria Carolina Robaina Vieira [a], Vagner Bezerra dos Santos [b], Joao Paulo Barbosa de Almeida[b]

[a] *Department of Chemistry, Federal University of Viçosa - UFV, Center for Exact Sciences and Technology, Viçosa, MG, Brazil* [b] *Fundamental Chemistry Department, Federal University of Pernambuco - UFPE, Recife, PE, Brazil*

ARTICLE INFO

*Keywords:*
Volatile acidity
Cachaça
Digital image RGB
Smartphone
Quality control

ABSTRACT

The present study reports the development and application of a novel method for the colorimetric determination of volatile acidity in *cachaça* using digital image. *Cachaça* is the most widely consumed beverage in Brazil and the development of efficient techniques for the determination of volatile acidity in this beverage is essentially important because this parameter directly reflects on the flavor and aroma of the drink. The method employed was digital image-based (DIB); this method involves the use of methyl orange as an indicator and the analysis of images captured and processed by a smartphone with a free application. A simple pretreatment of the samples employing a steam-dragging distillation for the extraction of volatile acids was performed before DIB analysis. The calibration curve related to anhydrous alcohol was found to be linear in the range of 25 to 275 mg/100 mL with an adjusted-$R^2$ = 0.9912 and limit of detection of 6.70 mg/100 mL based on acetic acid content. The recovery assays conducted yielded recoveries ranging from 89.5 and 112 %. The technique proposed in this study is an easy, inexpensive and rapid tool for the quality control of *cachaça*, especially for small producers of the beverage who have limited financial resources. Moreover, this method is applicable to *in situ* analysis allowing to measure this parameter along the cachaça are produced being useful to monitor the volatile acidity.

## 1. Introduction

Cachaça is a popular Brazilian beverage that is produced from the fermentation of sugar cane juice and which has very distinct characteristics and flavors [1]. Although the main components of *cachaça* are water and alcohol, the beverage also contains low concentrations of secondary components, which are formed mainly in the alcoholic fermentation process during its production [2–4]. Among the secondary compounds present in *cachaça*, acids - especially volatile acids, are essentially vital components in the beverage composition which directly influence the aroma and flavor of the distilled product [2]. The acidity of the beverage largely depends on factors such as the control of the raw material, the distillation mechanism, and most importantly, the fermentation process. The fermentation process is essentially crucial because it plays a major role in shaping the acidity and quality of *cachaça*; during the fermentation process, one must pay particular attention to the following important factors: yeast, time, purity of the medium, temperature and handling of the must; by carefully addressing these factors, one will be able to avoid the proliferation of acetic bacteria during the production process, which increase the acidity of the drink and decrease the production yield [5].

The volatile acidity of *cachaça* is a key parameter that directly reflects on the quality of the beverage since this parameter is essential to the sensory characteristics of the drink, including flavor and aroma [2]. The presence of an excessive volatile acidity in the beverage can lead to the production of *cachaça* with an undesirable and slightly aggressive taste for the consumer, and this will negatively affect the quality of the product [6,7].

Based on the findings of the study conducted by Miranda et al. (2008), the lower the volatile acidity of the beverage, the better the sensory characteristics of the brandy and the greater its acceptance by consumers; thus, it is extremely important to control the acidity levels of the beverage in order to ensure an excellent quality of the final, freshly made product [2].

In Brazil, the quality parameters of *cachaça* have been defined under the Normative Instruction No. 13 of the Ministry of Agriculture, Livestock and Extension (MAPA); based on the established regulatory standards, the volatile acidity of *cachaça* must not exceed 150 mg/100 mL of anhydrous alcohol (expressed in acetic

acid) [8]. In Brazil, the quality parameters of *cachaça* have been defined under the Normative Instruction No. 13 of the Ministry of Agriculture, Livestock and Extension (MAPA); based on the established regulatory standards, the volatile acidity of *cachaça* must not exceed 150 mg/100 mL of anhydrous alcohol (expressed in acetic acid) (MAPA 2005b).

Based on the studies reported in the literature, among the analytical methods employed for the determination of volatile acidity in alcoholic beverages include the following: gas chromatography-flame ionization detector (GC-FID) [9–12], capillary zone electrophoresis and electrochemical biosensors based on lactate oxidase, sarcosine oxidase, and a mixture of fumarase and sarcosine oxidase [13]. Other analytical methods reported in the literature which have been employed for the determination of acidity are spectrophotometric and colorimetric methods for the analysis of acetic anhydride [14], hydrolyzed wood [15], and urine [16]. As can be observed, none of the aforementioned methods have been employed specifically for the analysis of volatile acidity in *cachaça*, as proposed in the present study. However, to develop the DIB method, a simple pretreatment of the samples for the extraction of volatile acids is needed [17].

Analytical methods based on spot test of digital images have been employed as a useful alternative mechanism for the determination of different contaminants in alcoholic beverages, especially in *cachaça*, since the spot test technique is a rapid, simple, practical, low cost, portable, and environmental friendly method for the analysis of compounds of interest once the test involves the use of a few microliters of chemicals compounds [3,18–20].

The DIB technique (Digital Image-Based) [21–24] has been a powerful analytical tool in recent years, because it is inexpensive, fast, accessible and portable as it is compared to conventional spectrophotometry being applied in the most diverse scientific areas [25–26]. The first works based on the digital images for the quantification of analyte concentrations were proposed by Maleki et al and Gaiao et al. [27–28], and after, an exponential increase in the number of publications are reported mainly due to advances in devices such as cameras, scanners, webcams and smartphones and the use of free applications and software such as ImageJ, Color Grab, PhotoMetrix [21,22,29–31]. The applications and software decompose

the images into numerical data using different methods, and thus, different color systems such as RGB, CMYK, HSL, HSV, among others were developed. The most commonly used color system is RGB, as it is a simpler model. The intensities of the generated colors are stored in 256 levels, on a scale from 0 to 255 for each color channel (Red, Green and Blue), where the combination of these three channels (R, G and B) lead to 16 million combinations/colors covering the entire visible electromagnetic spectrum [27,28,30,31]. The value 0 for all channels represents the black color, while the value 255 for all channels represents the white color [27,28,30,31]. For the use of the DIB method, it is necessary to use platforms to accommodate the solutions containing the analyte. For this purpose, materials such as paper [32,33], conventional cuvettes [34], ceramic plates [35], polystyrene microplates [21] and polylactic acid (PLA) [24] are among the materials most used. In the DIB method, the control and/or homogenization of the radiation to capture the digital image is of fundamental importance, in order to avoid spurious radiation, and to obtain precise and accurate data [23,30] a chamber is commonly used [23,30,36]. The DIB method is based on the phenomenon of reflectance despite the transmittance/absorbance used in spectrophotometry [25,30,37–40].

To the best of our knowledge, to date, there have been no reports in the literature regarding the combined application of spot test and digital image-based (DIB) method using a smartphone as detector for the determination of volatile acidity in alcoholic beverages. Thus, the present work presents an innovative method for the determination of acidity level in commercial samples of cachaça for *in situ* analysis. The novel methodology presented here is based on the DIB of spot test which involves the use of methyl orange as an indicator – the methyl orange becomes red in the presence of acetic acid, and the images are captured by a camera containing a CCD type sensor. Among the outstanding advantages of the proposed analytical method are operational simplicity, low cost and low waste generation. The method was developed to be employed for the determination of volatile acidity in alcoholic beverages, specifically in *cachaça*. The technique proposed in this study is an important tool for the quality control of *cachaça*, especially for the small producers of this beverage who have limited financial resources. Moreover, this method is applicable to *in situ* analysis of volatile acidity along the cachaça production.

## 2. Materials and methods

### 2.1. Chemicals and Samples

The solutions were prepared using ultrapure water (resistivity > 18.0 MΩ cm) obtained from a Millipore Milli-Q system (USA). All the chemical reagents employed in the experiments were of analytical grade. The standard methyl orange solution 1.5 x $10^{-3}$ mol $L^{-1}$ was prepared by hot dissolving 0.5 g of commercial reagent (acquired from Sigma–Aldrich). The following chemical substances were also used in the experiments: acetic acid (99.7%, Vetec), ethanol (95%, Vetec), and sodium hydroxide (99%, Sigma Aldrich). All the nine *cachaça* samples (A1-A9) used in the experiments were obtained from supermarkets in the city of Viçosa - Minas Gerais, Brazil.

### 2.2. Apparatus and instrumentation

The apparatus for capturing images employed in this work was developed in order to simplify the approach employed in other previous works reported in the literature [41] and to enable the immediate application of the tool by *cachaça* producers. A box with dimensions of 20 × 10 × 6 $cm^3$ was used to accommodate the chemical reactions; the box had an opening for the placement of an Asus ZenFone 3 smartphone, which was used to capture the digital images for analysis.

Fig. 1 illustrates the equipment developed and used to capture the images for analysis. Plastic lids of glass vials of 2 cm in diameter were used to store the solutions for further digital analysis. The light source of the system came exclusively from the smartphone; this helped simplify the operation of the apparatus. The images were required to be decomposed in an algebraic model in order to be used for analysis; the image decomposition was performed using the free application ColorGrab (version 3.6.1, Loomatix ©) [42], which provides RGB values instantly.

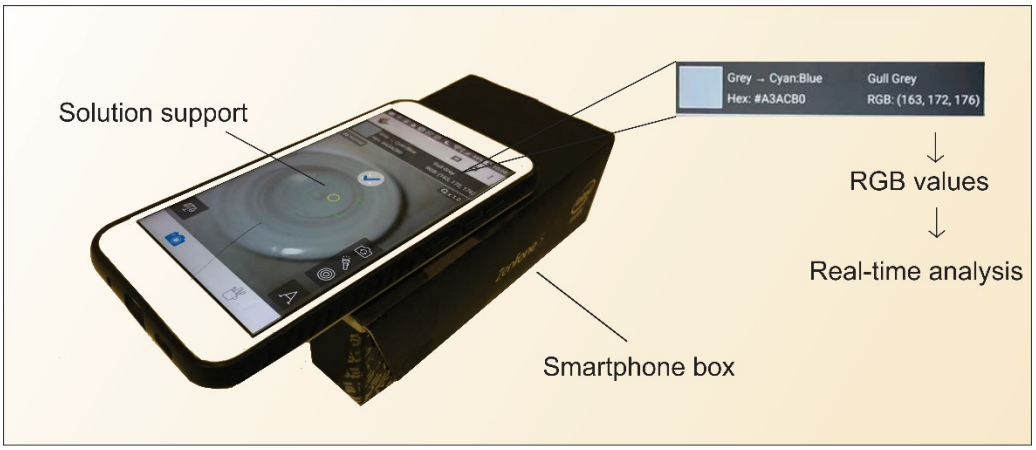


**Fig.1.** Apparatus developed for the determination of volatile acidity in cachaças.

### 2.3. Optimization of operational parameters

The apparatus employed for the acquisition of the analytical data was optimized in order to obtain satisfactory, accurate data and results for the proposed procedure. In this way, a thorough analysis was carried out in order to determine a suitable region (selected region) for the acquisition of the data inside the reaction lid and the size of the specific region; this procedure is found to be essentially important because the area analyzed is required to be free of shadows and excessive brightness, since these elements can impair the quality of the data obtained. In addition, one needs to ensure that the selected region is homogeneous; in other words, the selected region should be within the detection area itself, and the standard deviation should be as small as possible [30,35].

For a thorough analysis of these factors (selected region for analysis and the size of the selected region), the following three different pixel sizes were tested using the open access application Grab (version 3.6.1, Loomatix ©) (Loomatix, 2017): 20 × 20, 30 × 30, and 40 × 40 (length × height). To perform these tests, Tartrazine dye with a concentration of $10^{-5}$ mol/L was employed. To evaluate the effect of the variation in the size of the selected area, a comparative analysis was conducted using the results obtained from the values of the RGB channels found in each experiment. After obtaining the RGB values, a logarithmic equation was used to obtain the analytical response. As the R, G, and B signals from the colorimetric reactions ($I$) were lower than the analytical background ($I_0$), the equation -log ($I/I_0$)

was used to construct the analytical curve [30,41]. To perform this analysis, a single channel, the one which exhibited the best analytical sensitivity, was used in all the experiments. All the procedures were performed in triplicate ($n$ = 3). The reactions were carried out by transferring adequate volumes of solutions to the sample reservoir. Foam supports were placed inside the box in order to bind the sample reservoir tightly.

## 2.4. Otimização das condições reacionais.

The analysis of the digital images was performed after the *cachaça* samples were subjected to steam-dragging distillation for the extraction of volatile acids [17]. To perform this analysis, an amount of 10 mL of each sample was placed in a bubbler and an amount of 250 mL of distilled water was added to the generator connected to the condenser. The water was then boiled, with the steam tap open, to eliminate the air from the device and, eventually, the carbon dioxide in the distilled water. Subsequently, the faucet was closed so that the water vapor bubbled into the sample, dragging the volatile acids which were collected for digital image analysis.

## 2.5. Optimization of reaction conditions

The analysis of volatile acidity of *cachaça* in this work was carried out using methyl orange as an indicator responsible for the color change which is determined by the amount of acetic acid concentration in the spirits. This indicator was chosen due to the fact that the pH of the samples after extraction was within the turning range of the indicator, enabling its use.

The formation of red color observed when there is an increase in acetic acid concentration in the reaction medium is attributed to the protonation of the free amine of methyl orange, which leads to the formation of helianthin - which has a red color. The protonation of the methyl orange allows for the dislocation of free electrons by the molecule, as can be seen in Fig. 2.

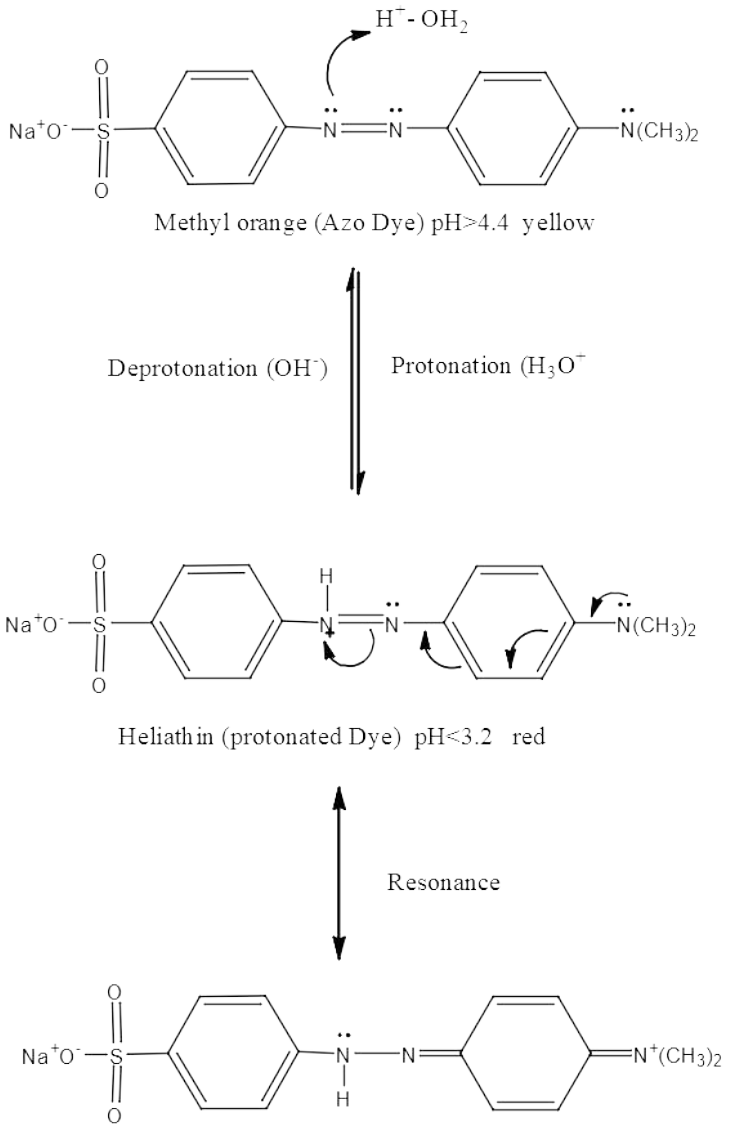


**Fig.2.** Methyl orange and its species in chemical equilibrium according to the protonation of the free amine.

The delocalization of electrons allows the light present to promote a quantum leap from the HOMO orbital to the LUMO due to the effect of hyperconjugation, which gives the molecule a red color. Hyperconjugation is also responsible for the stabilization of the molecule, so the equilibrium is shifted toward the formation of helianthin [43].

To optimize the experimental conditions applied for the determination of volatile acidity in *cachaça*, a Box – Behnken type experimental design was used to evaluate the adequate concentration of the variables investigated. In this sense, three variables (A, B and C) were studied with their respective levels: [methyl orange]

(3.40, 4.54 and 5.67 $\times 10^{-4}$ mol/ L); time of reaction (1, 5.5 and 10 min); and hydroalcoholic content (30, 40 and 50 %). In a system involving three significant independent variables – namely, A, B, and C, the mathematical relationship involving the response of these variables can be approximated by the quadratic polynomial equation.

The analytical response was calculated based on the difference in the values obtained by channel G between two different concentrations of acetic acid equivalent to 10 mg and 200 mg of acetic acid/100 mL of anhydrous alcohol. In this case, single and lower values of G would not necessarily be favorable for the reaction, since both concentrations could respond with the same tendency for the range analyzed and exhibit an inaccurate result in relation to the variables investigated. Thus, the goal here was to obtain the highest possible variation of G value, which pointed to a difference in the colors shown in the reactions for the two concentration levels. With that in mind, all experiments in the experimental design were carried out in triplicate ($n$ = 3) for both concentration levels, and the difference in the values obtained (Y) was used with an analytical response.

For this response (Y), the following polynomial model of the second degree was defined targeted at quantifying the influence of the variables:

$$Y = \beta_0 + \beta_1 A + \beta_2 B + \beta_{12} AB + \beta_{13} AC + \beta_{23} BC + \beta_{11} A^2 + \beta_{22} B^2 + \beta_{33} C^2$$

where A, B and C are the independent variables; $\beta_0$ is a constant; $\beta_1$, $\beta_2$, and $\beta_3$ are the linear coefficients of A, B and C, respectively; $\beta_{12}$, $\beta_{13}$ and $\beta_{23}$ are the coefficients of interactions between the variables; and $\beta_{11}$, $\beta_{22}$ and $\beta_{33}$ are the quadratic coefficients of the variables A, B and C.

After the optimization of the reaction, the samples were subjected to analysis. The analytical procedure employed was quite simple and straightforward. The procedure consisted of using 100 µL of distilled sample after steam-dragging and 300 µL of methyl orange in the sample reservoir; this was taken to the apparatus for image acquisition and the analytical response was obtained from the smartphone application.

All samples were also analyzed using the official method determined by the Ministry of Agriculture, Livestock and Supply – MAPA from Brazil. This method involves the titration of samples with 0.1 mol/L sodium hydroxide standard using

phenolphthalein as an indicator; after that, the samples are subjected to steam-dragging distillation [44]. The ethanol content in *cachaça* was measured using a pycnometer, based on the recommended guidelines of the AOAC [45].

## 3. Results and Discussion

### 3.1. Optimization of the Imaging System

The optimization process targeted at obtaining the analytical signals was performed carefully in order to avoid any inaccurate results. Initially, an analysis was conducted aiming at identifying which size of the selected area was adequate to be used with a view to obtaining a homogeneous and accurate response. This factor is essentially important because, in certain situations, the control of luminosity is not effective, and, as such, some regions of the sample reservoir may receive different intensities of light.

As previously reported in the literature, regions with shadows or excessive brightness pose a significant obstacle when it comes to obtaining the analytical signal [23,30,35]. In this sense, three levels of the selected area available through the application were tested, and all of them presented close results, with coefficient of variation (CV) of 1.2 % in relation to all the levels; the experiments were performed in triplicate ($n$ = 3). Thus, an area of 30 × 30 pixels was selected for the conduct of further studies.

In addition, an analysis was also performed in order to evaluate the maximum volume of solution that the sample reservoir could handle in order to obtain a maximum analytical response. As the cap has a small internal circular hole, this region has a capacity to pre-concentrate the solution and increase the optical path, resulting in a high analytical response. The results obtained from this analysis showed that the maximum volume that the internal hole could bear in a safe and stable manner was 400 µL; thus, this volume was chosen for the conduct of further experiments.

## 3.2. Reaction optimization

To provide a thoroughly accurate description of the behavior of experimental data, an experimental design must ensure that all variables are studied at least in three levels. This is possible when one employs experimental matrices that allow the adjustment of second order functions. Based on the response surface methodology (RSM) analysis, the second order quadratic model of coded units for the analytical response (Y) is presented as follows:

$Y = -95.24 + 20.62\ A - 1.67A^2 - 0.38B + 0.10B^2 + 3.8C - 0{,}04\ C^2 - 0.15\ AB - 0.AC - 0.01\ BC$

The experimental data was evaluated by the analysis of variance (ANOVA) and the significance of the regression coefficients was analyzed based on the corresponding p-values, as shown in Table 1.

**Table 1**. Analysis of variance for the response surface quadratic model

| | SQ | DF | MS | F-value | p-value |
|---|---|---|---|---|---|
| **Model** | 190.87 | 9 | 21.21 | 17.86 | < 0.01* |
| **A** | 0.02 | 1 | 0.02 | 0.05 | 0.84 |
| **$A^2$** | 17.17 | 1 | 17.17 | 51.52 | 0.02* |
| **B** | 21.08 | 1 | 21.08 | 63.25 | 0.02* |
| **$B^2$** | 16.03 | 1 | 16.03 | 48.08 | 0.02* |
| **C** | 3.11 | 1 | 3.11 | 9.33 | 0.09 |
| **$C^2$** | 72.03 | 1 | 72.03 | 216.08 | < 0.01* |
| **AB** | 2.23 | 1 | 2.23 | 6.70 | 0.12 |
| **AC** | 2.25 | 1 | 2.25 | 6.74 | 0.12 |
| **BC** | 1.00 | 1 | 1.00 | 3.00 | 0.23 |
| **Residual error** | 5.94 | 5 | 1.19 | | |
| **Lack-of-fit** | 5.27 | 3 | 1.76 | 5.27 | 0.16 |
| **Pure error** | 0.67 | 2 | 0.33 | | |
| **Total** | 184.93 | 14 | | | |

* Significant at 95% confidence;. SQ: Sum of squares, DF:degrees of freedom, MS: Mean square.

As can be observed, the model presented and the variables A, $A^2$, B, $B^2$, $C^2$ were found to be significant ($P < 0.05$); this shows that all the factors studied in the experimental design had significant influence in relation to the independent variable. In addition, it was also observed that there was no significant interaction between the variables studied, and the lack of fit of the method was not significant. The model was evaluated using the determination coefficient ($R^2$); the adjusted-$R^2$ value obtained was 0.967 – this value showed that the model was highly significant in predicting the variables investigated.

As can be seen in Fig. 3a**,** a high analytical response is obtained when there is a reduced reaction time - close to 1 min of reaction; this shows that the response of the indicator employed in the study is extremely efficient in the presence of acetic acid.

The reaction time is found to be extremely important; this is because, in spot test analysis, a reaction must respond in the shortest possible time. As can be observed, higher values of methyl orange concentration yielded superior analytical signals, and the analytical signal remained stable from the concentration of $4.8 \times 10^{-4}$ mol/L onwards (based on the model); this shows that the levels studied are within the optimal concentration range of the indicator.

Fig. 3b confirms that the concentration of methyl orange is precisely in the above range. This same figure also shows that the ideal hydro- alcoholic concentration range is approximately 40 %. The same results are observed in Fig. 3c with respect to hydro-alcoholic concentration and dye concentration. Thus, the following conditions were applied in subsequent experiments: methyl orange concentration of about $4.8 \times 10^{-4}$ mol/L; reaction time of 1 min; and hydro-alcoholic concentration of 40 %. Thus, the following conditions were applied in subsequent experiments: methyl orange concentration of about $4.8 \times 10^{-4}$ mol/L; reaction time of 1 minute; and hydro-alcoholic concentration of 40%.

Given that the hydro-alcoholic concentration in *cachaça* varies from one brand to another, it was essentially important to evaluate the real impact of this variable on the content of acetic acid in the beverage, since the variable proved to be highly significant in the experimental planning. This time, a robustness test was performed, and the following different hydro-alcoholic concentrations were tested: 38, 42, 44, 46,

48, 50, 53, and 54%. The result obtained showed that the values of channel B changed above 5 % only after the concentration of 44 %. Thus, when the *cachaça* has a hydro-alcoholic concentration below 44 %, no correction is required to be made. In contrast, when the hydro-alcoholic concentration is above 44 %, one is required to make some adjustments in order to correct the alcohol content to 40 % for further analysis. In fact, the content of alcohol doesn't change significatively the color of the methyl orange because the acid-base equilibrium is not shifted by alcohol, to be it a very weak acid substance. The hydroalcoholic content only changes the transfer rate of volatile acid. Thus, the RGB data is weakly affected by alcohol compounds [46].

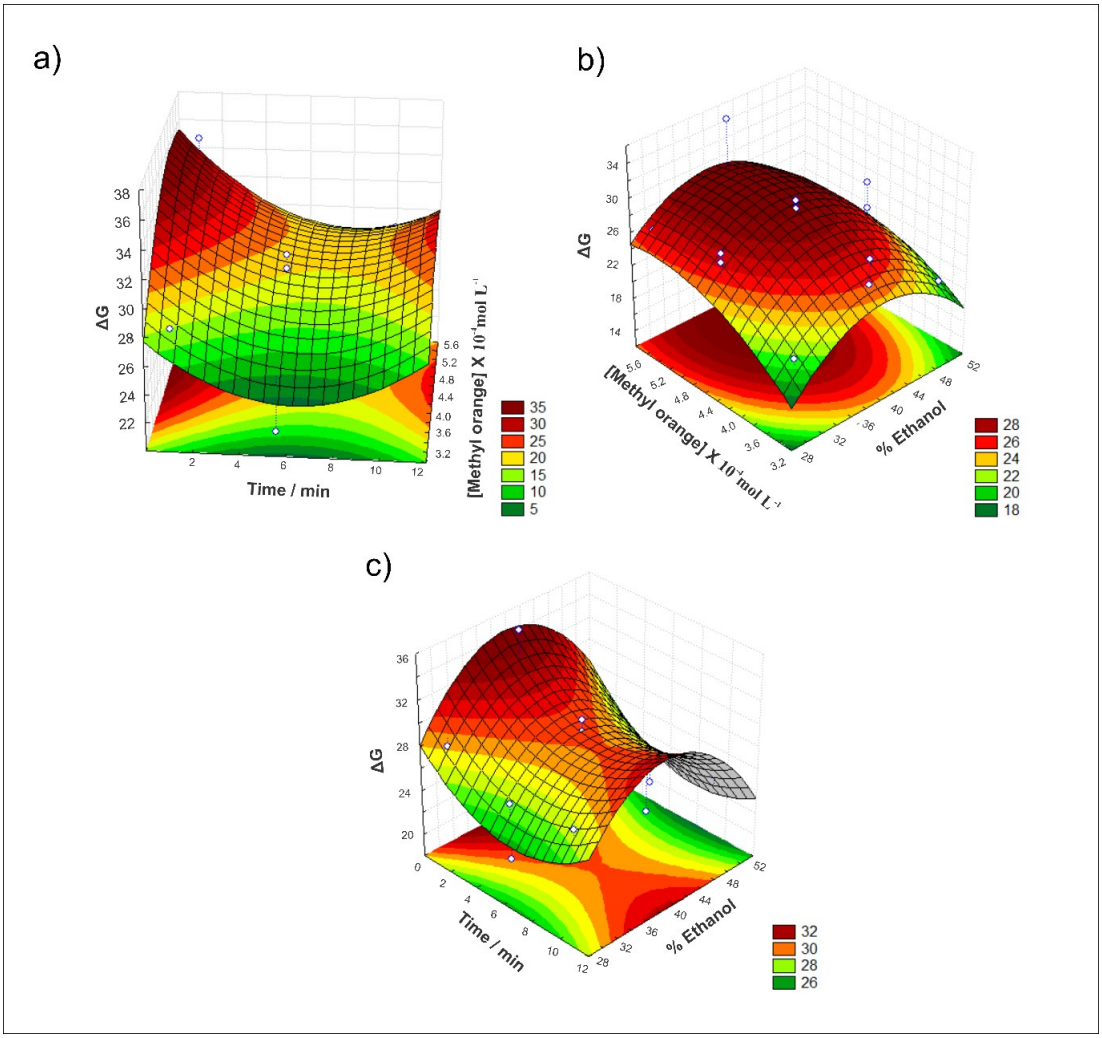


**Fig. 3.** Effect of interaction between: a) time and [methyl orange] and analytical response; b) [methyl orange], % ethanol and analytical response; c) % ethanol and analytical response. Variation of green channel (ΔG).

The variation of the color of the methyl orange due to the variation of pH is not a problem for quantification purposes using the RGB system. The variation of the RGB value of the methyl orange is in function of the volatile acids presented in the sample. Moreover, other volatile compounds such as signal of the sample (containing volatile acid compounds) [21,26,35].

In previous work we described this principle of the variation of the RGB using anthocyanins and acid-base indicator to microtitration to measure the total acidity in food and to evaluate the conformity of bleaching products [21,35]. The anthocyanin presents a purple color in pH 7, and the RGB data correlated with this color was used as background signal, and the RGB obtained from the shift to red color in funcion of the acidity of the food was used discounted from the RGB background [21]. This procedure was similarly studied by Shalaby & Mohamed [39] and Inagawa et al. [40] to evaluate acid-base dyes as alizarin red S, methyl orange, bromothymol blue and bromophenol blue. Thus, the change in the color solution characteristic of acid-base dyes does not present interference.

### 3.3. Analytical features

An analytical curve was constructed using the G channel and based on the application of acetic acid in the range of 25 to 275 mg acetic acid / 100 mL of anhydrous alcohol. The linearity of the proposed method was evaluated through the calibration curve using the least squares method (LSM). The following equation was fitted to the processed data from the images: $-\log (I/I_0) = 0.0006$ [acetic acid] + 0.0527, and an adjusted determination coefficient ($R^2$) of 0.9912 was obtained; this result points to a significant linearity over the working concentration range. The limit of detection (LOD) and limit of quantification (LOQ) were estimated based on the new IUPAC guidelines [47]; the values obtained were as follows: LOD = 3.70 mg/100 mL and LOQ = 11.1 mg/ 100 mL of anhydrous ethanol. Furthermore, the proposed method exhibited a reliable precision, with a relative standard deviation (RSD) of 5.3 % for acetic acid solution of 150 mg/100 mL of anhydrous ethanol ($n$ = 10).

Some organic compounds (referred to as potential interferents) present in *cachaça* were tested to evaluate their influence in terms of interaction with methyl

orange (employed as an indicator). The potential interferents shown in Table 2 were analyzed using the proposed method. Methanol, Propan-1-ol, butan-1-ol, acetaldehyde, furfural and ethyl acetate were tested in the molar ratios of 1:1 and 1:10 (interferent/ analyte). Normally, the absence of interference is considered when the response variation is<5 %. Based on the results obtained in this analysis, it can be concluded that acetaldehyde, furfural and ethyl acetate are potential interferents when it comes to the determination of volatile acidity in *cachaça* samples [46].

**Table 2.** Selectivity study for determination volatile acidity in cachaça (*n* =3)

| Interferent | Ratio of acetic acid/ interferent | Relative error (%) |
|---|---|---|
| Methanol | 1:1 | -5.52 |
| | 1:10 | -1.84 |
| Propan-1-ol | 1:1 | -5.50 |
| | 1:10 | -3.68 |
| Butan-1-ol | 1:1 | -9.20 |
| | 1:10 | 9.28 |
| Acetaldehyde | 1:1 | -9.20 |
| | 1:10 | 9.28 |
| Furfural | 1:1 | -1.80 |
| | 1:10 | 7.41 |
| Ethyl acetate | 1:1 | 11.21 |
| | 1:10 | 22.50 |

Recovery assays were carried out for the *cachaça* samples using three concentration levels: 55, 90 and 125 mg of acetic acid / 100 ml of anhydrous alcohol. The recovery rates obtained ranged between 89.50% and 111.80% (Table 3); this result shows that there was no significant matrix effect.

**Table 3**: Percentage of furfural recovered in the analyzed samples with *n* = 3.

| Sample [a] | Added[b] | Found[b] | Recovery (%) |
|---|---|---|---|
| A1 | 55.0 | 49.22 ± 3.21 | 89.49 |
| | 125.0 | 130.96 ± 5.66 | 104.77 |
| A2 | 55.0 | 53.76 ± 4.48 | 97.74 |
| | 125.0 | 124.68 ± 5.36 | 99.74 |
| A3 | 55.0 | 54.24 ± 2.36 | 98.60 |
| | 125.0 | 121.32 ± 6.25 | 97.05 |
| A4 | 55.0 | 51.15 ± 4.97 | 93.00 |
| | 125.0 | 136.16 ± 5.47 | 109.93 |
| A5 | 55.0 | 50.10 ± 3.5 | 91.10 |
| | 125.0 | 126.10 ± 7.46 | 100.88 |
| A6 | 55.0 | 61.50 ± 3.56 | 111.83 |
| | 125.0 | 112.42 ± 3.64 | 89.92 |
| A7 | 55.0 | 58.08 ± 4.78 | 105.62 |
| | 125.0 | 134.43 ± 6.21 | 107.54 |
| A8 | 55.0 | 57.59 ± 2.28 | 104.71 |
| | 125.0 | 127.07 ± 7.67 | 101.66 |
| A9 | 55.0 | 57.15 ± 3.91 | 103.90 |
| | 125.0 | 126.09 ± 4.63 | 100.87 |

The volatile acidity content of nine non-aged *cachaça* samples was determined using the proposed method and the reference method [44]. The results obtained from this analysis are summarized in Table 4. As can be observed, the two methods exhibited quite similar results, with relative errors varying between –14.5 % and 15.0 %.

**Table 4:** Acetic Acid concentrations found in samples of cachaça unaged tested by the DIB-spot test and comparative method with *n* = 3.

| Sample [a] | Reference Method [b] | DIB method [b] | Relative error (%) |
|---|---|---|---|
| A1 | 81.92 ± 0.45 | 70.02 ± 5.15 | -14,52 |
| A2 | 91.36 ± 2.80 | 88.37 ± 8.30 | -3.27 |
| A3 | 10.40 ± 0.56 | 9.02 ± 1.42 | -13.26 |
| A4 | 25.32 ± 0.60 | 29.36 ± 3.20 | 15.95 |
| A5 | 166.08 ± 0.48 | 150.23 ± 10.21 | --9.54 |

| Sample [a] | Reference Method [b] | DIB method [b] | Relative error (%) |
|---|---|---|---|
| A6 | 22.8 ± 1.2 | 25.65 ± 2.65 | 12.5 |
| A7 | 36.23 ± 0.24 | 38.52 ± 1.36 | 6.32 |
| A8 | 43.80 ± 0.13 | 50.36 ± 3.35 | 14.97 |
| A9 | 196.80 ± 0.50 | 215.68 ± 8.93 | 9.59 |

[a] Real alcoholic degree of cachaça samples: 41, 38, 39, 40, 38, 38, 42, 42, 45 %(v/v) respectively. [b] Concentration in mg / 100 mL of anhydrous ethanol.

The analysis of the results presented in Table 4 shows that two samples of cachaça, A4 and A9, exhibited volatile acidity above the levels established by the Brazilian legislation (MAPA)- 150 mg/100 mL of ethyl alcohol (this value is expressed in terms of acetic acid). According to Leite *et al.* [5], volatile acidity levels depend on factors such as adequate control of time and temperature during the fermentation process, type of yeast used, must management, and, most importantly, the hygienic condition during the manufacturing process. Thus, the results obtained in this study reinforce the importance of implementing good production practices, and a fast and *in situ* analysis as the DIB method using smartphone in order to obtain beverages with great sensory qualities, which will, consequently, lead to higher market acceptance.

Finally, the results obtained from the application of the proposed method and the reference method were statistically compared using the paired t-test with 95 % confidence level. The results of the paired t-test showed that the calculated t value (0.08) was lower than the critical t value (2.30); this implies that there were no statistically significant differences between the two methods.

## 4. Conclusions

The present work reported the development and application of a novel method for the determination of volatile acidity in non-aged *cachaça* samples using a smartphone as an analytical tool. Methyl orange was used as an indicator of color change according to the acidity of the medium, and the green channel was used based on the RGB model decomposed in a cell phone application. The method proposed in this study proved to be efficient, fast and environmentally friendly, since it generates a very small amount of waste. Apart from that, the proposed method can

be easily employed for the production of good quality *cachaça* with great sensory properties and volatile acidity levels that are within the limits stipulated by the Brazilian legislation. Two samples of *cachaça* failed to meet the standard criteria established by the Brazilian legislation; thus, the findings of this study point to the need for promoting good production practices and stricter quality control of the beverage.

**References**

[1] MAPA, Instruçao normativa no. 24, de 08 de setembro de 2005. Manual operacional de bebidas e vinagres, (2005).

[2] M.B.d. Miranda, N.G.S. Martins, A.E.d.S. Belluco, J. Horii, A.R. Alcarde, Perfil físico-químico de aguardente durante envelhecimento em toneis de carvalho, Food Sci. Technol. 28 (2008) 84–89.

[3] M. de Oliveira Krambeck Franco, W.T. Suarez, V.B.D. Santos, Digital Image Method Smartphone-Based for Furfural Determination in Sugarcane Spirits, Food Anal. Methods. 10 (2) (2017) 508–515.

[4] H.G.S. Luna, M.H. Canuto, G.M. de Lima, J.B.B. da Silva, Cachaça Artesanal de Minas, Inf. Agropecuario. 23 (2002) 59–62.

[5] J.J.d.R. Leite, E.N.A. Oliveira, F.L.C. Almeida, R.M. Feitosa, Caracterizaçao físico-quimica de aguardentes de cana-de-açúcar produzidas no rio grande do norte, Rev. Bras. Tecnol. Agroindustrial. 11 (1) (2017), https://doi.org/10.3895/RBTA.V11N1.3778.

[6] K. Chen, S. Li, H. Yang, J. Zou, L. Yang, J. Li, L. Ma, Feasibility of using gas chromatography-ion mobility spectrometry to identify characteristic volatile compounds related to brandy aging, J. Food Compos. Anal. 98 (2021), 103812, https://doi.org/10.1016/J.JFCA.2021.103812.

[7] J. Silva, M. Verruma-Bernardi, A. Belluco, S. Medeiros, A. Oliveira, Volatile compounds in cachaças obtained from three sugarcane varieties cultivated under the managements: organic, conventional and without fertilization.

[8] MAPA, Instruçao, Normativa,, de 30 de junho de 2005. Aprova o Regulamento Tecnico para Fixaçao dos Padr̃oes de Identidade e Qualidade para Aguardente de Cana̤ e para Cachaça, no. 13, 2005.

[9] A.M. Bortoletto, G.C. Silvello, A.R. Alcarde, Chemical and microbiological quality of sugar cane juice influences the concentration of ethyl carbamate and volatile congeners in cachaça, J. Inst. Brew. 121 (2015) 251–256, https://doi.org/10.1002/jib.213.

[10] A.M. Bortoletto, A.R. Alcarde, Assessment of chemical quality of Brazilian sugar cane spirits and cachaças, Food Control. 54 (2015) 1–6, https://doi.org/10.1016/j. foodcont.2015.01.030.

[11] R.F. Nascimento, D.R. Cardoso, B.S. Lima Neto, D.W. Franco, Determination of acids in Brazilian sugar cane spirits and other alcoholic beverages by HRGC-SPE, Chromatographia. 48 (1998) 751–757, https://doi.org/10.1007/BF02467643.

[12] A. Antonelli, M. Galli, Determination of volatiles in spirits using combined stationary phases in capillary GC, Chromatographia. 41 (1995) 722–725, https:// doi.org/10.1007/BF02267811.

[13] J. Zeravik, Z. Fohlerova, M. Milovanovic, O. Kubesa, M. Zeisbergerova, K. Lacina, A. Petrovic, Z. Glatz, P. Skladal, Various instrumental approaches for determination of organic acids in wines, Food Chem. 194 (2016) 432–440, https:// doi.org/10.1016/j.foodchem.2015.08.013.

[14] M. Gallart, S. Francioli, A. Viu-Marco, E. Lopez-Tamames, S. Buxaderas, ´ Determination of free fatty acids and their ethyl esters in musts and wines, J. Chromatogr. A. 776 (1997) 283–291, https://doi.org/10.1016/S0021-9673(97) 00383-X.

[15] T. Sakai, I. Hara, M. Tsubouchi, Spectrophotometric determination of quinine, emethine and ephedrine in pharmaceutical preparations with tetrabromophenolphthalein ethyl ester by solvent extraction, Chem. Pharm. Bull. (Tokyo) 24 (1976) 1254–1259, https://doi.org/10.1248/cpb.24.1254.

[16] K. Oono, A colorimetric method for the determination of acetic acid in the urine, J. Biochem. 39 (1952) 133–135,

[17] C.A. Machado, F.O. Oliveira, M.A. de Andrade, K.V.S. Hodel, H. Lepikson, B.A. S. Machado, Steam Distillation for Essential Oil Extraction: An Evaluation of Technological Advances Based on an Analysis of Patent

Documents, Sustainability 14 (2022) 7119–7134, https://doi.org/10.3390/su14127119.

[18] J.M. Prats-Montalban, A. Juan, A. Ferrer, Multivariate image analysis: A review ´ with applications, Chemom. Intell. Lab. Syst. 107 (2011) 1–23, https://doi.org/ 10.1016/j.chemolab.2011.03.002.

[19] S. Paciornik, A.V. Yallouz, R.C. Campos, D. Gannerman, Scanner image analysis in the quantification of mercury using spot-tests, J. Braz. Chem. Soc. 17 (2006) 156–161, https://doi.org/10.1590/S0103-50532006000100022.

[20] B.G. Botelho, L.P. De Assis, M.M. Sena, Development and analytical validation of a simple multivariate calibration method using digital scanner images for sunset yellow determination in soft beverages, Food Chem. 159 (2014) 175–180, https:// doi.org/10.1016/j.foodchem.2014.03.048.

[21] L.M.A. de Oliveira, V.B. dos Santos, E.K.N. da Silva, A.S. Lopes, H.A. Dantas-Filho, An environment-friendly spot test method with digital imaging for the micro- titration of citric fruits, Talanta. 206 (2020), 120219, https://doi.org/10.1016/j. talanta.2019.120219.

[22] F.C. Bock, G.A. Helfer, A.B. Costa, M.B. Dessuy, M.F. Ferr¨ao, PhotoMetrix and ˜ colorimetric image analysis using smartphones, Journal of Chemometrics. 34 (2020) 1–19, https://doi.org/10.1002/cem.3251.

[23] E.K.N. da Silva, V.B. dos Santos, I.S. Resque, C.A. Neves, S.G.C. Moreira, M.d.O. K. Franco, W.T. Suarez, A fluorescence digital image-based method using a 3D- printed platform and a UV-LED chamber made of polyacid lactic for quinine quantification in beverages, Microchemical Journal. 157 (2020), https://doi.org/ 10.1016/j.microc.2020.104986.

[24] J.P.B. de Almeida, V.B. dos Santos, G.A. do Nascimento, W.T. Suarez, W.M. de Azevedo, A.F. Ferreira, M.V. Maia, A fluorescence digital image-based method using carbon quantum dots to evaluate the compliance of a biocidal agent, Analytical Methods. 14 (26) (2022) 2631–2641.

[25] S. Soares, F.R.P. Rocha, Spot test for determination of uric acid in saliva by smartphone-based digital images: A new proposal for detecting kidney dysfunctions, Microchemical Journal. 162 (2021), 105862, https://doi.org/ 10.1016/j.microc.2020.105862.

[26] M.F. Filgueiras, P.C. de Jesus, E.M. Borges, Quantification of Nitrite in Food and Water Samples Using the Griess Assay and Digital Images Acquired Using a Desktop Scanner, Journal of Chemical Education. 98 (2021) 3303–3311, https:// doi.org/10.1021/acs.jchemed.0c01392.

[27] N. Maleki, A. Safavi, F. Sedaghatpour, Single-step calibration, prediction and real samples data acquisition for artificial neural network using a CCD camera, Talanta. 64 (2004) 830–835, https://doi.org/10.1016/j.talanta.2004.02.041.

[28] E.N. Gaiao, V.L. Martins, W.S. Lyra, L.F. de Almeida, E.C. da Silva, M.C.U. Araújo, Digital image-based titrations, Anal Chim Acta. 570 (2006) 283–290, https://doi. org/10.1016/j.aca.2006.04.048.

[29] M.V. Maia, W.T. Suarez, V.B. dos Santos, J.P.B. de Almeida, Carbon dots on paper for determination of $Cu^{2+}$ in sugar cane Spirits samples for fluorescence digital image-based method, Microchemical Journal. 179 (2022), 107500, https://doi. org/10.1016/j.microc.2022.107500.

[30] L.P.S. Benedetti, V.B. dos Santos, T.A. Silva, E.B. Filho, V.L. Martins, O. Fatibello- Filho, A digital image-based method employing a spot-test for quantification of ethanol in drinks, Analytical Methods. 7 (2015) 4138–4144, https://doi.org/ 10.1039/C5AY00529A.

[31] V.L.F. Capitan, N.L. Ruiz, A.M. Olmos, M.M. Erenas, A.J. Palma, Recent ´ developments in computer vision-based analytical chemistry: a tutorial review, Analytica Chimica Acta. 899 (2015) 23–56.

[32] K. Mahato, P. Chandra, Paper-based miniaturized immunosensor for naked eye ALP detection based on digital image colorimetry integrated with smartphone, Biosensors and Bioelectronics. 128 (2019) 9–16, https://doi.org/10.1016/j. bios.2018.12.006.

[33] M. Rastislav, V.B. dos Santos, L. Angnes, A simple paper-strip colorimetric method utilizing dehydrogenase enzymes for analysis of food components, Anal. Methods. 7 (2015) 8177–8184, https://doi.org/10.1039/C5AY01556A.

[34] C.T. Gee, E. Kehoe, W.C.K. Pomerantz, R.L. Penn, Quantifying Protein

Concentrations Using Smartphone Colorimetry: A New Method for an Established Test, Journal of Chemical Education. 94 (2017) 941–945.

[35] I.S. Resque, V.B. dos Santos, W.T. Suarez, An environmentally friendly analytical approach based on spot test and digital image to evaluate the conformity of bleaching products, Chemical Papers. 73 (2019) 1659–1668, https:// doi.org/ 10.1007/s11696-019-00717-w.

[36] W. Li, X. Zhang, C. Miao, R. Li, Y. Ji, Fluorescent paper–based sensor based on carbon dots for detection of folic acid, Analytical and Bioanalytical Chemistry. 412 (2020) 2805–2813, https://doi.org/10.1007/s00216-020-02507-w.

[37] W.R.F. Silva, W.T. Suarez, C. Reis, V.B. dos Santos, F.A. Carvalho, E.L. Reis, F. C. Vicentini, Multifunctional Webcam Spectrophotometer for Performing Analytical Determination and Measurements of Emission, Absorption, and Fluorescence Spectra, Journal of Chemical Education. 98 (2021) 1442–1447, https://doi.org/10.1021/acs.jchemed.0c01085.

[38] W.T. Suarez, O.D. Pessoa-Neto, V.B. dos Santos, A.R.A. Nogueira, R.C. Faria, O. Fatibello-Filho, M. Puyol, J. Alonso, A compact miniaturized continuous flow system for the determination of urea content in milk, Analytical and Bioanalytical Chemistry. 398 (2010) 1525–1533, https://doi.org/10.1007/s00216-010-4052-6.

[39] A.A. Shalaby, A.A. Mohamed, Determination of acid dissociation constants of alizarin red S, methyl orange, bromothymol blue and bromophenol blue using a digital camera, RSC Advances. 10 (2020) 11311–11316, https://doi.org/10.1039/ C9RA10568A.

[40] A. Inagawa, K. Saito, A. Sasaki, N. Uehara, Dataset for reproducing absorption spectra of methyl orange from the RGB values of microscopic images, Data in Brief. 31 (2020), 105998, https://doi.org/10.1016/j.dib.2020.105998.

[41] M.d.O.K. Franco, W.T. Suarez, V.B. dos Santos, I.S. Resque, A novel digital image method for determination of reducing sugars in aged and non-aged cachaças employing a smartphone, Food Chem. 338 (2021), https://doi.org/10.1016/j. foodchem.2020.127800.

[42] Loomatix, Color Grab, (2022). https://play.google.com/store/apps/details? id=com.loomatix.colorgrab&hl=pt_BR.

[43] A.M. Sanchez, M. Barra, R.H. de Rossi, On the Mechanism of the Acid/ Base- Catalyzed Thermal *Cis − Trans* Isomerization of Methyl Orange, J. Org. Chem. 64 (1999) 1604–1609, https://doi.org/10.1021/jo982069j.

[44] MAPA- Ministry of Agriculture Livestock and Supply, Acidez total ou titulavel, in: Man. Métodos Análises Bebidas e Vinagres, 2004.

[45] G.W. Latimer Jr, The Official Methods of Analysis of AOAC International, 19th Editi, USA, Rockville, 2012.

[46] J. Clayden, N. Greeves, S. Warren, P. Wothers, Organic Chemistry, Oxford University Press Inc., New York, 2001.

[47] L.A. Currie, Nomenclature in evaluation of analytical methods including detection and quantification capabilities (IUPAC Recommendations 1995), Anal. Chim. Acta. 391 (1999) 105–126, https://doi.org/10.1016/S0003-2670(99)00104-X.

# CAPÍTULO 4 –

## Uma nova reação seletiva e altamente sensível para a determinação de $Cu^{2+}$ em bebidas destiladas empregando imagens digitais

Analytica Chimica Acta 1177 (2021) 33884

Contents lists available at ScienceDirect

Analytica Chimica Acta

journal homepage: www.elsevier.com/locate/ac

# A color reaction for the determination of $Cu^2$ in distilled beverages employing digital imaging

Mathews de Oliveira Krambeck Franco [a], Gabriel Abranches Dias Castro [b], Castelo Vilanculo [a], Sergio Antonio Fernandes [b], Willian Toito Suarez [a, *]

[a] Departamento de Química, Centro de Ci^encias Exatas e Tecnologica, Universidade Federal de Viçosa, Viçosa, MG, 36570-900, Brazil

[b] Grupo de Química Supramolecular e Biomimetica (GQSB), Departamento de Química, Centro de Ci^encias Exatas e Tecnologica, Universidade Federal de Viçosa, Viçosa, MG, 36570-900, Brazil

ARTICLE INFO

Keywords:
Digital image analysis
Copper determination
Thiocarbazones
Copper complex
Distilled beverages

ABSTRACT

In this work, we describe for the first time the synthesis of thiocarbazones for the selective determination of $Cu^{2+}$ in distilled beverages. The method was based on the complexation reaction of $Cu^{2+}$ with thiocarbazones, and the colored product was analyzed using a smartphone application. The thiocarbazones react with $Cu^{2+}$ to form a 1:1 (metal:ligand) complex. The $Cu^{2+}$ complex was characterized by UV, IR and NMR spectral analyses. The proposed reaction yields a yellow color, and therefore, channel B of the RGB system was used in the analysis. After optimizing the reaction conditions, an analytical curve was obtained to determine $Cu^{2+}$ concentrations ranging between 0.25 and 6.75 mg $L^{-1}$; the use of 400 μL sample volumes led to a relative standard deviation (n = 5) of 3.2% and a detection limit of 0.18 mg $L^{-1}$. Recovery experiments were performed with sugar cane spirits, whiskies and tequilas to evaluate the accuracy of the method, and the recovery obtained ranged from 80.5–112.2%.

## 1. Introduction

According to a recent global status report on alcohol and health, approximately 2.3 billion people currently consume alcoholic beverages and that number has steadily increased. As a result, peoples' awareness of the consumption of quality products has also been growing, and this has generated the need to develop the products they seek in accordance with the norms and standards defined by regulatory bodies [1–3]. In this context, beverages that are usually distilled in traditional equipment made of copper deserve special attention, since when manufacturers do not promote the proper hygiene of distillers, there may be contamination of copper in the distillates [4]. In this scenario, we can cite mainly whiskey, tequila and sugar cane spirits, since their production and consumption have been growing worldwide [5–8]. In general, it has been reported that when these beverages are produced in copper-based equipment, they are more widely accepted, which can be explained by the unique ability of copper to reduce acidity and the levels of aldehydes and sulfur-based compounds; these characteristics reduce the organoleptic quality of drinks [9–11]. The Ministry of Agriculture, Supply and Livestock of Brazil (MAPA) established that the maximum allowed $Cu^{2+}$ concentration in drinks is 5 mg/L, which applies to sugar cane spirits, whiskey and tequila [12].

In this sense, it is of utmost importance to develop simpler and more robust methods for analyzing $Cu^{2+}$ concentrations in beverages. Some studies have already reported the determination of this ion by using a smartphone as an analytical instrument with several samples, such as water and blood, mushrooms and effluent [13,14]. Therefore, chemical analyses are becoming more accessible since webcams, smartphones and cameras can be used as analytical tools, thereby allowing the determination of analyte dosages in a simple and inexpensive way [15–22]. In addition, methods that involve the analysis of digital images are fast, do not require sophisticated technical knowledge in the area and only require that the product formed from the reaction with analyte be colored. In addition, the advantages of this type of platform over conventional methods of analysis are numerous, including low reagent consumption, small sample volumes, simplicity, portability and disposability [23].

Shiff bases (or imines) play a very important role, since they have already proven countless times to be useful in the determination of metals by colorimetric methods [24–27]. They were first reported by Hugo Shiff in 1864 and are organic molecules that can be identified by the presence of a double bond between a carbon and a nitrogen (C=N) [28]. Among the Shiff bases already studied, thiocarbazones have been gaining prominence. They are commonly produced from the condensation of an aldehyde, or ketone, with a thiocarbohydrazine. This class of compounds is structurally similar to thiosemicarbazones and thioureas [29–31]. In general, these compounds have already been reported in the literature because they have several applications in which they serve as antioxidants, antifungal and antibacterial agents, and as urease inhibitors [29,32–35]. In addition, thiocarbazones have been reported several times because they have the ability to complex metals selectively and produce colored coordination compounds [29,30,36–38].

In view of the above, a method based on digital image analysis with a smartphone is proposed for the use of thiocarbazones to determine the $Cu^{2+}$ content in whiskey, tequila and sugar cane spirits. The reaction employed in this method is unprecedented in the literature and has proven to be highly sensitive and selective for the determination of the metal in beverages. The method is simple, fast, robust and can be used for quality control of the $Cu^{2+}$ content in manufactured drinks, thereby guaranteeing the food safety of the final product.

## 2. Experimental

### *2.1. Chemical and Samples*

Carbon sulfide ($CS_2$, >99%, Sigma Aldrich), hydrazine hydrate ($NH_2NH_2$, 80% in water, Sigma Aldrich), acetic acid (99,7%, Vetec), ethanol (95%, Vetec), 4-methoxybenzaldehyde (98%, Sigma Aldrich), 4-nitrobenzaldehyde (98%, Sigma Aldrich), 4-(dimethylamino)benzaldehyde (>95%, Eastman Organic Chemicals), 4-aminobenzaldehyde (>99%, Sigma Aldrich), 2-nitrobenzaldehyde (98%, Sigma Aldrich), deuterated dimethylsulfoxide (DMSO-$d_6$, 99%, Sigma Aldrich), and copper sulfate pentahydrate ($CuSO_4.5H_2O$, >98%, Sigma Aldrich) were used. All chemical reagents were of analytical grade.

The solutions were prepared with ultrapure water (resistivity > 18.0 MΩ) obtained from a Millipore Milli-Q system (USA). A stock solution of $Cu^{2+}$ 75.375 mg $L^{-1}$ (0.00125 mol $L^{-1}$) was prepared by dissolving 0.0312 g $CuSO_4.5H_2O$ in 100 mL of distilled water and then stored at room temperature. Ligand (**1A-1E**) stock solutions (0.001 mol $L^{-1}$) were prepared in anhydrous ethanol and stored at 4 °C.

Solutions of 0.1 mol $L^{-1}$ phthalate buffer with pH 4.0 and 0.1 mol $L^{-1}$ borate buffer with pH 9.0 were prepared by dissolving 2.042 g of potassium hydrogen phthalate ($KHC_8H_4O_4$) and 3.814 g of sodium tetraborate decahydrate $Na_2B_4O_7{\cdot}10H_2O$ in 100 mL of distilled water, respectively, and these solutions were stored at room temperature. Hydrochloric acid (HCl) and sodium hydroxide (NaOH) solution with concentrations of 0.1 mol $L^{-1}$ were prepared and used to adjust the pH.

All samples of sugar cane spirits, whisky and tequila used for our studies were obtained from supermarkets in the city of Viçosa-MG-Brazil.

### *2.2. Instrumentation and Apparatus*

Infrared spectra were recorded on neat samples using an FT-IR Varian 660 Fourier transform infrared spectrometer. Values are expressed in wavenumbers ($cm^{-1}$) for spectra recorded in the range 4000−400 $cm^{-1}$. NMR spectra were recorded at 25 °C in DMSO-$d_6$ on a Varian Mercury 300 spectrometer operating at 300 MHz for $^1H$ and 75 MHz for $^{13}C$. All chemical shifts are reported in parts per million (ppm) and were measured relative to the solvent in which the sample was analyzed (DMSO-$d_6$, $\delta$ = 2.49 for $^1H$ NMR and $\delta$ = 39.5 for $^{13}C$ NMR). Coupling constants ($J$) are reported in hertz (Hz), and the signals were characterized as singlet (s), doublet (d), triplet (t), quartet (q), multiplet (m), double doublet (dd) and triple doublet (td). The masses of compounds were determined by mass spectrometry using a SHIMADZU GCMS-QP2010C Ultra.

For $Cu^{2+}$ determination in distilled beverages, the procedure was performed according to the protocol described in our previous works with some adaptations [39]. Briefly, the colorimetric reactions were performed directly with samples on porcelain plaques containing 6 vessels, and after each reaction, an aliquot was transferred to the reaction module that consisted of lids of glass vials that were 2 cm in diameter.

To accommodate the lids in the box for image acquisition, a foam was cut into a circular shape to avoid movements of solutions.

In the present work, an Asus ZenFone 3 smartphone camera with 16.0 megapixel resolution was used as the detector. Camera parameters were fixed in the application to avoid automatic configurations of the mobile phone. The focus mode was set by considering that the distance between the camera lens and the reaction module containing a sample was less than five centimeters. Additionally, the application uses the automatic focus option, which avoids capturing out-of-focus pictures of the target sample. The resolution of the pictures was set to the highest available value in the smartphone to guarantee a high number of pixels in each sensing area for the image analysis. As shown in Fig. 1, the reaction module containing a sample was placed at the bottom of the equipment. A box with dimensions of 20 x 10 x 6 cm was used as an apparatus for image capture. The smartphone was placed on the top of the box. After entering optimized parameters for image capturing, the reaction module containing a sample was placed into the box in an appropriate position to allow the camera flashlight to focus on the sample solution and therefore capture an image with high quality and good resolution.

When a new picture was required, the application, with the camera parameters fixed, started the capture process by turning on the flashlight. This step ensured that pictures were always taken with the same orientation, thereby simplifying the processing by ensuring that the user did not place the camera in an incorrect position. For image treatment, the free software Color Grab was used [40]. This application was chosen mainly for its simplicity and because the RGB values are offered in real time, which made it easier for the analyst to control and interpret the responses obtained in each procedure.

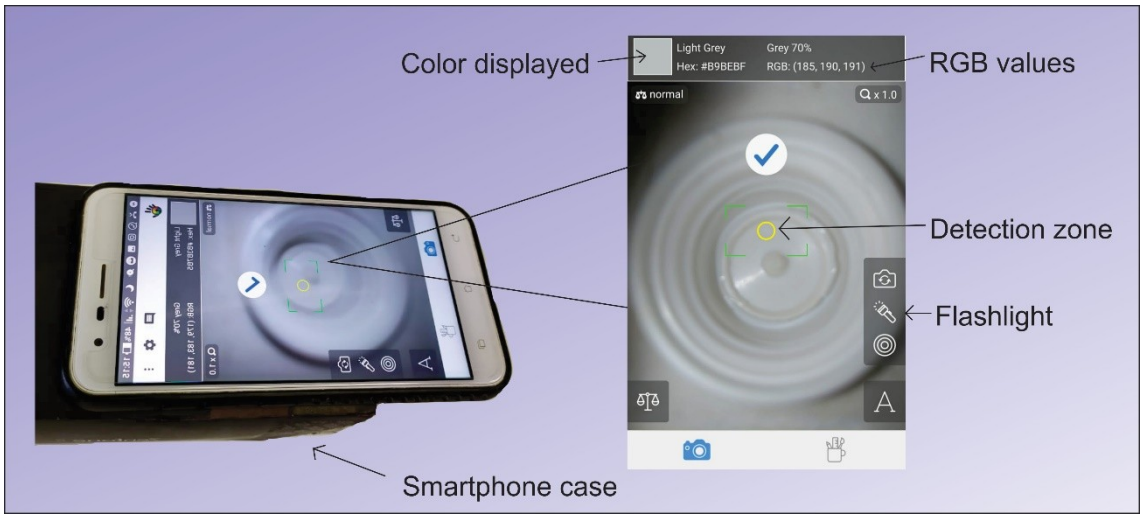


**Fig. 1**. Apparatus developed for the determination of $Cu^{2+}$ in distilled beverages.

### *2.3. Image acquisition and data analysis*

The digital images can be decomposed with several color models, with the RGB model being that most known and used. In this model, the images were decomposed into related algebraic matrices for the present colors, red (R), green (G) and blue (B) [41]. In this way, an appropriate relationship was established between the values of the channel components and the concentration of the analyte. The values relating to RGB colorimetric reaction responses (I) were compared with the values acquired for the R, G, or B values obtained from the analytical background ($I_0$). The equation $y = -\log(I/I_0)$ supplied the value needed to construct the analytical curve [42].

The application Color Grab was used to decompose the images into RGB data. The program provides the average signal value of each channel (R, G, or B), as well as the standard deviation for the selected area. The phenomena involved in the process required the incidence of electromagnetic radiation on the solution contained in the reaction module. Part of this radiation was reflected and reached the CCD detector of the smartphone.

Three rectangular areas were selected for analysis in each reaction module, and they were of different dimension (20 × 20, 30 × 30, and 40 × 40). The dimensions were given in pixels (length × height), and the regions that presented the lowest coefficients of variation were chosen, thereby avoiding regions with brightness

and shadow. The settings used to capture the images with the devices were as follows: camera left cell (RGB); reference standard (RAL classic), locking indication (active), noise cancellation (smart with active flashlight option).

### *2.4. Synthesis of thiocarbohydrazine*

With the aid of an addition funnel, carbon disulfide (1 mL) was dripped into a solution of hydrazine hydrate (3.3 mL) in water (10 mL) contained in a 25 mL flask, and the mixture was stirred with a magnetic stir bar for one hour. At the end of this period, the mixture was heated under reflux for two hours (**Fig. 2**). Subsequently, it was allowed to cool to room temperature, and the formation of a yellow precipitate was observed; this was vacuum filtered and washed with cold ethanol [43].

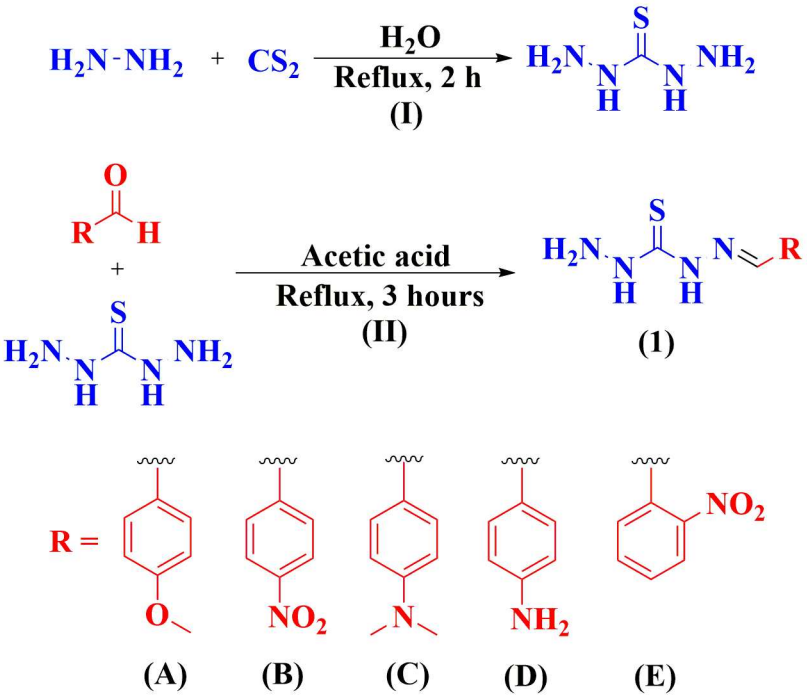


**Fig. 2**. Synthesis route for thiocarbazide and synthesis route for compounds **1A-1E**.

### *2.5. Spectroscopic data for thiocarbohydrazine*

The spectral images are contained in the supplementary material (**Fig. S1 – Fig. S4**).Thiocarbohydrazine: White crystals, yield 56%. M.p. 171.1–172.5 °C. IR ($cm^{-1}$) $\bar{\nu}_{max}$: 3271, 3172, 2964, 1630, 1529, 1488, 1285, 1006. GC-MS (*m/z*) (abundance %):

106 (100, $M^+$), 75 (30), 60 (40). $^1$H NMR (DMSO-$d_6$) $\delta$ 8.37 (s, 2H), 5.63 (s, 4H). $^{13}$C NMR (DMSO-$d_6$) $\delta$ 181.8.

### *2.6. General synthesis of ligands 1A-1E*

Thiocarbohydrazine (0.11 mmol) was dissolved in a mixture of water (3 mL) and ethanol (2 mL), and an aromatic aldehyde (0.10 mmol) and 33 µL of acetic acid were added. The mixture was maintained under reflux for three hours (**Fig. 2**). The precipitate was collected by filtration and washed with cold water. For purification, it was recrystallized from a mixture of ethanol/water in a 1:1 ratio [44].

### *2.7. Spectroscopic data of thiocarbazones*

The spectra images are found in the supplementary material (**Fig. S5 – Fig. S24**).

1-(4-methoxybenzaldehyde)thiocarbazone (**1A**): White solid, yield 80%. M.p. 182.2–183.3 °C. IR ($cm^{-1}$) $\bar{\nu}_{max}$: 3165, 2998, 1606, 1504, 1241, 1176, 979, 848, 586. GC-MS (*m/z*) (abundance %): 224 (85, $M^+$), 193 (59), 134 (100), 91 (50). $^1$H NMR (DMSO-$d_6$) $\delta$ 11.27 (s, 1H), 9.67 (s, 1H), 7.93 (s, 1H,), 7.74 (d, $J$ = 8.7 Hz, 2H), 6.93 (d, $J$ = 8.7 Hz, 2H), 4.81 (s, 2H), 3.76 (s, 3H). $^{13}$C NMR (DMSO-$d_6$) $\delta$ 175.8, 160.6, 142.1, 126.9, 129.0, 114.1, 55.3.

1-(4-nitrobenzaldehyde)thiocarbazone (**1B**): Yellow solid, yield 73%. M.p. 203.5–203.9 °C. IR ($cm^{-1}$) $\bar{\nu}_{max}$: 3300, 3163, 2966, 1561, 1503, 1335, 1241, 1088, 1008, 943, 861, 783, 703, 624. GC-MS (*m/z*) (abundance %): 239 (100, $M^+$), 208 (25), 103 (35), 76 (32). $^1$H NMR (DMSO-$d_6$) $\delta$ 11.72 (s, 1H), 10.15 (s, 1H), 8.23–8.06 (m, 5H), 4.93 (s, 2H). $^{13}$C NMR (DMSO-$d_6$) $\delta$ 175.7, 147.4, 140.9, 139.3, 128.2, 123.7.

1-(4-(dimethylamino)benzaldehyde)thiocarbazone (**1C**): Yellow solid, yield 92%. M.p. 186.6–187.6 °C. IR ($cm^{-1}$) $\bar{\nu}_{max}$: 3385, 3279, 3155, 2900, 1596, 1496, 1358, 1273, 1176, 1008, 804. GC-MS (*m/z*) (abundance %): 237 (85, $M^+$), 205 (58), 148 (100). $^1$H NMR (DMSO-$d_6$) $\delta$ 11.14 (s, 1H), 9.49 (s, 1H), 7.87 (s, 1H), 7.59 (d, $J$ = 9.0 Hz, 2H), 6.67 (d, $J$ = 9.0 Hz, 2H), 4.77 (s, 2H); 2.93 (s, 6H). $^{13}$C NMR (DMSO-$d_6$) $\delta$ 175.6, 151.3, 143.2, 128.6, 121.6, 111.7, 39.8.

1-(4-aminobenzaldehyde)thiocarbazone (**1D**): Orange solid, yield 39%. M.p. 183.2–183.8 °C. IR ($cm^{-1}$) $\bar{\nu}_{max}$: 3424, 3323, 3279, 3155, 2989, 1605, 1497, 1277, 1176, 1008, 833, 586, 528. GC-MS (*m/z*) (abundance %): 209 (68, $M^+$), 178 (42), 135 (48),

119 (100), 92 (66), 65 (65). $^{1}$H NMR (DMSO-$d_6$) $\delta$ 11.11 (s, 1H), 9.45 (s, 1H), 7.81 (s, 1H), 7.25 (d, $J$ = 8.4 Hz, 2H), 6.53 (d, $J$ = 8.4 Hz, 2H), 5.53 (s, 2H), 4.84 (s, 2H). $^{13}$C NMR (DMSO-$d_6$) $\delta$ 175.6, 150.8, 143.6, 128.9, 121.4, 113.4.

1-(2-nitrobenzaldehyde)thiocarbazone (**1E**): Yellow solid, yield 58%. M.p. 187.4–188.8 °C. IR (cm$^{-1}$) $\bar{\nu}_{max}$: 3130, 2922, 2798, 1510, 1343, 1227, 1022, 782, 746, 601. GC-MS (*m/z*) (abundance %): 239 (28, M$^{+}$), 222 (39), 104 (56), 91 (100), 75 (67), 60 (66), 44 (75). $^{1}$H NMR (DMSO-$d_6$) $\delta$ 11.71 (s, 1H), 10.00 (s, 1H), 8.53 (dd, $J$ = 8.0 and 1.5 Hz, 1H), 8.43 (s, 1H), 8.00 (dd, $J$ = 8.0 and 1.5 Hz, 1H), 7.75–7.69 (m, 1H), 7.62–7.57 (m, 1H), 4.92 (s, 2H). $^{13}$C NMR (DMSO-$d_6$) $\delta$ 175.8, 148.2, 136.9, 133.3, 130.2, 128.5, 128.4, 124.5.

## 3. Results and Discussions

### *3.1. Optimization of system parameters*

For the capture of digital images, the built system was submitted to precision assays based on the obtained RGB data. First, it was observed that all areas selected to capture the images obtained satisfactory responses, with standard deviations less than 1.8%. This showed that the apparatus developed to obtain the digital images was adequate and allowed us to acquire homogeneous illumination.

### *3.2. Study of the best complexant for $Cu^{2+}$*

Five ligands (**1A**-**1E**) were synthetized and evaluated while seeking the sensitive and selective determination of $Cu^{2+}$. Thus, all were used at a fixed concentration of 2 x 10$^{-4}$ mol L$^{-1}$, while the metal concentrations were varied from 1.60 to 31.75 mg L$^{-1}$. As shown in **Fig. 3**, all metals showed good sensitivity until a concentration of 3.71 mg L$^{-1}$ was reached, while only ligand **1C** showed sensitivity at concentrations higher than this. In this study, the solution was kept at pH 7, and the reaction time was 10 minutes.

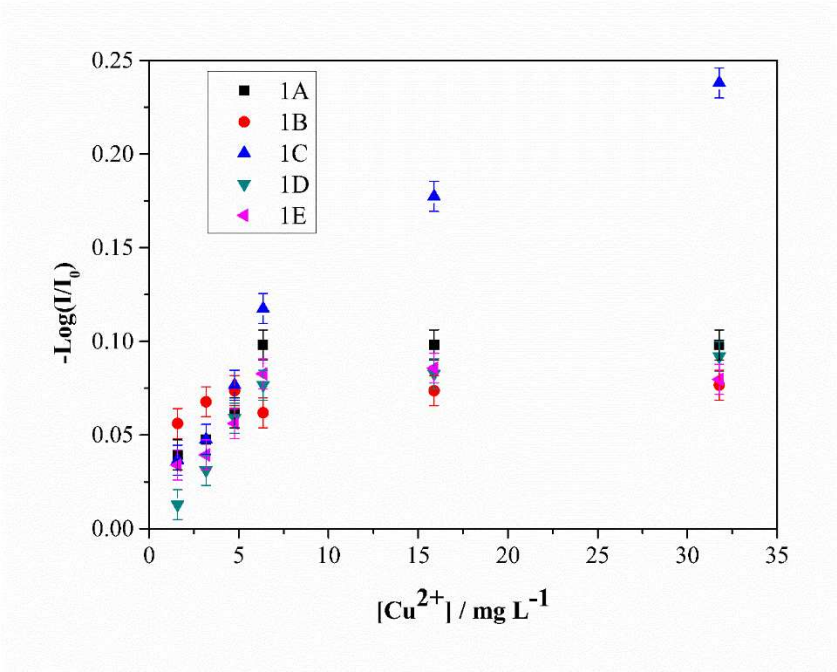


**Fig. 3.** Study of complexes for determination of $Cu^{2+}$.

The sensitivity of the ligan is directly related to its ability to coordinate with the metal. In this case, the substituents on the aromatic rings of the thiocarbazones influence the coordination reaction with their ability to donate electronic density to the ring, since the aromatic ring is conjugated with the imine group, which is one of the copper binding sites. Therefore, when comparing the substituents we used in the aromatic ring ($OCH_3$, $NO_2$, $N(CH_3)_2$ and $NH_2$), it is possible to state that the dimethylamino group of ligand **1C** was capable of donating more electronic density compared to the other ligands; with this, the nitrogen electron pair of the imine functional group became more available for coordination with copper. The dimethylamino group is a better donor group since methyl groups donate electronic density to nitrogen by induction, and the nitrogen atom uses its electron pair to conjugate with the aromatic ring [45–47]. Therefore, ligand **1C** was selected for further studies.

### *3.3. Effect of pH and selectivity*

The pH plays a significant role in the formation of metal complexes and the selectivity of the reactions, since it determines the nature of the ions present in the matrix. To evaluate the reaction selectivity as a function of pH, different metal ions

that could possibly interfere with determinations of copper in real samples were treated with synthesized ligand **1C** with solution pH values varied from 4.0 – 10.0. The reaction times was fixed at 10 minutes.

In this study, the effect of pH on complexation was observed, and simultaneously, the pH was affected by the interferents that may be contained in the drink. Thus, as shown in **Fig. 4**, the pH at which the reaction showed the highest analytical response was 10.0. However, with increasing pH, the other metals also showed increases in analytical response and, consequently, increased ability to complex with the ligand. This effect was more pronounced for nickel, at for pH 10.0 supported effective complexation. This occurred because at basic pH, the ligand binding sites were deprotonated and therefore more susceptible to formation of complexes. At pH values lower than 4.0, the Cu2+/**1C** complex did form with high efficiency, probably because of the competition between protons $H^+$ and $Cu^{2+}$ for the active site of the ligand. In addition, even at acidic pH, the analytical signal remained high, demonstrating that $Cu^{2+}$/**1C** complexation was strongly favored. Therefore, pH 4 was found to be optimal and was selected for the following experiments.

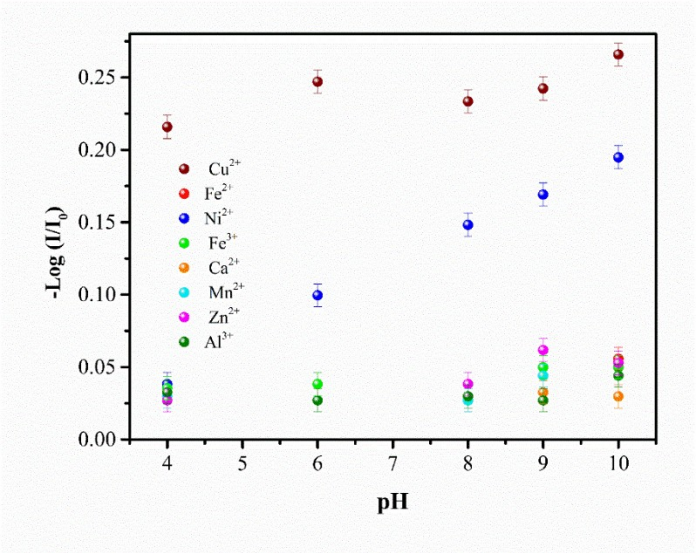


**Fig. 4.** Effect of pH and reaction selectivity**.**

*3.4. Effect of ligand concentration*

The effect of ligand concentration was also studied over the ligand concentration range 0.05 to 0.5 mmol $L^{-1}$. At a concentration of 0.38 mmol, the

analytical response was maximal and therefore this ligand concentration was chosen for further studies (**Fig. S25**). At lower concentrations, complexation was less effective, and at higher concentrations, there was a decline in the analytical signal due to the immediate precipitation of the complex, which was observed when excess ligand was present. In this study, the solution was maintained at pH 4, and the reaction time was 10 minutes.

*3.5. Effect of reaction time on $Cu^{2+}$/1C complex formation*

An optimal reaction time for formation of the complex is necessary to complete the reaction and achieve a strong analytical signal. The reaction kinetics of $Cu^{2+}$ ions with ligand **1C** were evaluated over a time range of 1-20 minutes. The analytical signal increased for the first 5 minutes and was stable for up to 12 minutes of reaction, as shown in **Fig. S26**. After this time, there was a decrease in the analytical signal, probably due to the low stability of the generated complex. For this reason, we selected a minimum time that showed good complex stability. Thus, a reaction time of 5 minutes was shown to be appropriate, and it was selected for further experiments. In this experiment, the pH of the solution was maintained at 4, and the concentration of the ligand was fixed at 0.38 mmol.

*3.6. Determination of the stoichiometric ratio of the $Cu^{2+}$/1C reaction*

The continuous variation method, also known as the Job method, is the technique most commonly used to determine the stoichiometric ratio due to its simplicity [48]. Thus, this method was used to obtain the stoichiometric relationship of the Cu2+/**1C** complex. In this study, 3 mmol solutions of the metal and the ligand were used and tested with different metal/ligand ratios. The Job curve was constructed by plotting the results obtained for the analytical signal based on the equilibrium concentration of $Cu^{2+}{}_{\alpha}$/**1C**$_{\beta}$ against the molar fraction of **1C**. The α/β value was obtained from the abscissa of the maximum point of the Job curve.

**Fig. 5** illustrates the Job diagram for the Cu2+$_{\alpha}$/1C$_{\beta}$ reaction. The largest analytical signal was observed when the molar fraction of the ligand was equivalent to 0.5. When the free ligand mole fraction value was used in a calculation with the equation $X_{1C}$ = n/(n+1), the number of moles (n) was seen to equal 1. In this way, it

could be concluded from the Job method that the stoichiometric ratio of the $Cu^{2+}$/**1C** reaction is 1:1.

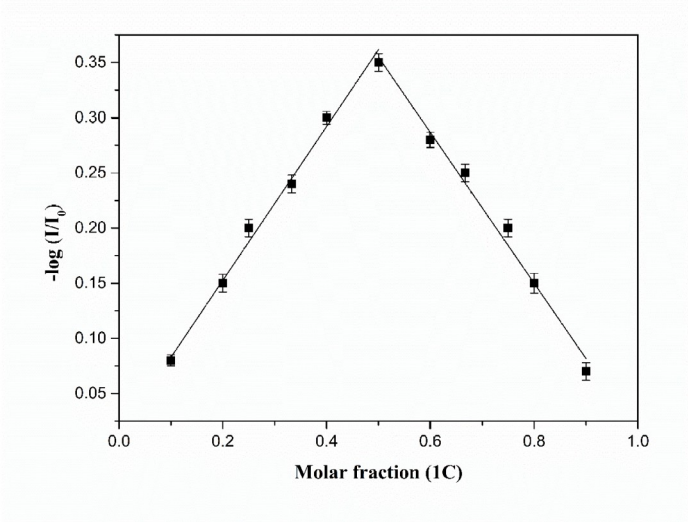


**Fig. 5.** Job`s Method to determine the stoichiometric relationship of the $Cu^{2+}$ with ligand **1C** reaction.

*3.7. Proposal for the structure of the $Cu^{2+}$/1C complex*

The architecture of the $Cu^{2+}$/**1C** complex was proposed from the analysis of UV, IR, $^1$H NMR data (**Fig. S27 – Fig. S29**) and stoichiometry (Job plot) for the complex. The proposed structure is shown in **Fig. 6**, in which the nitrogen groups of the $NH_2$ and N=CH groups coordinate with $Cu^{2+}$, forming a six-membered ring. A similar structural proposal was offered by Magdy and coworkers in 2010 [49].

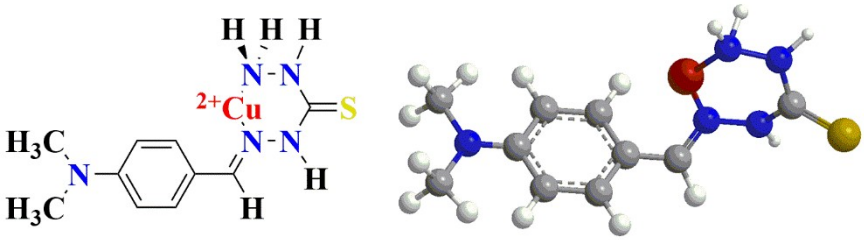


**Fig. 6**. Proposed structure for the $Cu^{2+}$/**1C** complex.

The uv-vis spectrum of ligand **1C** contained a high-intensity band with a maximum absorption wavelength of 359 nm. After complexation with $Cu^{2+}$, the absorption maximum of this band was shifted to 387 nm (**Fig. S27**), indicating a bathochromic displacement. This change occurred as a result of coordination of two nitrogen atoms ($NH_2$ and N=CH) to $Cu^{2+}$.

When comparing the infrared spectrum of thiocarbazone **1C** with that of its respective copper complex ($Cu^{2+}$/**1C**) (**Fig. S28**), it was possible to observe a change in the frequencies of N-H, $NH_2$, and C=N vibrations (**Table 1**). There were no changes in stretching frequencies for vibrations NH (NH), N-N and C=S bonds, which exhibited the same values for the free ligand and the complex.

**Table 1**. Infrared bands characteristic of ligand **1C** and its coordination compound $Cu^{2+}$/**1C** (400 – 4000 $cm^{-1}$).

| Compound | $\bar{\nu}_{max}$ ($cm^{-1}$) | | | | |
|---|---|---|---|---|---|
| | N-H ($NH_2$) | N-H (NH) | C=N | N-N | C=S |
| **1C** | 3386 | 3146 | 1590 | 1168 | 806 |
| $Cu^{2+}$/**1C** | 3379 | 3146 | 1572 | 1168 | 808 |

To carry out $^1$H NMR and COSY NMR analyses, 5.0 mg (21 µmol) of ligand **1C** and 15.8 mg (63 µmol) of $CuSO_4.5H_2O$ were added to 600 µL of DMSO-$d_6$. This sample was analyzed ($^1$H NMR and COSY NMR) at 50 °C, and the spectra shown below were obtained and compared with the spectrum of free thiocarbazone **1C** (**Fig. 7** and **Fig. S29**). By comparing the $^1$H NMR of the free **1C** ligand (**Fig. 7(a)**) with that of the $Cu^{2+}$/**1C** complex (**Fig. 7(b)**), it was possible to observe increases in the chemical shifts of all signals for thiocarbazone after the addition of $Cu^{2+}$. It is important to highlight the changes in the signals for $NH_2$ and HC=N hydrogen resulting from direct coordination of copper to these nitrogen groups, which led to greater electronic deshielding of the hydrogens of these groups. The $NH_2$ signal for the free **1C** ligand (**Fig. 7(a)**) is a singlet found at 4.77 ppm. After the addition of $Cu^{2+}$, this signal was converted to two singlets at 7.23 and 7.06 ppm (**Fig. 7(b)**), which can be explained by the formation of a six-membered ring that generates different chemical environments for each of the $NH_2$ hydrogens and makes them nonequivalent. The HC=N signal in ligand **1C** was a singlet at 7.87, and after adding $Cu^{2+}$, it became a multiplet at 8.75–8.38. It is also possible to observe changes in the signals for the four aromatic hydrogens; in the free thiocarbazone **1C** there are two doublets (at 7.59 (H9 and H11) and 6.67 (H8 and H12) ppm), and in the $Cu^{2+}$/**1C** complex there are two doublets (at 7.91 (H8) and 6.86 (H9) ppm) and two multiplets (at 7.72–7.60 (H12) and 6.80–6.73 (H11) ppm), which were assigned with the help of COSY NMR (**Fig.**

**S29**). This multiplicities of the signals can be explained by the alteration of the chemical environment of the aromatic ring after the formation of the six-membered ring. The signals for the six hydrogens of the methyls (H14 and H15) also changed after the addition of $Cu^{2+}$; **1C** displayed a singlet at 2.94 ppm and the spectrum of the $Cu^{2+}$/**1C** complex contained two singlets at 3.10 and 3.01 ppm.

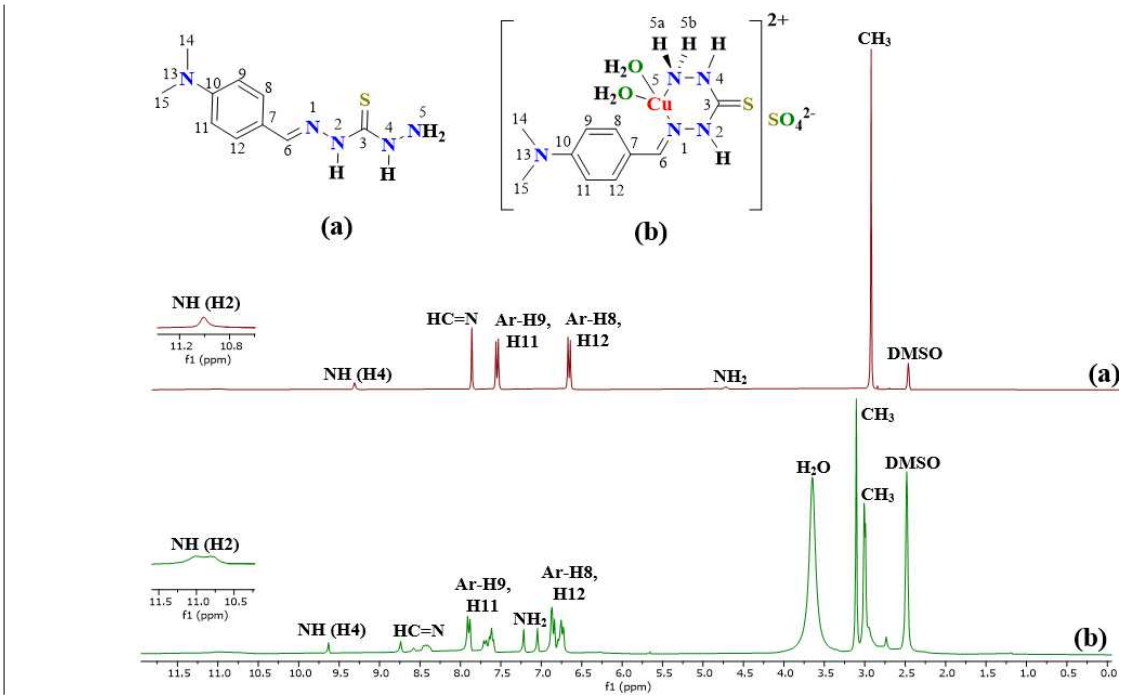


**Fig. 7.** $^1$H NMR spectrum (300 MHz; DMSO; $\delta_{DMSO}$ = 2.49) **a) 1C** free and **b)** $Cu^{2+}$/**1C** complex.

*3.8. Analytical performance*

An analytical curve was constructed for $Cu^{2+}$ concentrations in the range 0.25-6.75 mg $L^{-1}$, and the linear range of the developed method was verified by analysis of the calibration curve using the least squares methods (LSM) for the RGB channels. As seen in Fig. 8, channel B showed higher analytical sensitivity than the other channels, which can be explained by the fact that absorption of incident radiation occurred mainly for the complementary color. Since the complex is yellow, high sensitivity was observed in the B channel. Table S1 presents the analytical parameters obtained in the construction of the curves for all channels. The B channel was used in the calibration, and the following calibration regression was obtained: $-\log (I/I_0) = -0.0011 + 0.0427 \times [Cu^{2+}]$, where $[Cu^{2+}]$ is expressed in mg $L^{-1}$ ($n$=5). The

calculated calibration curve showed a high level of linearity and a determination coefficient ($R^2$) of 0.998.

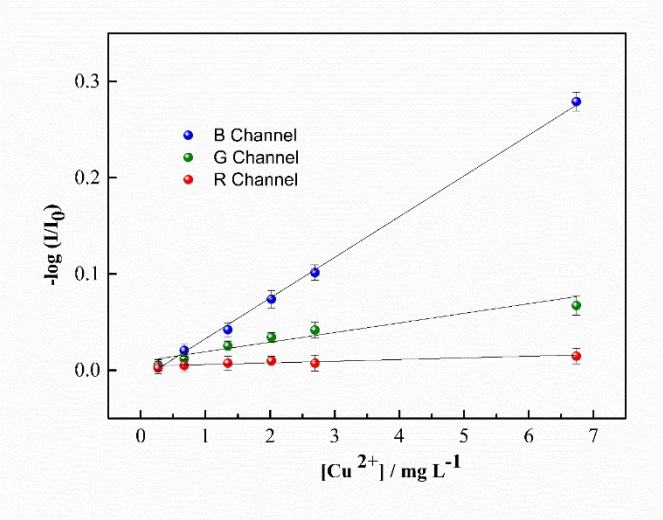


**Fig. 8.** Analytical curve for $Cu^{2+}$ determination in distilled beverages spirits.

The limits of detection (LODs) and quantification (LOQs) were calculated using the quantities 3 ×σ/m and 10 ×σ/m, respectively, where σ is the standard deviation the blank analytical curve and m is the slope of the analytical curve. Thus, the LOD and LOQ were 0.18 mg $L^{-1}$ and 0.62 mg $L^{-1}$, respectively. In addition, the developed method showed reliable precision with an RSD of 3.2% for a $Cu^{2+}$ solution of 5 mg $L^{-1}$ (*n* =10), while a 4.5% RSD was obtained over a period of seven days (interday precision, *n*=10). These results indicated good precision of the proposed method, which proves it value for the determination of $Cu^{2+}$ in distilled beverages.

The influence of coexisting ions on the determination of $Cu^{2+}$ in distilled beverage spirits was investigated under the optimized conditions and according to the recommended procedure. The tolerance limit of a competitor ion is defined as the largest amount causing a variation of less than ± 5% in the determination of $Cu^{2+}$. Some metallic ions that could be present in beverages and could compete with $Cu^{2+}$ for complexation with **1C** were investigated, as was previously described [50].

As shown in **Table 2**, the analyzed metallic ions did not act as interferents in the determination of $Cu^{2+}$ in distilled beverages with the proposed method. Moreover, only $Ni^{2+}$ showed significant interference for a 1:10 ratio of analyte/interferent; it is rarely found in distilled beverages, and when present, it is at a lower concentration than $Cu^{2+}$. The effect of a species was considered interference when the signals in

the presence of the species differed by more than 5% from those obtained in the absence of the foreign ion.

**Table 2**. Selectivity study for the determination of $Cu^{2+}$ in distilled beverages. (*n=3*).

| Interferent | Ratio $Cu^{2+}$: Interferent | Relative error (%) |
|---|---|---|
| $Fe^{3+}$ | 1:1 | -0.20 |
| | 1:10 | -1.19 |
| $Ca^{2+}$ | 1:1 | -1.19 |
| | 1:10 | -1.98 |
| $Mn^{2+}$ | 1:1 | +0.38 |
| | 1:10 | -0.39 |
| $Fe^{2+}$ | 1:1 | -0.45 |
| | 1:10 | +0.32 |
| $Zn^{2+}$ | 1:1 | -0.78 |
| | 1:10 | +0.37 |
| $Al^{3+}$ | 1;1 | +0.79 |
| | 1:10 | -1.19 |
| [a]$Ni^{2+}$ | 1:1 | +2.77 |
| | 1:10 | +9.92 |

[a]Ratio 1:10 showed an intense interference.

Pessoa and collaborators proposed a method based on digital image analysis to determine $Cu^{2+}$ in Brazilian sugar cane spirits, and they used cuprizone as a complexing agent [39]. The results obtained by that group indicated that all metals tested were possible interferents, with the exception of $Zn^{2+}$, which showed significant interference. In addition, $Ni^{2+}$ with concentrations 10 times lower than that of the analyte already presented an interference level greater than 12%. Thus, the complexing agent synthesized in this work showed higher selectivity for $Cu^{2+}$, and the method serves as a new alternative for determining the metal content in distilled beverages.

Recovery studies were run for samples of sugar cane spirits (S), whiskeys (W) and tequilas (T) at two concentration levels: 1.50 and 3.00 mg $L^{-1}$. The resulting recoveries for $Cu^{2+}$ were reasonable and ranged from 87.3–109.3%. These results were compared with the values described in the Official Methods of Analysis - AOAC

[51], which recommends a recovery percentage between 80 and 110% for concentration levels of 0.1 mg $L^{-1}$ to 10 mg $L^{-1}$.

The $Cu^{2+}$ levels in the distilled beverage samples were determined using the proposed method and a reference method (Flame Atomic Absorption Spectrophotometry). The results are summarized in the **Table 3**.

**Table 3**. Analysis of distilled beverages using the proposed method and the reference method, as well as a recovery study for the analyzed beverages.

| Samples | Proposed method / mg $L^{-1}$ | Reference method / mg $L^{-1}$ | R.E./ % | Added / mg $L^{-1}$ | Found / mg $L^{-1}$ | Recovery/ % |
|---|---|---|---|---|---|---|
| S1 | 3.92 ± 0.15 | 4.35 ± 0.05 | -9.78 | 1.5 | 5.55 ± 0.12 | 108.7 |
| | | | | 3.0 | 6.98 ± 0.14 | 102.0 |
| S2 | 2.77 ± 0.05 | 2.54 ± 0.04 | 9.24 | 1.5 | 4.23 ± 0.08 | 97.3 |
| | | | | 3.0 | 5.74± 0.09 | 99.0 |
| S3 | 0.68 ± 0.04 | 0.74 ± 0.02 | -4.23 | 1.5 | 2.25 ± 0.04 | 108.0 |
| | | | | 3.0 | 3.87 ± 0.09 | 108.0 |
| S4 | 0.94 ± 0.08 | 1.01 ± 0.02 | -6.28 | 1.5 | 2.34 ± 0.04 | 93.3 |
| | | | | 3.0 | 4.02 ± 0.08 | 102.6 |
| S5 | 0.94 ± 0.07 | 0.95 ± 0.02 | -0.37 | 1.5 | 2.25 ± 0.05 | 87.3 |
| | | | | 3.0 | 3.98 ± 0.11 | 101.3 |
| S6 | 0.90 ± 0.07 | 0.81 ± 0.06 | 11.98 | 1.5 | 2.29 ± 0.04 | 92.6 |
| | | | | 3.0 | 3.90 ± 0.06 | 100.0 |
| W1 | 1.40 ± 0.07 | 1.30 ± 0.05 | 7.69 | 1.5 | 3.00 ± 0.07 | 106.6 |
| | | | | 3.0 | 4.25 ± 0.07 | 95.0 |
| W2 | <LD | 0.01 | - | 1.5 | 1.52 ± 0.03 | 101.3 |
| | | | | 3.0 | 3.21 ± 0.03 | 107.0 |
| W3 | 0.65 ± 0.03 | 0.62 ± 0.03 | 4.83 | 1.5 | 2.21 ± 0.02 | 104.0 |
| | | | | 3.0 | 3.75 ± 0.03 | 103.3 |
| W4 | 0.68 ± 0.04 | 0.72 ± 0.10 | -5.55 | 1.5 | 2.32 ± 0.05 | 109.3 |
| | | | | 3.0 | 3.87 ± 0.05 | 106.3 |
| T1 | 0.68 ± 0.05 | 0.72 ± 0.04 | -5.55 | 1.5 | 1.45 ± 0.04 | 96.6 |
| | | | | 3.0 | 3.02 ± 0.08 | 100.6 |
| T2 | <LD | 0.01 | - | 1.5 | 1.59 ± 0.07 | 106.0 |

| | | | | | | |
|---|---|---|---|---|---|---|
| | | | | 3.0 | 3.12 ± 0.05 | 104.0 |
| T3 | <LD | <LD | - | 1.5 | 1.38 ± 0.04 | 92.0 |
| | | | | 3.0 | 3.25 ± 0.06 | 108.3 |
| T4 | 0.89 | 0.95 | -6.31 | 1.5 | 2.45 ± 0.05 | 104.0 |
| | | | | 3.0 | 3.75 ± 0.09 | 95.3 |

Mean ± d Standard deviation. Samples: S = sugar cane spirits; W = whiskies; T = tequilas. R.E %= Relative error = ((proposed method - reference method)/ reference method) *100

As seen in **Table 3**, the levels of [$Cu^{2+}$] determined by the proposed method and the reference method are relatively close, indicating the accuracy of the proposed method. The -0.51 t value calculated was lower than the critical t (2.26); therefore, no statistically significant differences in the results were generated by either method at a confidence level of 95%. Of the 14 beverage samples, none presented values above that allowed by Brazilian legislation (5 mg $L^{-1}$). However, samples S1 and S2 would be at odds with European legislation, which is stricter, since it advocates a maximum of 2 mg $L^{-1}$.

*3.9. Comparison with other analytical $Cu^{2+}$sensors*

**Table 4** shows several sensors that have already been reported in the literature for the determination of $Cu^{2+}$ ions in several samples, such as water and wastewater [13,52,53], distilled drinks [39], and biological, environmental, and food samples [14]. Compared to other systems, the proposed method presents a more extensive linear range [13,39,54,55], lower detection limit [54,56] and better relative standard deviation [13,14,39,56]. In addition, the use of a manufactured portable device and a smartphone as an analytical tool for capturing the image immediately with a cell phone application is highlighted. When compared with the work of Pessoa and collaborators [39], the dimensions of the apparatus used for acquiring images in our work are smaller, and the method does not require external light sources such as LEDs to capture images. Furthermore, it does not require any sample preparation,

unlike studies involving two-phase liquid-liquid extraction [56] or liquid-liquid microextraction [14], and it presents the highest precision (lowest RSD) among the studies that employ smartphones [13,14,52,56]; this is due to the reduced size of the apparatus and, mainly, to the use of the contained light source. In addition, the present work brings some considerable advantages, such as the limited use of reagents (400 µL per analysis), displaying agreement, therefore, with the precepts of green chemistry. In addition, the method is highly portability since analyses can be done with the smartphone itself and the device for acquisition is the cell box itself. All of these factors make the method a highly promising alternative for analyzing copper in distilled beverages.

**Table 4**. Comparison between the results obtained by the proposed method and other methods used for $Cu^{2+}$ ions determination.

| **Reference** | **Linear Range / (mg $L^{-1}$)** | **Detection limit / (mg $L^{-1}$)** | **Detection method** | **R.S.D./ %** |
|---|---|---|---|---|
| [39] | 0.75 – 5.0 | 0.078 | Digital camera | 5.9 |
| [54] | 0 - 0.64 | 0.32 | Spectrophotometric | - |
| [55] | 0.13- 0.64 | 0.13 | Spectrophotometric | - |
| [52] | 5.0 - 571.9 | 0.08 | Smartphone | 2.5 |
| [53] | 0.006 - 6.00 | 0.001 | Smartphone | 3.0 |
| [56][a] | 3.18 -12.7 | 3.05 | Smartphone | <5 |
| [14][b] | 0.3 - 40 | 0.1 | Smartphone | 4.1–5.3 |
| [13] | 0.25-1.17 | 0.053 | Smartphone | 8.3 |
| **Proposed Method** | 0.25- 6.75 | 0.18 | Smartphone | 3.2 |

[a] demands a sample preparation involving two-phase liquid-liquid extraction;

[b] demands a sample preparation involving and liquid-liquid microextraction.

However, the method has a disadvantage because it requires the synthesis of thiocarbazone, which makes the method more time consuming than would a commercial reagent that could be used immediately.

## Conclusions

The proposed method for determining $Cu^{2+}$ in distilled beverages proved to be accurate, precise, simple, and robust since the smartphone itself can be used as an analytical instrument. In addition, it dispenses with a complex electronic system and LEDs to focus electromagnetic radiation on the samples, and a producer seeking to control beverage quality in the production environment can easily use it.

In addition, the reaction used to determine $Cu^{2+}$ is unprecedented and was shown to be sensitive and selective for metals at acidic pHs. The method generates a low amount of waste (approximately 400 µL), and it only takes 5 minutes to acquire the images, demonstrating the speed of the method. For further studies, it is possible to use paper or thread to immobilize the ligand, thereby generating a test strip for $Cu^{2+}$ determination.

## Acknowledgments

The authors are thankful for the financial support provided by Fundação de Amparo à Pesquisa do Estado de Minas Gerais – Brazil (FAPEMIG), Conselho Nacional de Desenvolvimento Científico e Tecnológico - Brazil (CNPq), and Coordenação de Aperfeiçoamento de Pessoal de Nível Superior - Brasil (CAPES - Finance Code 001). SAF is supported by Research Fellowships from CNPq.

**Supplementary Material**

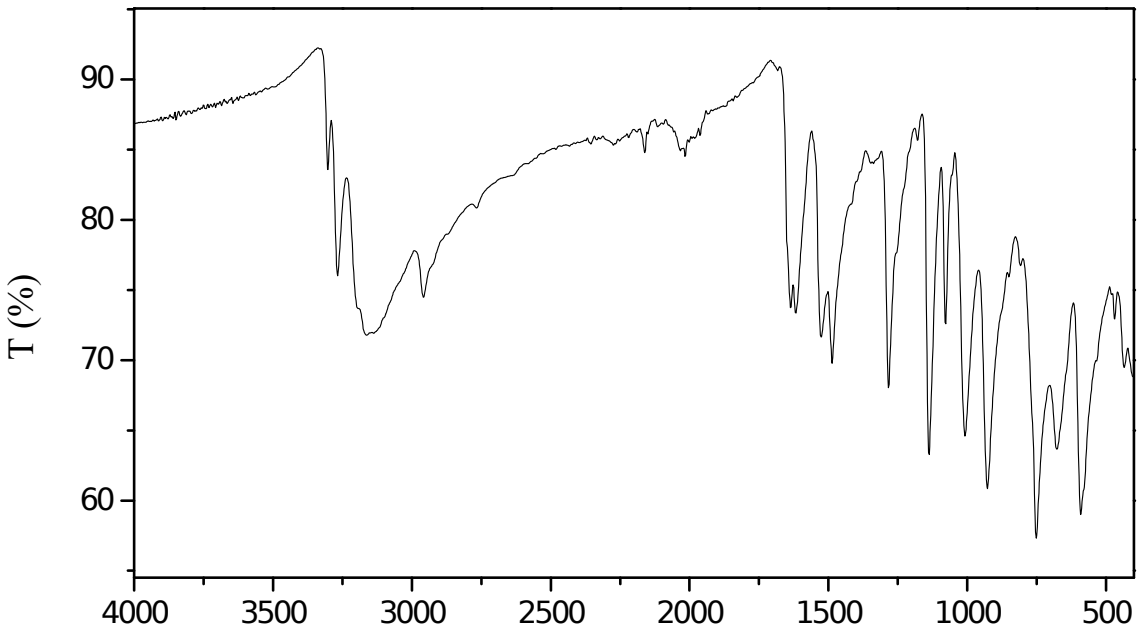


**Fig. S1.** Infrared spectrum of thiocarbohydrazine.

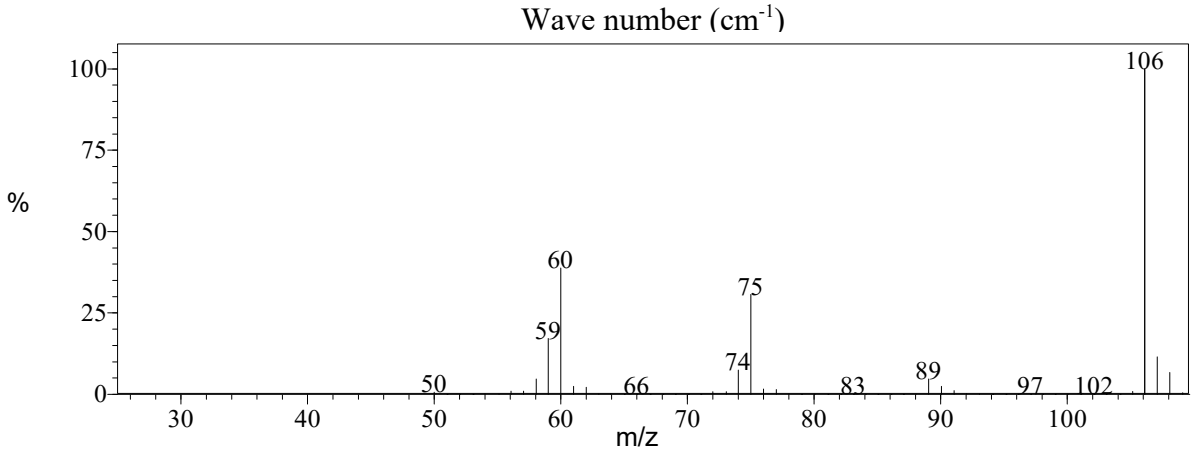


**Fig. S2.** Mass spectrum of thiocarbohydrazine.

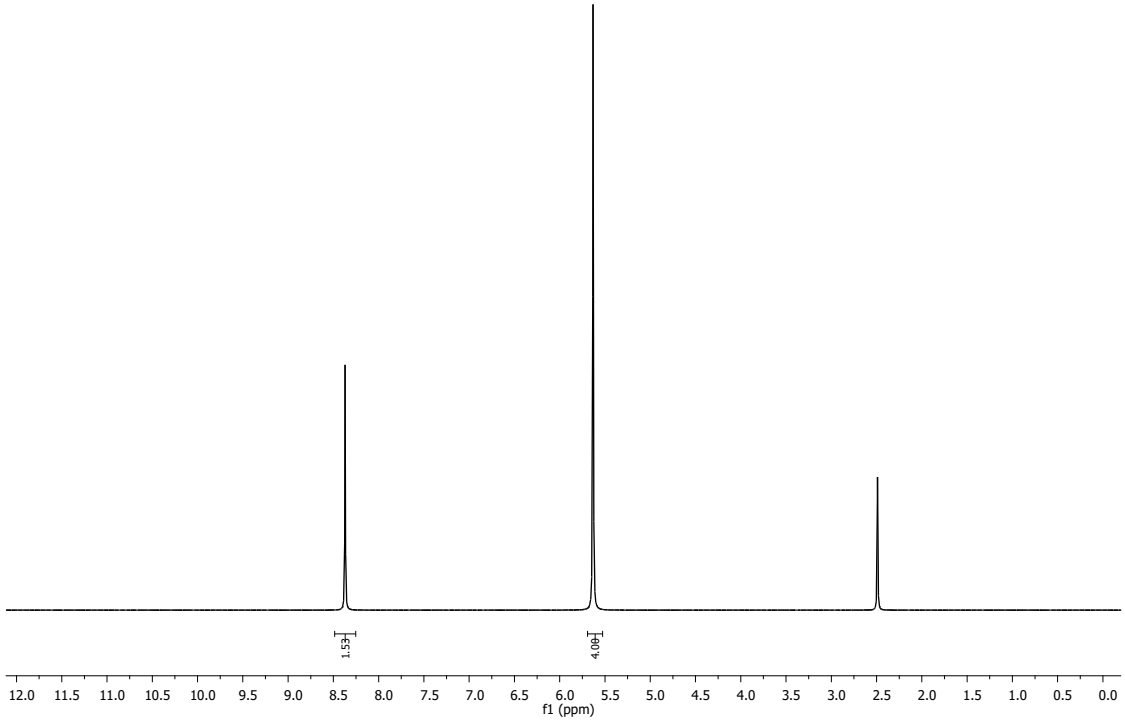


**Fig. S3**. $^{1}$H NMR spectrum of thiocarbohydrazine.

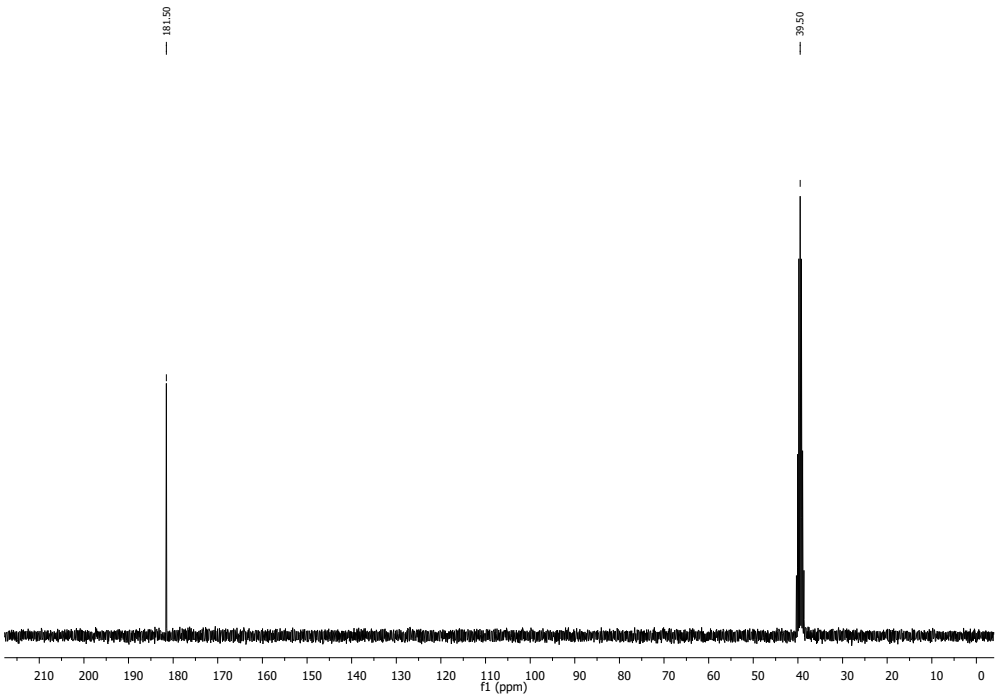


**Fig. S4.** $^{13}$C NMR spectrum of thiocarbohydrazine.

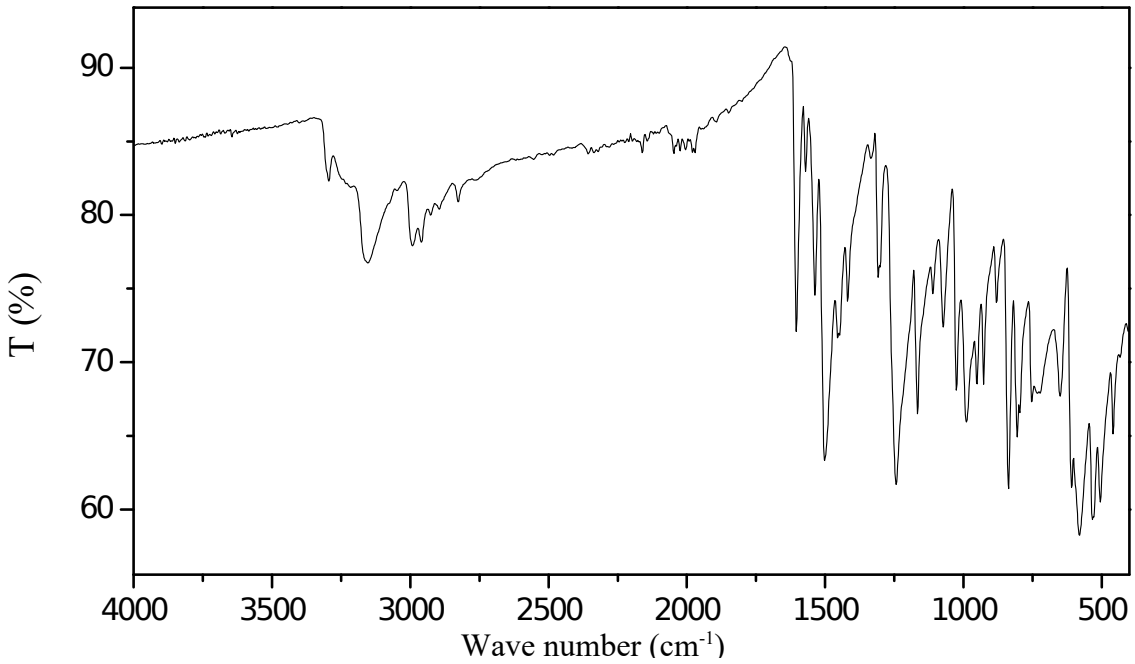


**Fig. S5.** Infrared spectrum of 1-(4-methoxybenzaldehyde)thiocarbazone (**1A**).

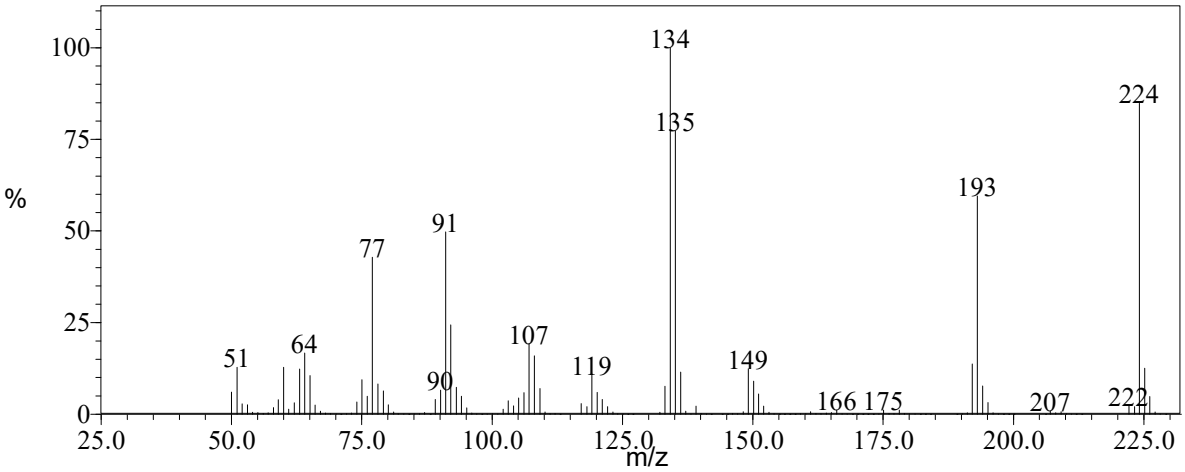


**Fig. S6.** Mass spectrum of 1-(4-methoxybenzaldehyde)thiocarbazone (**1A**).

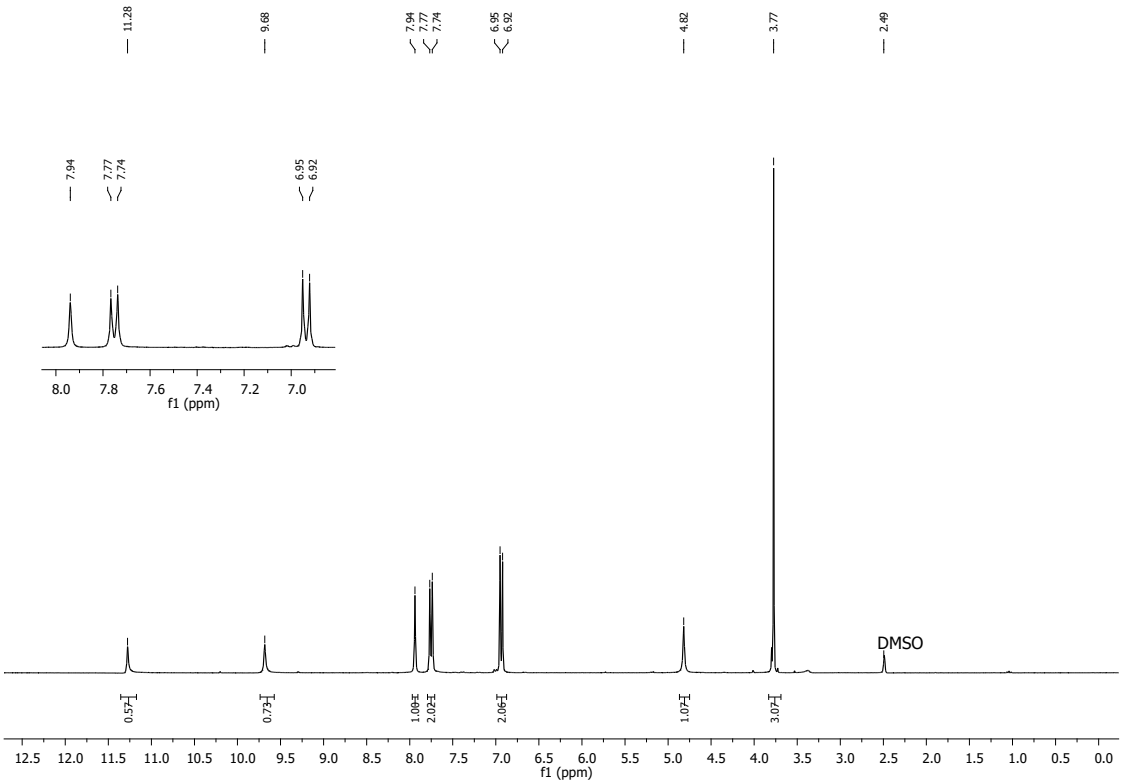


**Fig. S7**. [1]H NMR spectrum of 1-(4-methoxybenzaldehyde)thiocarbazone (**1A**).

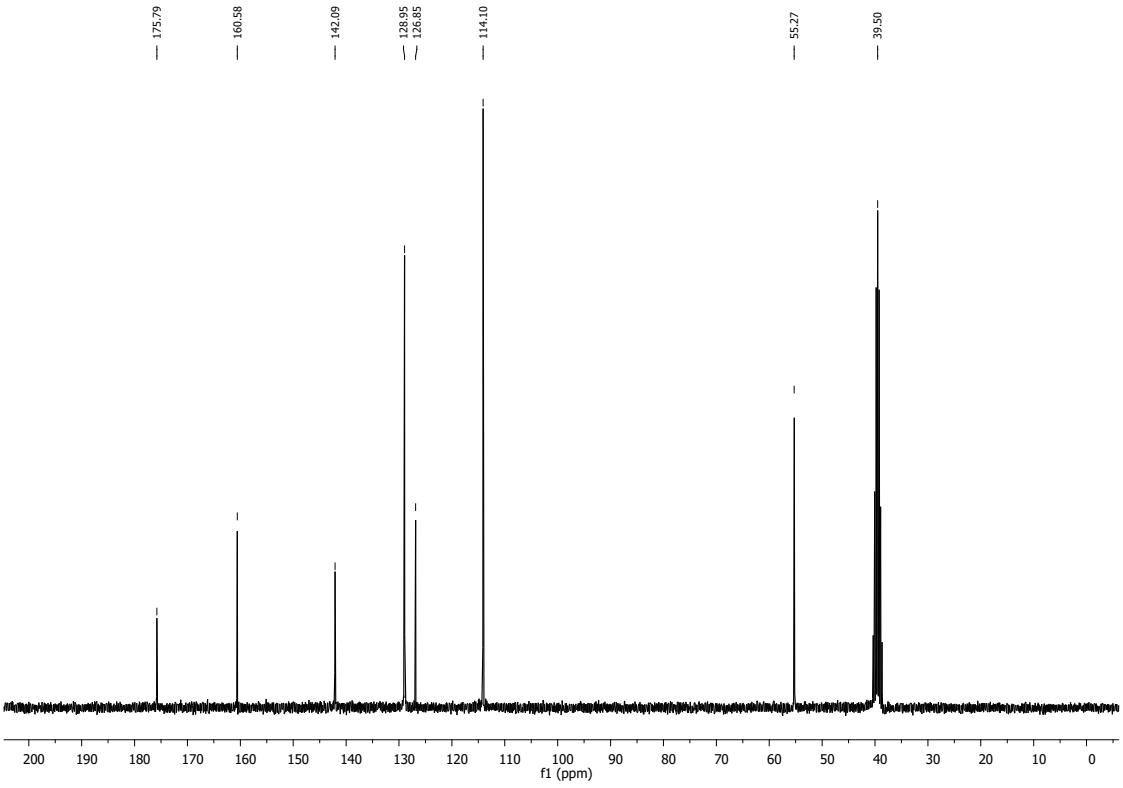


**Fig. S8.** [13]C NMR spectrum of 1-(4-methoxybenzaldehyde)thiocarbazone (**1A**).

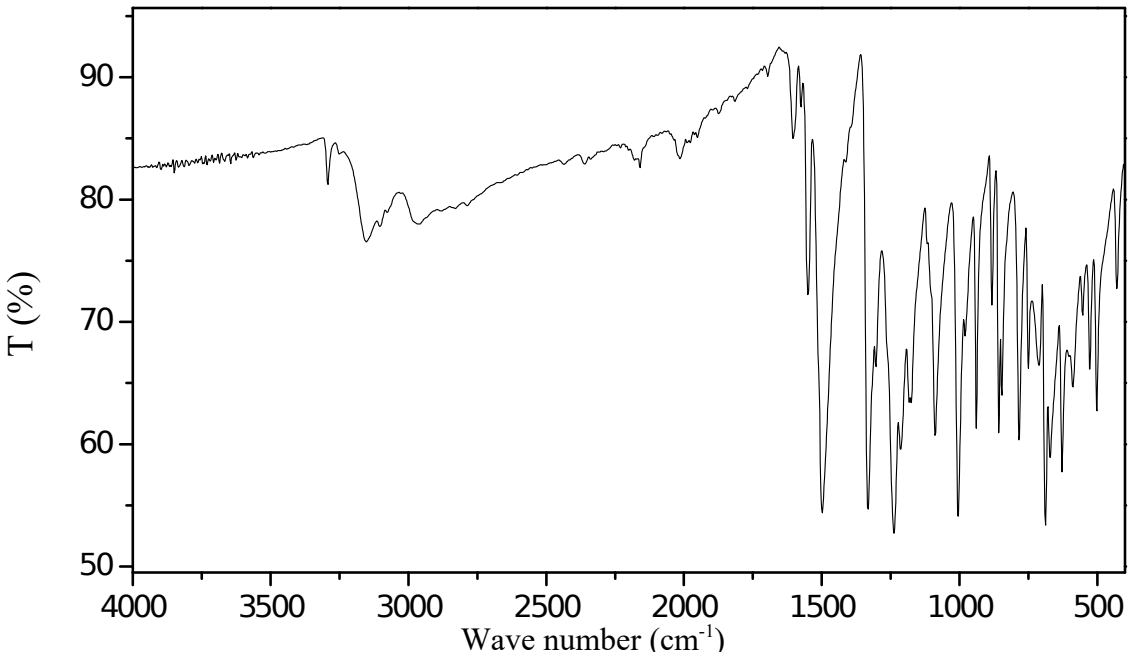


**Fig. S9.** Infrared Spectrum of 1-(4-nitrobenzaldehyde)thiocarbazone (**1B**).

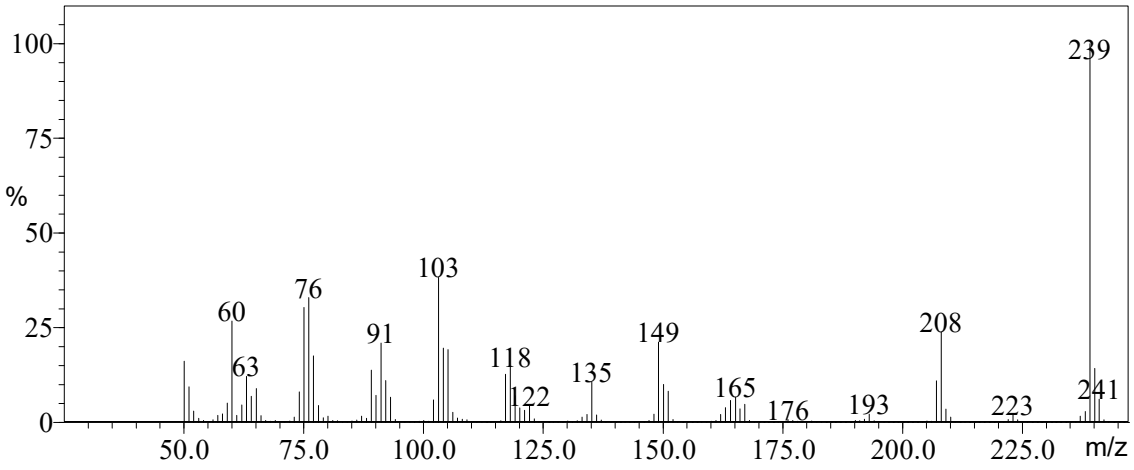


**Fig. S10.** Mass spectrum of 1-(4-nitrobenzaldehyde)thiocarbazone (**1B**).

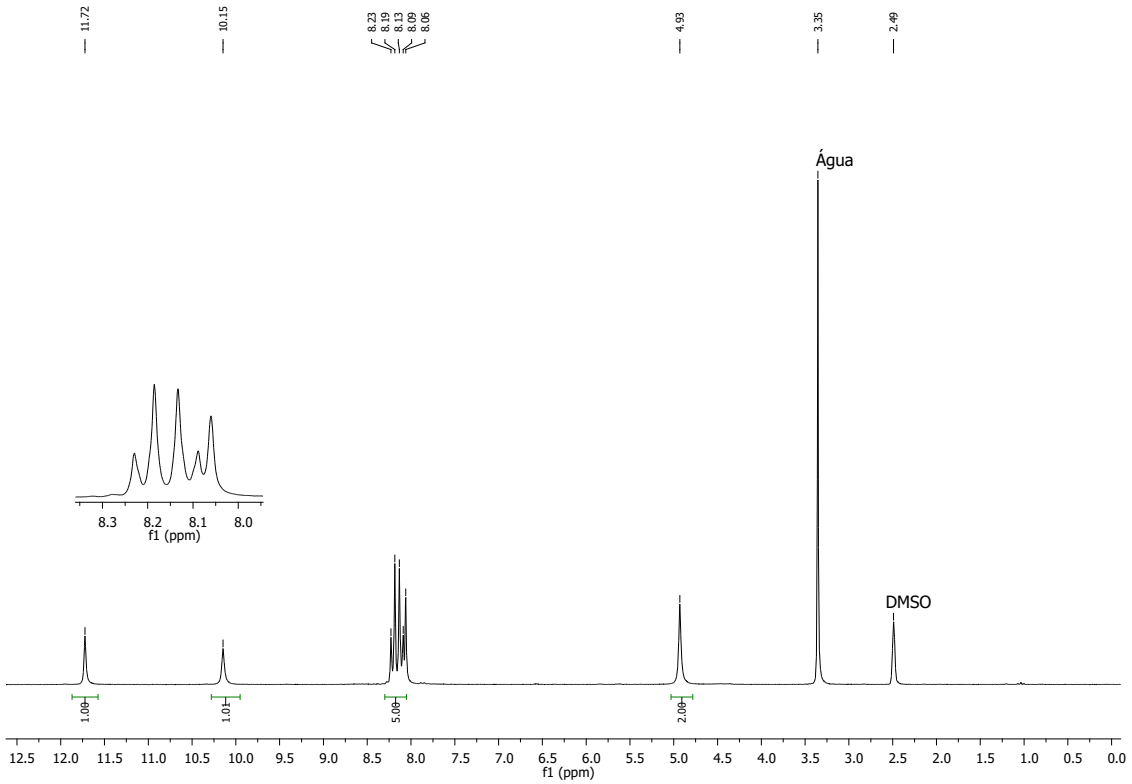


**Fig. S11.** $^{1}$H NMR spectrum of 1-(4-Nitrobenzaldehyde)thiocarbazone (**1B**).

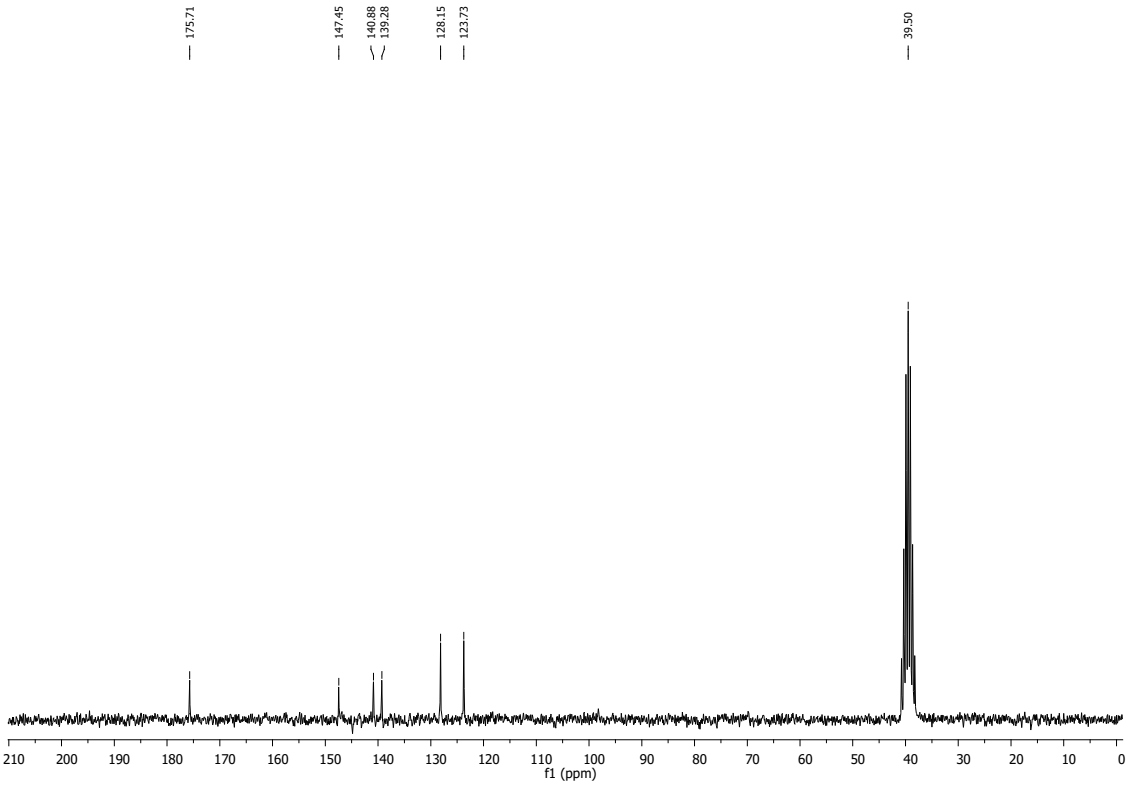


**Fig. S12.** $^{13}$C NMR spectrum of 1-(4-Nitrobenzaldehyde)thiocarbazone (**1B**).

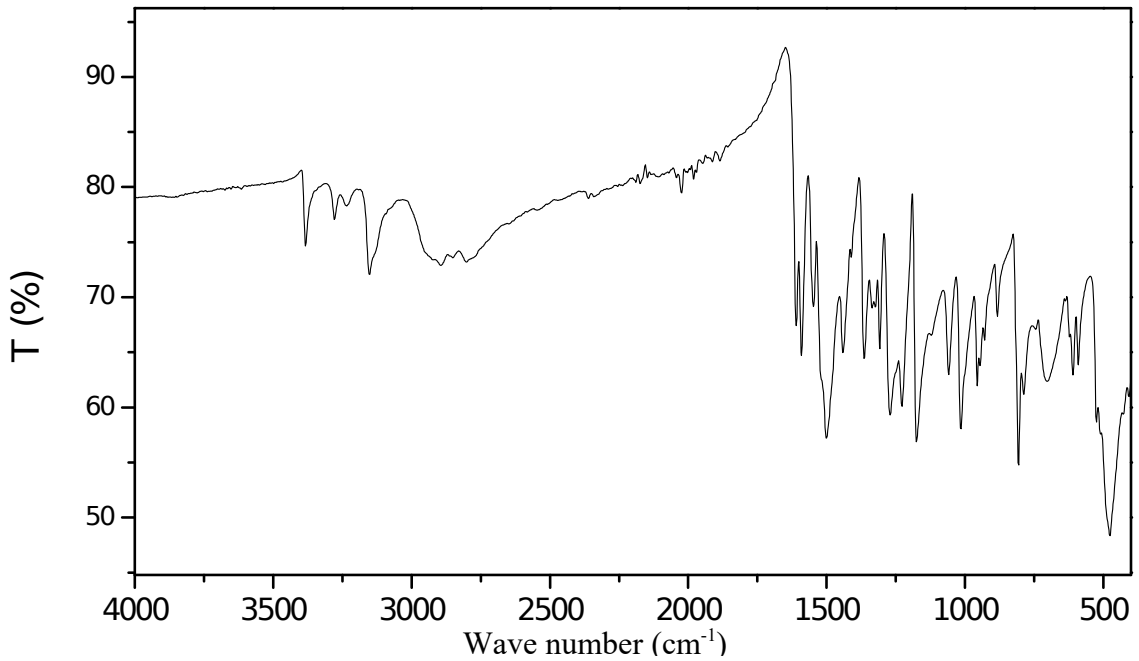


**Fig. S13.** Infrared spectrum of 1-(4-(dimethylamino)benzaldehyde)thiocarbazone (**1C**).

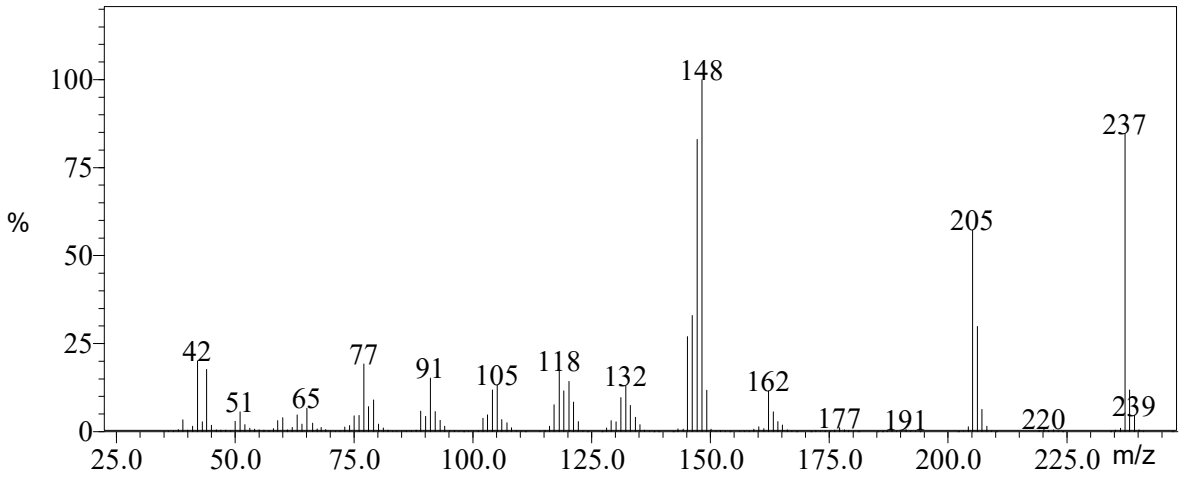


**Fig. S14.** Mass spectrum of 1-(4-(dimethylamino)benzaldehyde)thiocarbazone (**1C**).

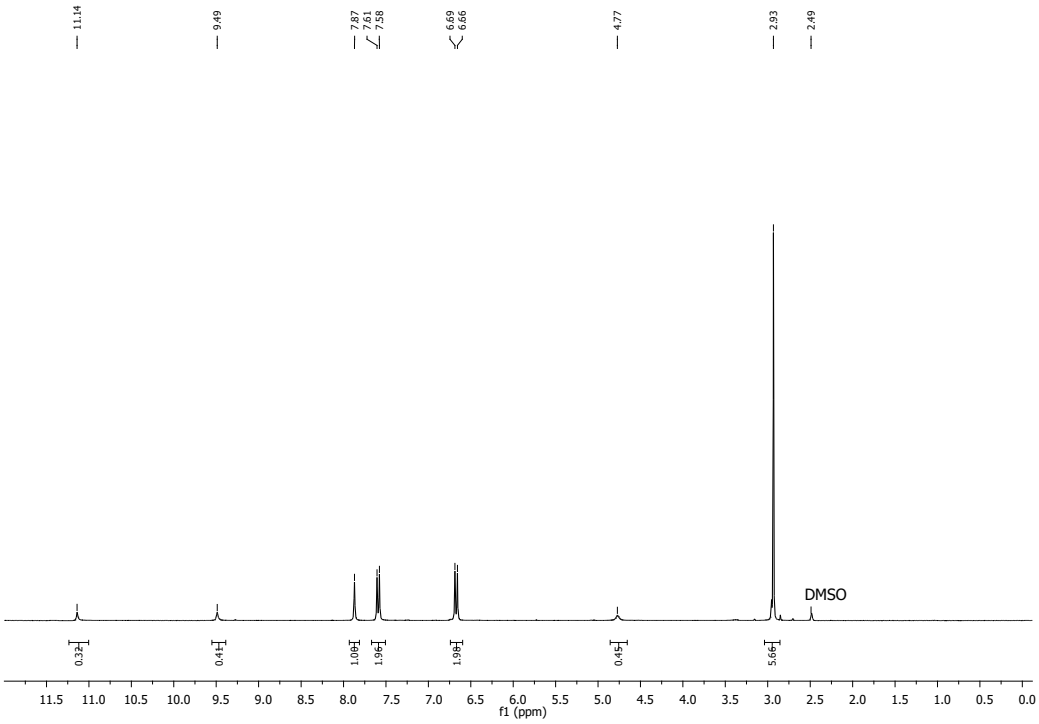


**Fig. S15**. $^{1}$H NMR spectrum of 1-(4-(dimethylamino)benzaldehyde)thiocarbazone (**1C**).

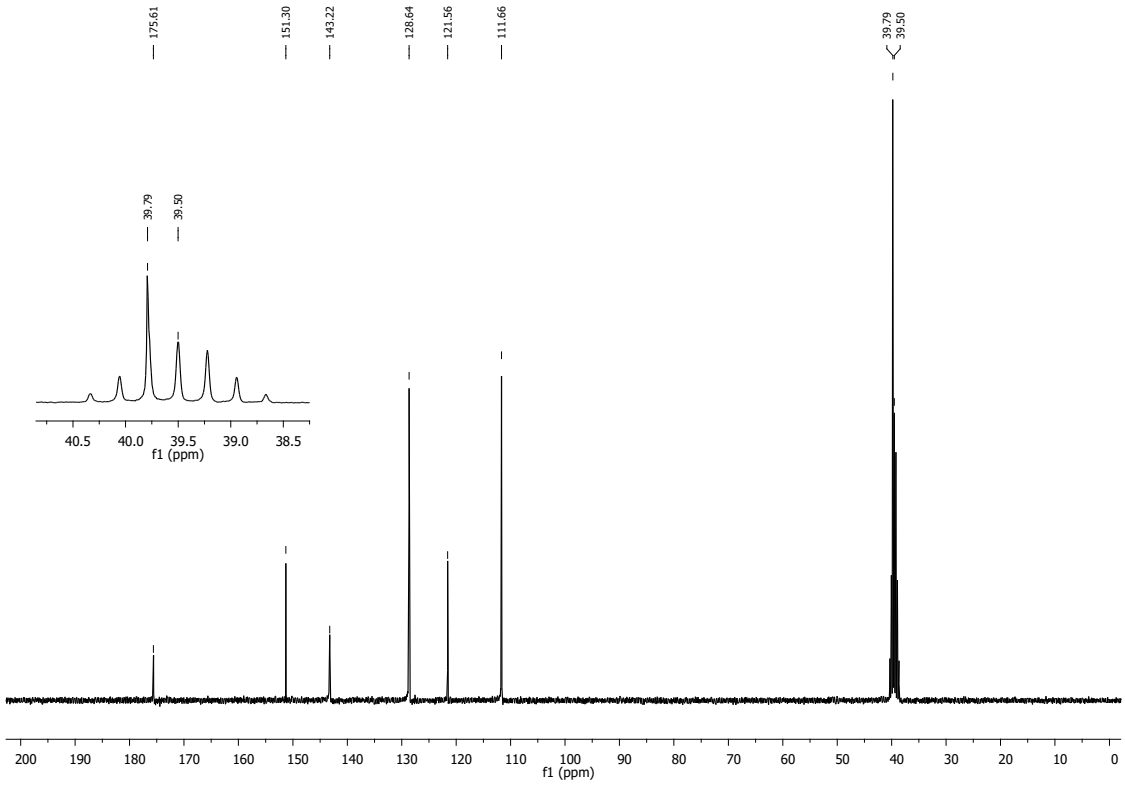


**Fig. S16**. $^{13}$C NMR spectrum of 1-(4-(dimethylamino)benzaldehyde)thiocarbazone (**1C**).

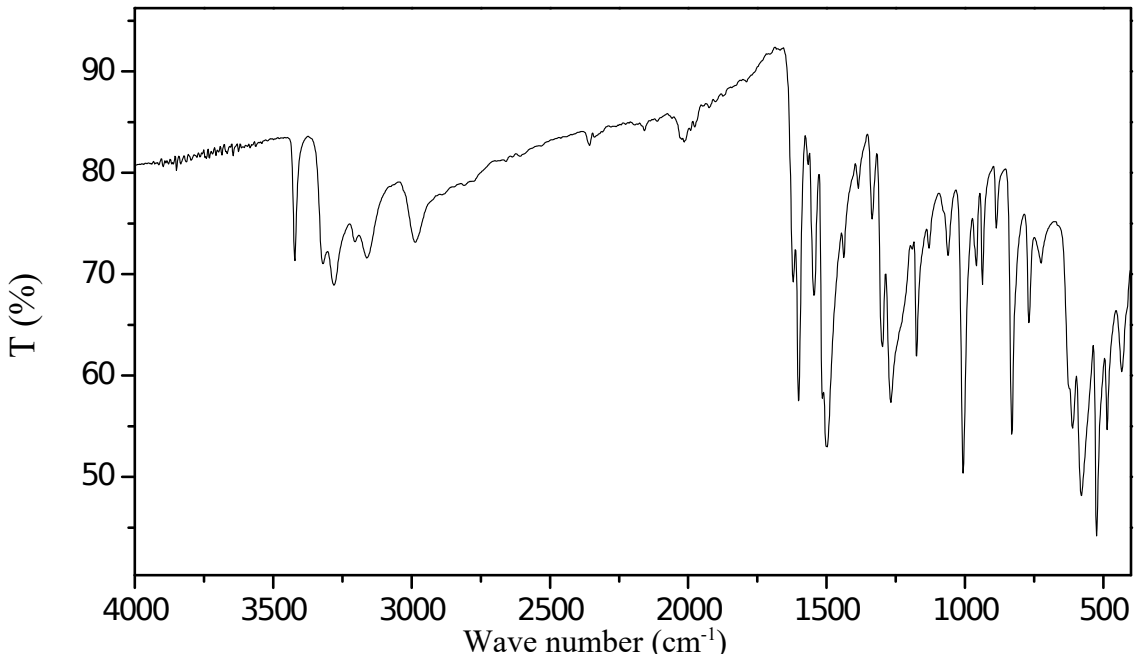


**Fig. S17.** Infrared spectrum of 1-(4-aminobenzaldehyde)thiocarbazone (**1D**).

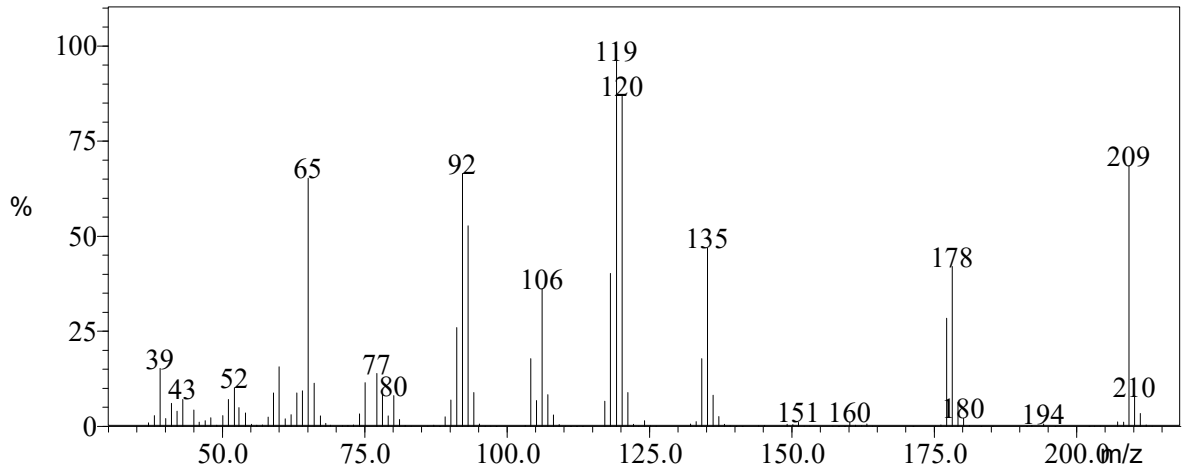


**Fig. S18.** Mass spectrum of 1-(4-aminobenzaldehyde)thiocarbazone (**1D**).

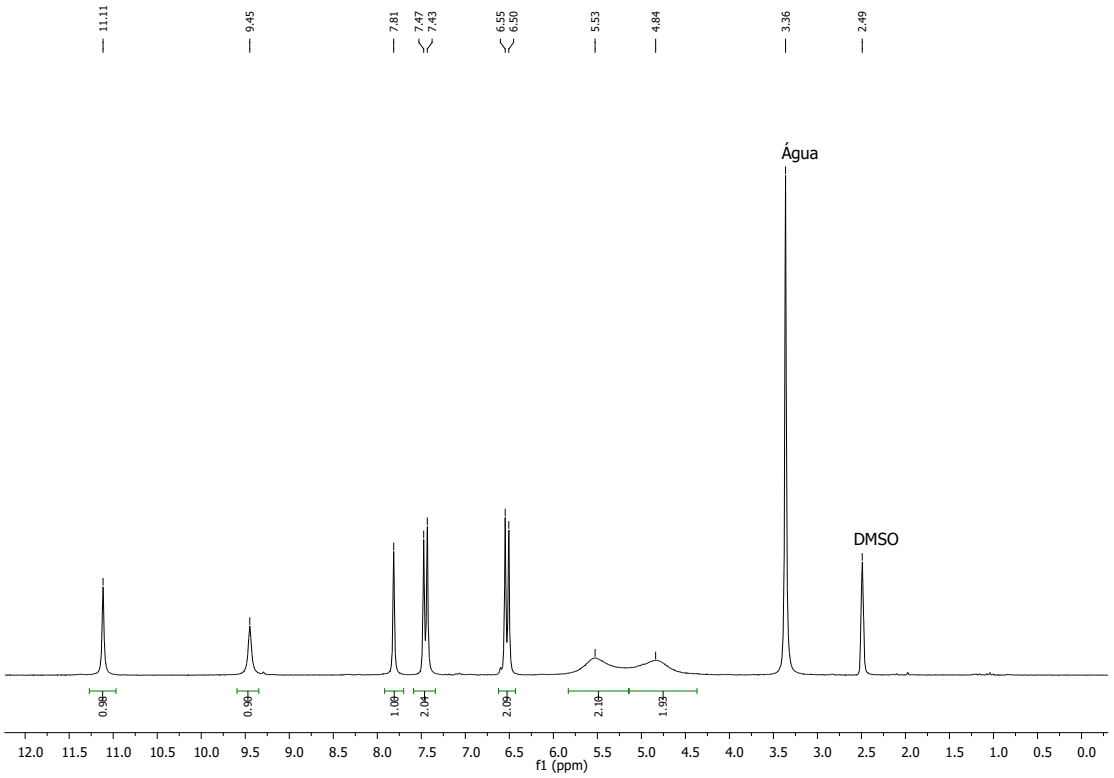


**Fig. S19**. $^{1}$H NMR spectrum of 1-(4-aminobenzaldehyde)thiocarbazone (**1D**).

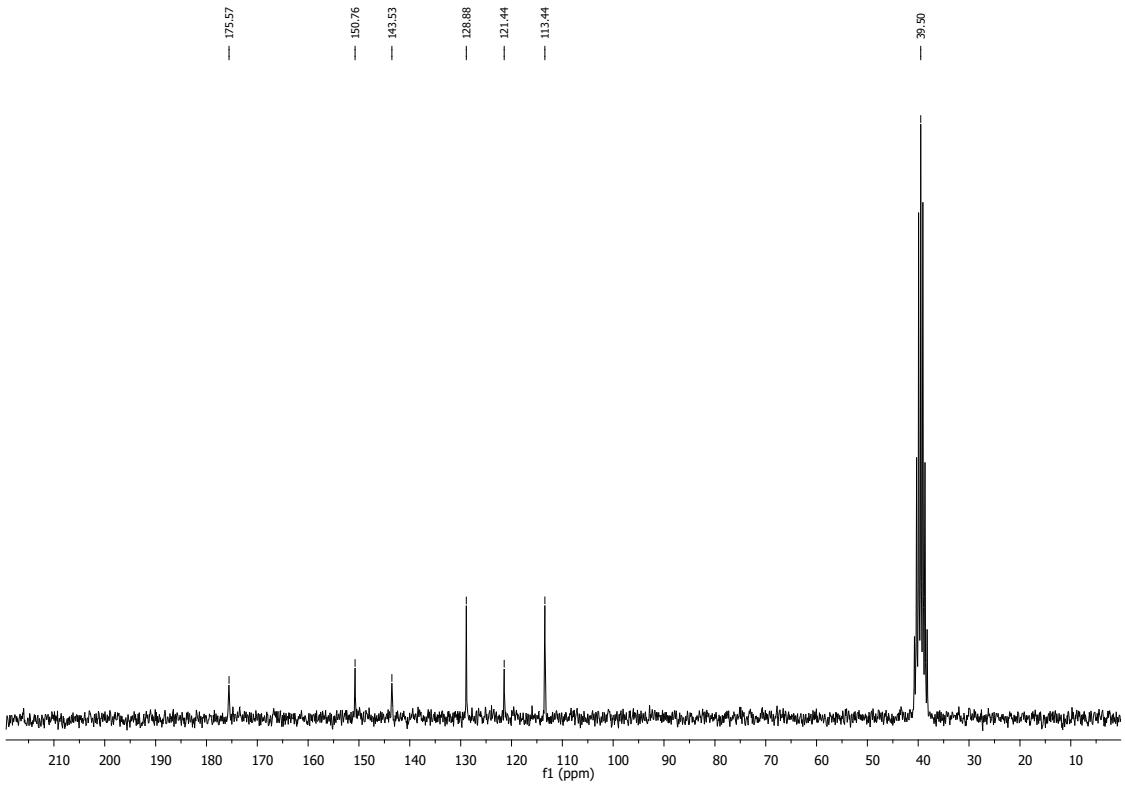


**Fig. S20**. $^{1}$H NMR spectrum of 1-(4-aminobenzaldehyde)thiocarbazone (**1D**).

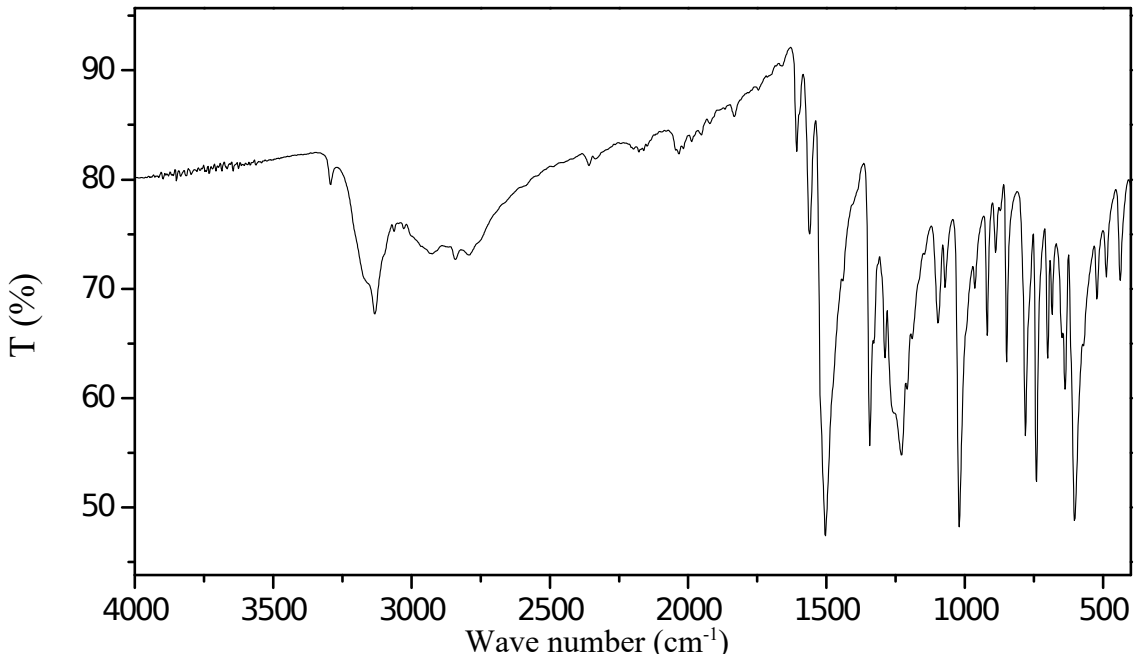


**Fig. S21.** Infrared spectrum of 1-(2-nitrobenzaldehyde)thiocarbazone (**1E**).

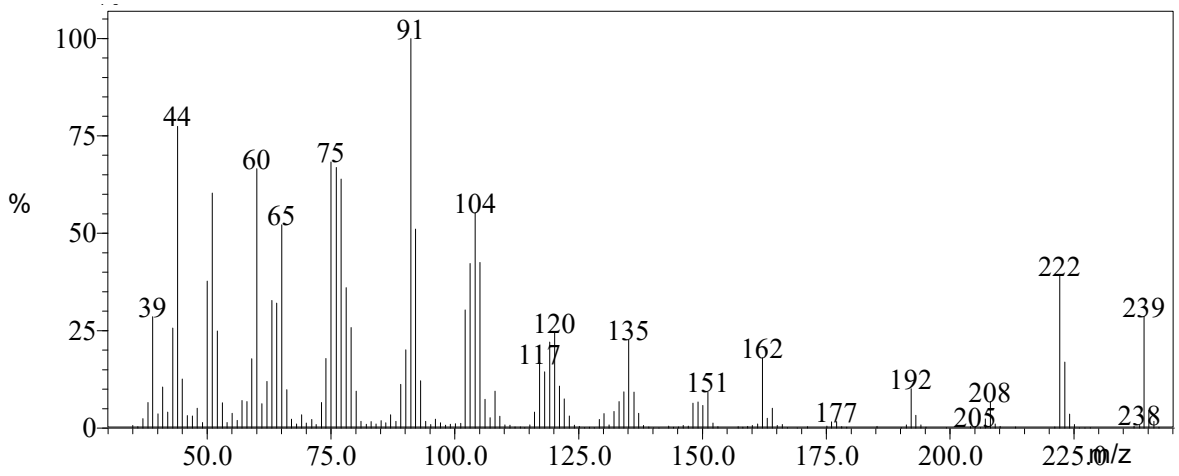


**Fig. S22.** Mass spectrum of 1-(2-nitrobenzaldehyde)thiocarbazone (**1E**).

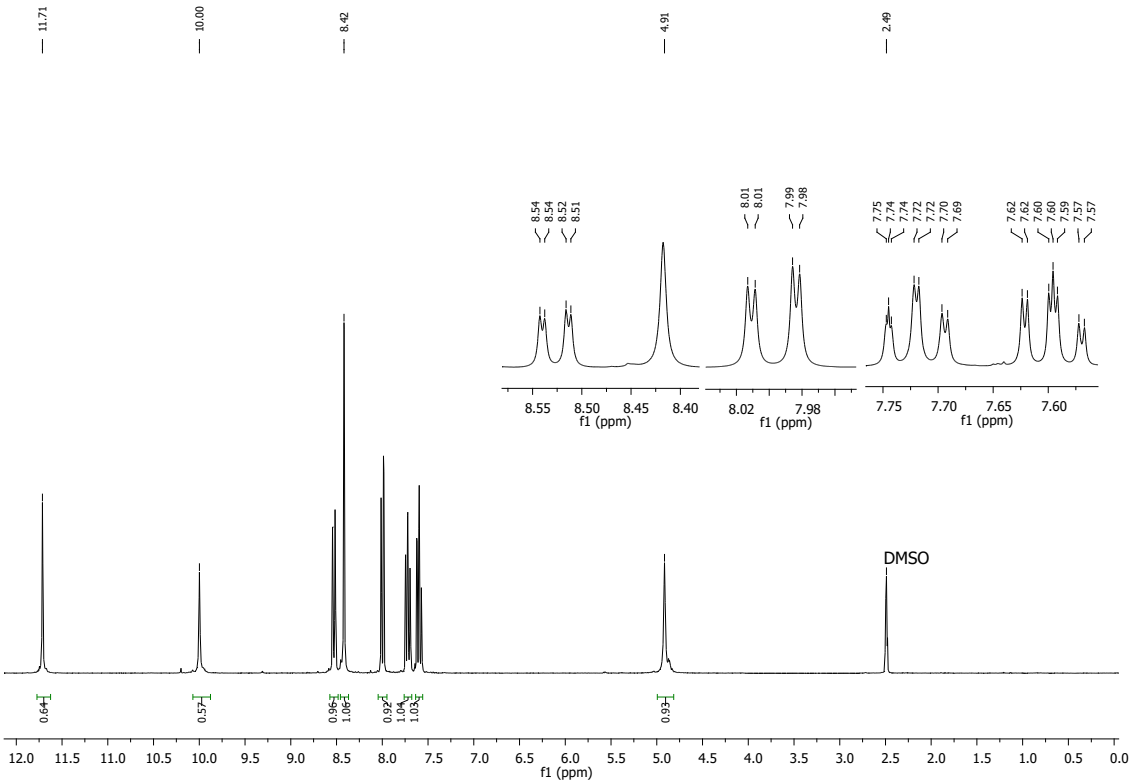


**Fig. S23.** $^{1}$H NMR spectrum of 1-(2-nitrobenzaldehyde)thiocarbazone (**1E**).

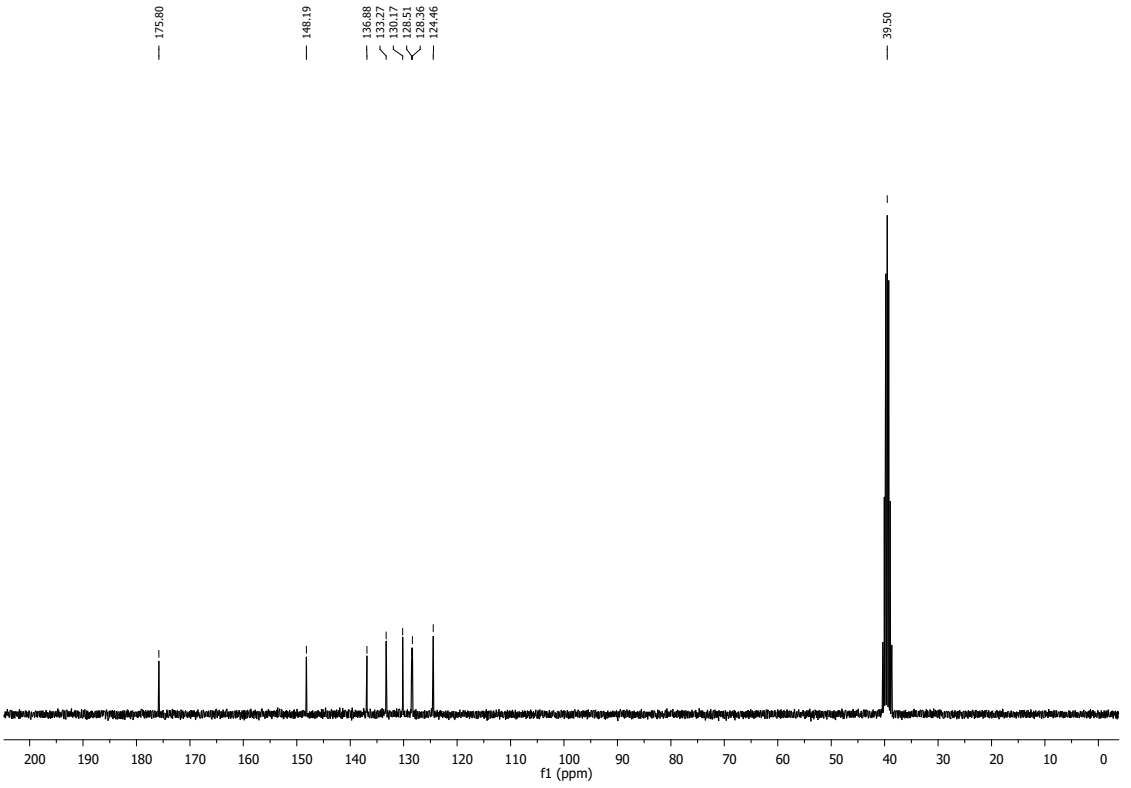


**Fig. S24.** $^{13}$C NMR spectrum of 1-(2-nitrobenzaldehyde)thiocarbazone (**1E**).

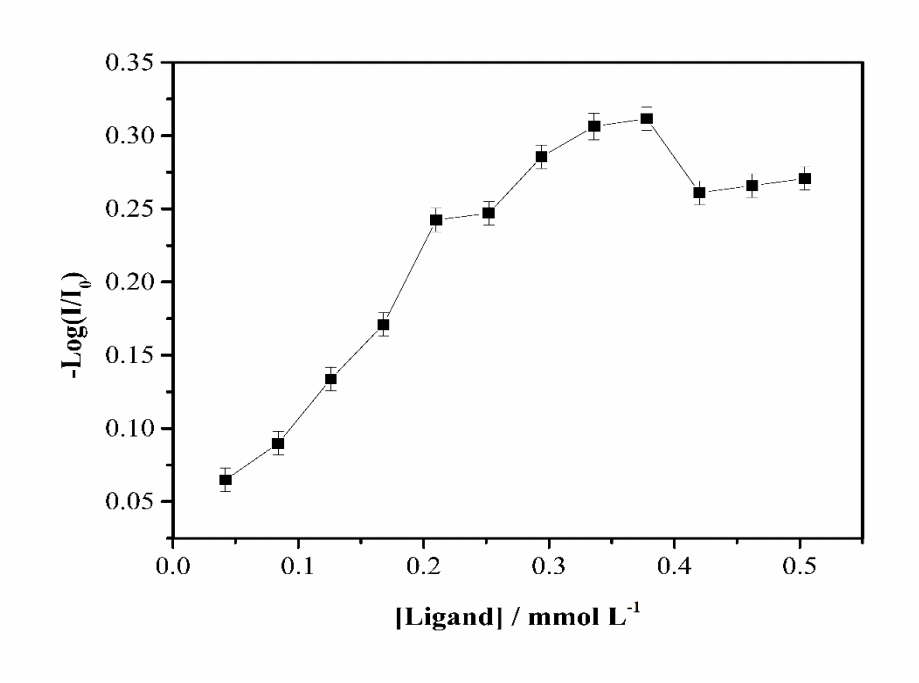


**Fig. S25**. Effect of ligand concentration.

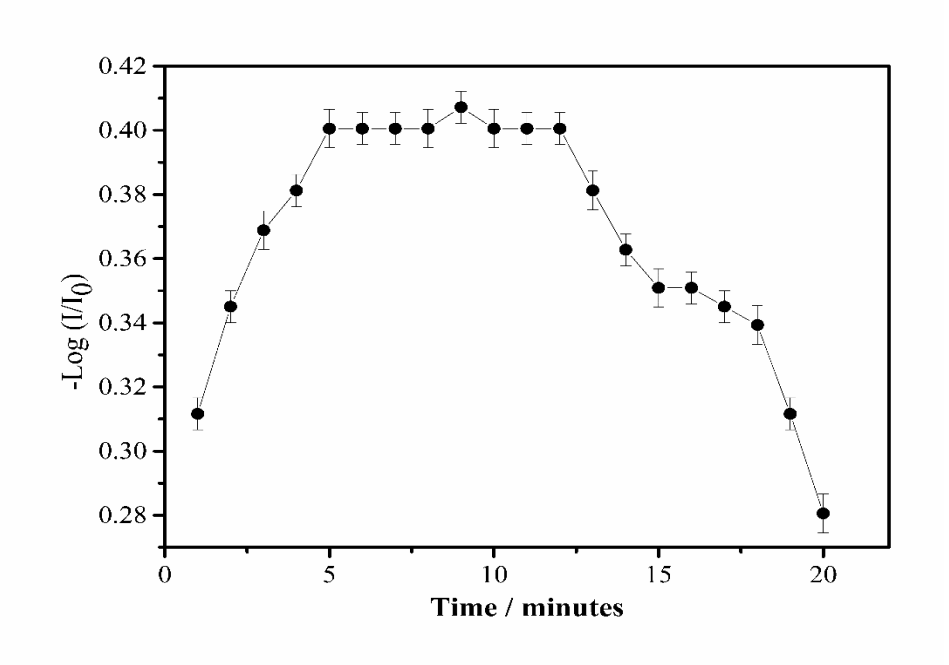


**Fig. S26**. Effect of reaction time for the $Cu^{2+}$-**1C** complex formation.

## 1. 1C – $Cu^{2+}$ Complex

### 1.1. Ultraviolet experiment

Two solutions were prepared, one of copper sulfate pentahydrate and the other of thiocarbazone 1C, both 0.04 mmol $L^{-1}$. Readings were performed on a spectrophotometer of the isolated ligand solution and a 1: 1 mixture of the ligand solution and $CuSO_4.5H_2O$. The spectra obtained are shown below (**Fig. S27**). It is possible to observe the formation of the 1C-$Cu^{2+}$ complex, with maximum absorption at 387 nm. The maximum absorption wavelength of the binder is 359 nm.

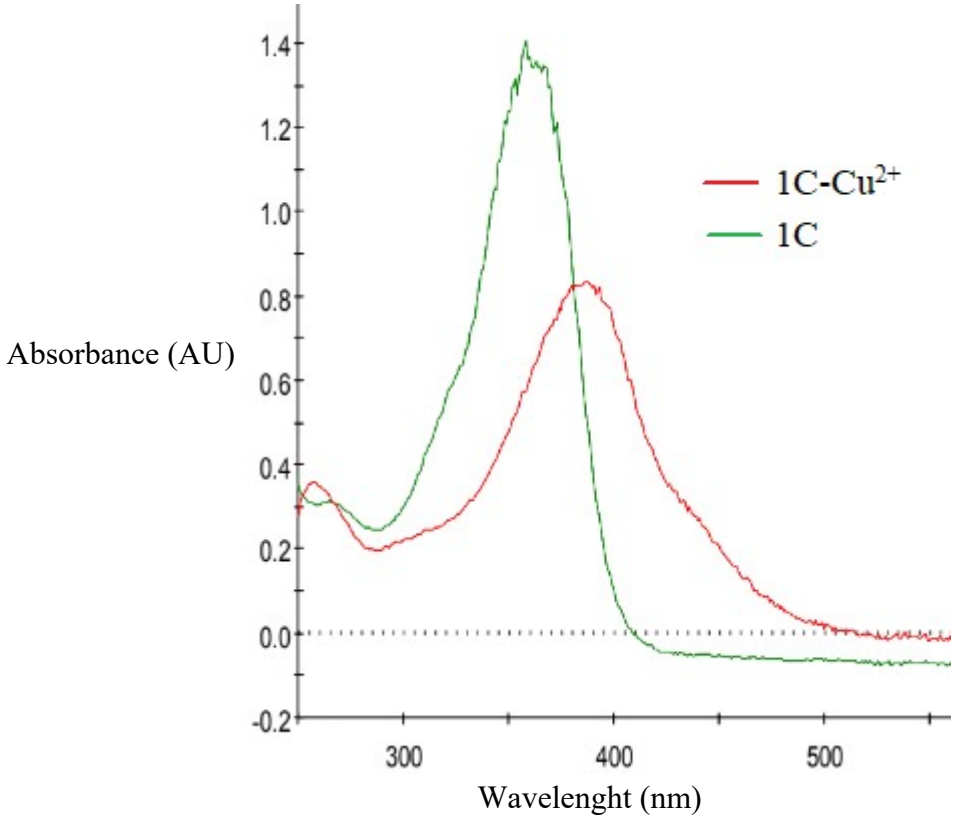


**Fig. S27**. UV spectrum of the 1C-$Cu^{2+}$ complex and the 1C ligand.

### 1.2. Infrared experiment

An experiment was carried out in which the 1C-$Cu^{2+}$ complex and the isolated 1C ligand were analyzed on an FTIR spectrophotometer (**Fig. S28**).

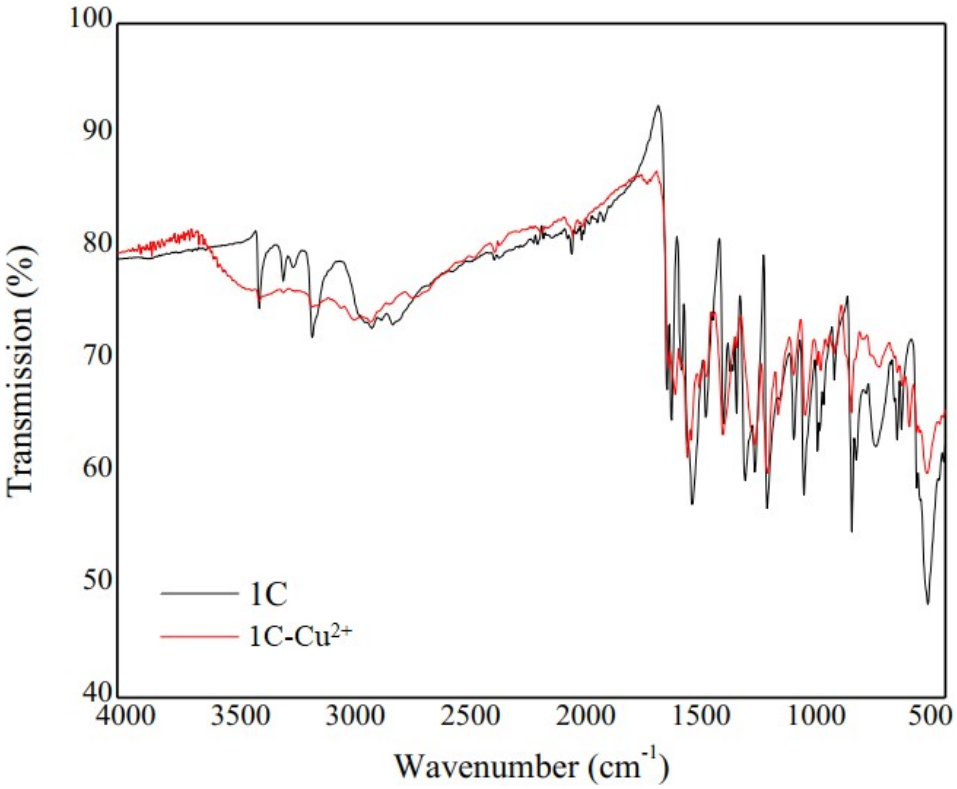


**Fig. S28.** Spectrum in the infrared of the 1C-$Cu^{2+}$ complex and of the 1C ligand.

## 1.3. COSY NMR experiment

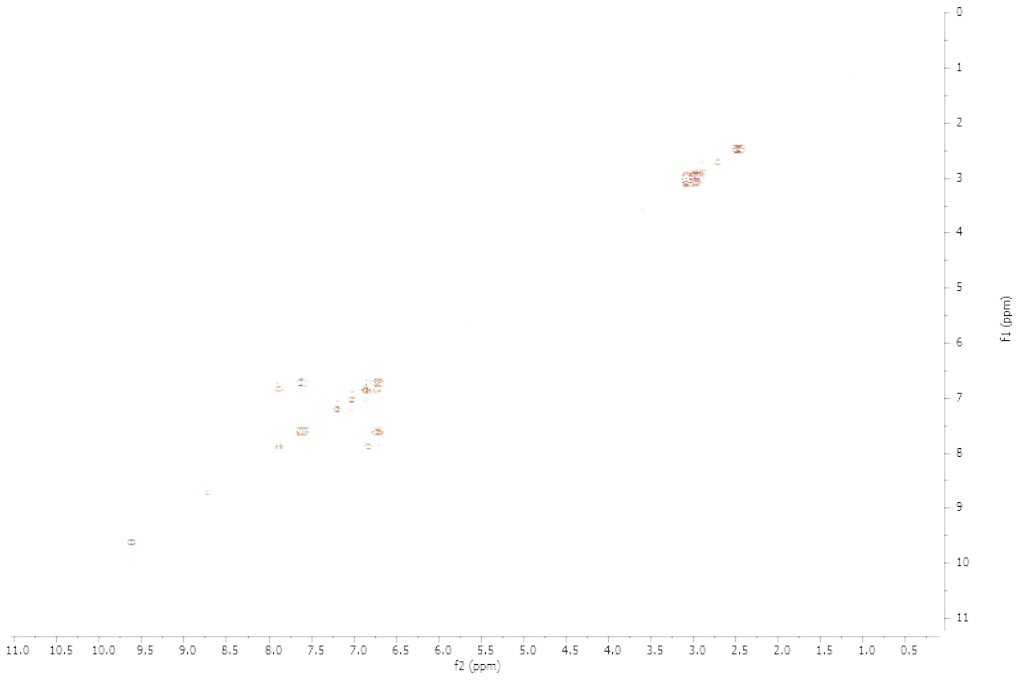


**Fig S29.** COSY NMR spectrum (300 MHz; DMSO; $\delta_{DMSO}$ = 2.49) $Cu^{2+}$/**1C** complex.

**Table S1.** Comparison between analytical parameters obtained for RGB channels

| Channel | Calibration equation [a] | Determination coefficient ($R^2$) |
|---|---|---|
| **R** | $0.0017 \times [Cu^{2+}] + 0.0040$ | 0.75 |
| **G** | $0.0099 \times [Cu^{2+}] + 0.0099$ | 0.87 |
| **B** | $0.042 \times [Cu^{2+}] - 0.0011$ | 0.99 |

[a] calibration equation = Sl. × $[Cu^{2+}]$ + Lc., where Sl. is the slope and Lc. is the linear coefficient, and $[Cu^{2+}]$ is expressed in mg $L^{-1}$ (*n*=5)

## References


[1] World Health Organization, Global status report on alcohol and health, Geneva, 2018. https://apps.who.int/iris/bitstream/handle/10665/274603/9789241565639-eng.pdf?ua=1.

[2] F.L.E. Viana, Indústria de Bebidas Alcóolicas, Cad. Setorial ETENE. 2 (2017) 2–15.

[3] P.R. Oliveira, A.C. Lamy-Mendes, E.I.P. Rezende, A.S. Mangrich, L.H. Marcolino Junior, M.F. Bergamini, Electrochemical determination of copper ions in spirit drinks using carbon paste electrode modified with biochar, Food Chem. 171 (2015) 426–431. doi:10.1016/j.foodchem.2014.09.023.

[4] Y. Boza, J. Horii, Influência do grau alcóolico e da acidez do destilado sobre o teor de cobre na aguardente, Ciência e Tecnol. Aliment. 20 (2000) 279–284. doi:10.1590/S0101-20612000000300001.

[5] J.C. Souza, H.R. Pezza, L. Pezza, A simple and green analytical method for determination of copper(II) in whisky and sugarcane spirit by diffuse reflectance spectroscopy, Anal. Methods. 8 (2016) 1867–1875. doi:10.1039/C5AY03073K.

[6] CRT, Consejo Regulador del Tequila, (2018). https://www.crt.org.mx/EstadisticasCRTweb/.

[7] E.S.F. Coutinho, D. França-Santos, E. Da Silva Magliano, K.V. Bloch, L.A. Barufaldi, C. De Freitas Cunha, M.T.L. De Vasconcellos, M. Szklo, ERICA: Patterns of alcohol consumption in Brazilian adolescents, Rev. Saude Publica. 50 (2016) 1s-9s. doi:10.1590/S01518-8787.2016050006684.

[8] R.A. Labanca, M. Beatriz, A. Glória, V. José, P. Gouveia, Determinação dos teores de cobre e grau alcoólico em aguardentes de cana produzidas no estado de Minas Gerais, Quim. Nov. 29 (2006) 1110–1113.

[9] A.D.J.B. Lima, M.D.G. Cardoso, M.C. Guerreiro, F.A. Pimentel, Emprego do carvão ativado para remoção de cobre em cachaça, Quim. Nova. 29 (2006) 247–250. doi:10.1590/S0101-20612008000500014.

[10] S.J. Villanueva-Rodríguez, B. Rodríguez-Garay, R. Prado-Ramírez, A. Gschaedler, Tequila: Raw Material, Classification, Process, and Quality Parameters, in: Encycl. Food Heal., Elsevier Inc., 2015: pp. 283–289. doi:10.1016/B978-0-12-384947-2.00688-7.

[11] M.B. Rota, Efeito do processo de bidestilação na qualidade sensorial da cachaça, Universidade Estadual Paulista “Júlio de Mesquita Filho,” 2008. https://repositorio.unesp.br/bitstream/handle/11449/88206/rota_mb_me_arafcf.pdf?sequence=1&isAllowed=y.

[12] MAPA, Instrução normativa n° 15, de 31 de março de 2011, 2011. https://www.gov.br/agricultura/pt-br/assuntos/vigilancia-agropecuaria/ivegetal/bebidas-arquivos/in-no-15-de-31-de-marco-de-2011.pdf/view.

[13] Y. Cao, Y. Liu, F. Li, S. Guo, Y. Shui, H. Xue, L. Wang, Portable colorimetric detection of copper ion in drinking water via red beet pigment and smartphone, Microchem. J. 150 (2019) 104176. doi:10.1016/j.microc.2019.104176.

[14] A. Shahvar, D. Shamsaei, M. Saraji, N. Arab, S. Alijani, Microfluidic-based liquid-liquid microextraction in combination with smartphone-based on-chip detection for the determination of copper in biological, environmental, and food samples, Microchem. J. 160 (2021) 105655. doi:10.1016/j.microc.2020.105655.

[15] J. Singkhonrat, A. Sriprai, S. Hirunwatthanakasem, T. Angkuratipakorn, P. Preechaburana, Digital image colorimetric analysis for evaluating lipid oxidation in oils and its emulsion, Food Chem. 286 (2019) 703–709.

[16] W. Wongniramaikul, W. Limsakul, A. Choodum, A biodegradable colorimetric film for rapid low-cost field determination of formaldehyde contamination by digital image colorimetry, Food Chem. 249 (2018) 154–161.

[17] V.B. dos Santos, E.K.N. da Silva, L.M.A. de Oliveira, W.T. Suarez, Low cost in

situ digital image method, based on spot testing and smartphone images, for determination of ascorbic acid in Brazilian Amazon native and exotic fruits, Food Chem. 285 (2019) 340–346. doi:10.1016/j.foodchem.2019.01.167.

[18] A.A. Mohamed, A.A. Shalaby, Digital imaging devices as sensors for iron determination, Food Chem. 274 (2019) 360–367. doi:10.1016/j.foodchem.2018.09.014.

[19] H. V. Dantas, M.F. Barbosa, A. Pereira, M.J.C. Pontes, P.N.T. Moreira, M.C.U. Araújo, An inexpensive NIR LED Webcam photometer for detection of adulterations in hydrated ethyl alcohol fuel, Microchem. J. 135 (2017) 148–152. doi:10.1016/j.microc.2017.08.014.

[20] I.S.A. Porto, J.H. Santos Neto, L.O. dos Santos, A.A. Gomes, S.L.C. Ferreira, Determination of ascorbic acid in natural fruit juices using digital image colorimetry, Microchem. J. 149 (2019). doi:10.1016/j.microc.2019.104031.

[21] C.G. Ravazzi, M. de O. Krambeck Franco, M.C.R. Vieira, W.T. Suarez, Smartphone application for captopril determination in dosage forms and synthetic urine employing digital imaging, Talanta. 189 (2018) 339–344. doi:10.1016/j.talanta.2018.07.015.

[22] L.F. Capitán-Vallvey, N. López-Ruiz, A. Martínez-Olmos, M.M. Erenas, A.J. Palma, Recent developments in computer vision-based analytical chemistry: A tutorial review., Anal. Chim. Acta. 899 (2015) 23–56. doi:10.1016/j.aca.2015.10.009.

[23] V.H.M. Luiz, L.S. Lima, E.L. Rossini, L. Pezza, H.R. Pezza, Paper platform for determination of bumetanide in human urine samples to detect doping in sports using digital image analysis, Microchem. J. 147 (2019) 43–48. doi:10.1016/j.microc.2019.03.006.

[24] V.K. Gupta, A.K. Singh, M.R. Ganjali, P. Norouzi, F. Faridbod, N. Mergu, Comparative study of colorimetric sensors based on newly synthesized Schiff bases, Sensors Actuators, B Chem. 182 (2013) 642–651. doi:10.1016/j.snb.2013.03.062.

[25] W. Zhu, L. Yang, M. Fang, Z. Wu, Q. Zhang, F. Yin, Q. Huang, C. Li, New carbazole-based Schiff base: Colorimetric chemosensor for Fe3+ and fluorescent turn-on chemosensor for Fe3+ and Cr3+, J. Lumin. 158 (2015) 38–

43. doi:10.1016/j.jlumin.2014.09.020.

[26] D. Udhayakumari, S. Saravanamoorthy, M. Ashok, S. Velmathi, Simple imine linked colorimetric and fluorescent receptor for sensing Zn2+ ions in aqueous medium based on inhibition of ESIPT mechanism, Tetrahedron Lett. 52 (2011) 4631–4635. doi:10.1016/j.tetlet.2011.06.097.

[27] D. Udhayakumari, S. Velmathi, Colorimetric chemosensor for multi-signaling detection of metal ions using pyrrole based Schiff bases, Spectrochim. Acta - Part A Mol. Biomol. Spectrosc. 122 (2014) 428–435. doi:10.1016/j.saa.2013.11.083.

[28] H. Schiff, Eine neue Reihe organischer Basen, Justus Liebigs Ann. Chem. 131 (1864) 118–119. doi:10.1002/jlac.18641310113.

[29] Â. de Fátima, C. de P. Pereira, C.R.S.D.G. Olímpio, B.G. de Freitas Oliveira, L.L. Franco, P.H.C. da Silva, Schiff bases and their metal complexes as urease inhibitors – A brief review, J. Adv. Res. 13 (2018) 113–126. doi:10.1016/j.jare.2018.03.007.

[30] A.A. Aly, S. Bräse, P. Weis, Tridentate and bidentate copper complexes of [2.2]paracyclophanyl-substituted thiosemicarbazones, thiocarbazones, hydrazones and thioureas, J. Mol. Struct. 1178 (2019) 311–326. doi:10.1016/j.molstruc.2018.10.036.

[31] L. Li, Y. Jiang, X. Liu, Z. Zhao, Microwave-assisted synthesis and antibacterial activity of unsymmetrical indolyl/aryl bis-thiosemicarbazones, J. Chem. Res. 37 (2013) 372–374. doi:10.3184/174751913X13688155249983.

[32] G. Kiran, T. Maneshwar, Y. Rajeshwar, M. Sarangapani, Microwave-Assisted Synthesis, Characterization, Antimicrobial and Antioxidant Activity ofSome New Isatin Derivatives, J Chem. 2013 (2013) 1–7.

[33] G. Li, Z. Shi, X. Li, Z. Zhao, Synthesis of new ferrocene bis thiocarbazones under solvent-free conditions using microwave, J. Chem. Res. (2011) 278–281. doi:https://doi.org/10.3184/174751911X13043447062703.

[34] T.E.-S. Ali, Utility of thiocarbohydrazide in heterocyclic synthesis, J. Sulfur Chem. 30 (2009) 611–647. doi:10.1002/chin.201022220.

[35] Z. Shi, Z. Zhao, M. Liu, X. Wang, Comptes Rendus Chimie Solvent-free synthesis of novel unsymmetric chenodeoxycholic acid bis thiocarbazone

derivatives promoted by microwave irradiation and evaluation of their antibacterial activity, Comptes Rendus - Chim. 16 (2013) 977–984. doi:10.1016/j.crci.2013.05.009.

[36] B.K. Momidi, V. Tekuri, D.R. Trivedi, Multi-signaling thiocarbohydrazide based colorimetric sensors for the selective recognition of heavy metal ions in an aqueous medium, Spectrochim. Acta - Part A Mol. Biomol. Spectrosc. 180 (2017) 175–182. doi:10.1016/j.saa.2017.03.010.

[37] A.D. Tiwari, A.K. Mishra, S.B. Mishra, B.B. Mamba, B. Maji, S. Bhattacharya, Synthesis and DNA binding studies of Ni(II), Co(II), Cu(II) and Zn(II) metal complexes of N 1,N 5-bis[pyridine-2-methylene]- thiocarbohydrazone Schiff-base ligand, Spectrochim. Acta - Part A Mol. Biomol. Spectrosc. 79 (2011) 1050–1056. doi:10.1016/j.saa.2011.04.018.

[38] D. Maity, A.K. Manna, D. Karthigeyan, T.K. Kundu, Visible – Near-Infrared and Fluorescent Copper Sensors Based on Julolidine Conjugates : Selective Detection and Fluorescence Imaging in Living Cells, (2011) 11152–11161. doi:10.1002/chem.201101906.

[39] K.D. Pessoa, W.T. Suarez, M.F. dos Reis, M. de Oliveira Krambeck Franco, R.P.L. Moreira, V.B. dos Santos, A digital image method of spot tests for determination of copper in sugar cane spirits, Spectrochim. Acta - Part A Mol. Biomol. Spectrosc. 185 (2017) 310–316. doi:10.1016/j.saa.2017.05.072.

[40] Loomatix, Color Grab. Loomatix Ltd. http://www.loomatix.com/.

[41] S. Paciornik, A. V. Yallouz, R.C. Campos, D. Gannerman, Scanner image analysis in the quantification of mercury using spot-tests, J. Braz. Chem. Soc. 17 (2006) 156–161. doi:10.1590/S0103-50532006000100022.

[42] L.P. dos S. Benedetti, V.B. dos Santos, T.A. Silva, E.B. Filho, V.L. Martins, O. Fatibello-Filho, A digital image analysis method for quantification of sulfite in beverages, Anal. Methods. 7 (2015) 7568–7573. doi:10.1039/C5AY01372K.

[43] X.-H. Liu, J.-Q. Weng, B.-L. Wang, Y.-H. Li, C.-X. Tan, Z.-M. Li, Microwave-assisted synthesis of novel fluorinated 1,2,4-triazole derivatives, and study of their biological activity, Res. Chem. Intermed. 40 (2014) 2605–2612. doi:10.1007/s11164-013-1113-4.

[44] Z. Shi, Z. Zhao, X. Liu, L. Wu, Synthesis of new deoxycholic acid bis

thiocarbazones under solvent-free conditions using microwave irradiation, J. Chem. Res. (2011) 198–201.

[45] J. Clayden, N. Greeves, S. Warren, P. Wothers, Organic Chemistry, Oxford University Press, 2000.

[46] P.Y. Bruice, Organic Chemistry, Pearson, 1987.

[47] H.L.C. Barros, Química Inorgânica uma introdução, Editora UFMG, Belo Horizonte, 1992.

[48] J.S. Renny, L.L. Tomasevich, E.H. Tallmadge, D.B. Collum, Method of Continuous Variations: Applications of Job Plots to the Study of Molecular Associations in Organometallic Chemistry, Angew. Chemie Int. Ed. 52 (2013) 11998–12013. doi:10.1002/anie.201304157.

[49] M. Shebl, S.M.E. Khalil, F.S. Al-Gohani, Preparation, spectral characterization and antimicrobial activity of binary and ternary Fe(III), Co(II), Ni(II), Cu(II), Zn(II), Ce(III) and UO 2(VI) complexes of a thiocarbohydrazone ligand, J. Mol. Struct. 980 (2010) 78–87. doi:10.1016/j.molstruc.2010.06.040.

[50] F.G. Pinto, S.S. Roch, M.H. Canuto, Siebald Hemulth G L, J.B.B. Silva, Determinação de Cobre e Zinco em cachaça por espectrometria de absorção atômica com chama usando calibração por ajuste de matriz, Rev. Anal. 17 (2005) 48–50.

[51] AOAC, AOAC, Official Methods of Analysis, Distilled Liquors, Copper in Distilled Liquors ZDBT Colorimetric Method, 2000, 7 (Chapter 26)., (2000).

[52] M. Trigo-López, A. Muñoz, S. Ibeas, F. Serna, F.C. García, J.M. García, Colorimetric detection and determination of Fe(III), Co(II), Cu(II) and Sn(II) in aqueous media by acrylic polymers with pendant terpyridine motifs, Sensors Actuators, B Chem. 226 (2016) 118–126. doi:10.1016/j.snb.2015.11.116.

[53] Y. Zhou, H. Zhao, Y. He, N. Ding, Q. Cao, Colorimetric detection of Cu2+ using 4-mercaptobenzoic acid modified silver nanoparticles, Colloids Surfaces A Physicochem. Eng. Asp. 391 (2011) 179–183. doi:10.1016/j.colsurfa.2011.07.026.

[54] X. Bai, Y. Li, H. Gu, Z. Hua, Selective colorimetric sensing of Co2+ and Cu2+ using 1-(2-pyridylazo)-2-naphthol derivative immobilized polyvinyl alcohol microspheres, RSC Adv. 5 (2015) 77217–77226. doi:10.1039/c5ra12765c.

[55] S. Hu, J. Song, F. Zhao, X. Meng, G. Wu, Highly sensitive and selective colorimetric naked-eye detection of Cu2+ in aqueous medium using a hydrazone chemosensor, Sensors Actuators, B Chem. 215 (2015) 241–248. doi:10.1016/j.snb.2015.03.059.

[56] I.J. Chang, M.G. Choi, Y.A. Jeong, S.H. Lee, S.K. Chang, Colorimetric determination of Cu2+in simulated wastewater using naphthalimide-based Schiff base, Tetrahedron Lett. 58 (2017) 474–477. doi:10.1016/j.tetlet.2016.12.066.

# CAPÍTULO 5

## Determinação simultânea de cobre e furfural em cachaças utilizando sistema bifásico e análise de imagens digitais com ferramentas quimiométricas

# Simultaneous determination of copper and furfural in cachaças using a biphasic system and digital images analysis with chemometric tools

Mathews de O.K. Franco[1], Wilson J. Cardoso[1], Castelo B. Vilanculo[1], Vagner B. dos Santos[2] , João Paulo Barbosa de Almeida[2] , Willian T. Suarez[1*]

[1] Department of Chemistry, Federal University of Viçosa, Center for Exact Sciences and Technology, Viçosa-MG 36570-900, Brazil

[2] Fundamental Chemistry Department, Federal University of Pernambuco, Recife-PE 50670-901, Brazil

## ABSTRACT

For the first time, a method based on digital image analysis was proposed for the simultaneous determination of $Cu^{2+}$ and furfural in cachaças samples using a two-phase system and chemometrics tools. Furfural reacts with aniline in acidic medium forming furfulidenanelline, which presents a pink color. On the other hand, $Cu^{2+}$ reacts with CPZ in a basic medium to form a blue complex. The two reactions were performed on a porcelain plaque, and a smartphone was used to capture the colorimetric images. Partial least squares (PLS) regression was used to build the prediction models for $Cu^{2+}$ and furfural contents in cachaças samples. After finding the best PLS models, the ordered predictors selection (OPS) was performed to select the most predictive variables. The developed method was effective to estimate the values of $Cu^{2+}$ and furfural in cachaças, with a mean absolute error of 0.2 mg/L for $Cu^{2+}$ model, and 0.3 mg/100 mL of anhydrous alcohol for the furfural model. Furthermore, the method is simple, does not require complex technical knowledge and can be used by the producers themselves in the *cachaça* manufacturing process.

**KEYWORDS:** Partial least squares; Multivariate calibration; Two-phase system; Alcoholic beverages; Chemometric; Smartphone

## 1. Introduction

Analytical chemistry has recently advanced in the development of simpler analytical methodologies, with low-cost, using low amounts of reagents, corroborating the principles of green chemistry. In this sense, the use of analytical instruments associated with low-cost home-built equipment, adequate for *in situ* analysis, and miniaturized apparatus has been widely used quantification several compounds in diverse samples of foods and beverages [1–6].

Sugarcane spirits (cachaça) is a Brazilian alcoholic beverage with an alcohol content of 38% to 48% by volume at 20°C. It is obtained from the distillation of fermented must from sugarcane juice [7]. Cachaça is a typical distilled beverage produced in Brazil and, after beer, is the most consumed alcoholic beverage in the country, occupying the fourth position worldwide [8].

Recently, numerous studies have pointed to cachaças with components that do not comply with the standards established by Brazilian legislation [9], ~~como~~such as: furfural [10,11], $Cu^{2+}$ [2,12–14] methanol [11,15], reducing sugars [16], ethyl carbamate [11,14], acrolein [17,18] among others. Furfural and hydroxymethylfurfural (HMF) are aromatic aldehydes and are some of the undesirable components present in cachaças. These compounds are formed mainly from the pyrolysis of organic matter deposited at the bottom of stills [19]. Prolonged or repeated contact with furfural can affect the central nervous system, produce dermatitis, irritation of the mucosa and respiratory tract, in addition to having carcinogenic potential [20]. According to Brazilian legislation, the maximum content of furfural and HMF allowed in cachaças is 5 mg per 100 mL of anhydrous alcohol [9].

Furthermore, in the distillation process, the formation of acidified alcoholic vapors occurs by the dissolution of part of the basic $Cu^{2+}$ carbonate present on the walls of the stills. Depending on the amount of metal transferred to the beverage, the quality of the final product is impaired, as the presence of $Cu^{2+}$ in high concentrations is undesirable because it is harmful to humans [21]. Wilson's disease is the most well-known disease caused by the accumulation of $Cu^{2+}$ in the body, clinically characterized by hepatic and neurological manifestations and accumulation of $Cu^{2+}$ in the liver and corneas [22]. Brazilian legislation limits the $Cu^{2+}$ content in distilled

beverages to 5 mg/L [9]. Nevertheless, the European Union, for example, does not tolerate more than 2 mg/L of $Cu^{2+}$ in alcoholic distillates [23].

Therefore, Analytical Chemistry has introduced, due to the fast image capture and background stability, the use of cameras and smartphones, since they provide the development of new analytical methods with high sensitivity, robustness, quick, portable, accessible due to its low implementation cost [24]. These smartphones due to its sensors are capable of converting the intensity of incident light into storable digital values which are used to construct the digital image. For analytical purposes, softwares are employed to decompose this image in the original data at a specific color model [15]. The widely used colors models used are RGB, HSV, HSI color model data among others [25–29]. The RGB (Red-Green-Blue) color model is a color representation standard in which each color is expressed by combining the R, G and B colors. RGB images are mathematically represented by three distinct two-dimensional matrices, one for each channel. Each element of these matrices is a number which represents the color intensity of a pixel [27,29]. Therefore, each pixel contains three values that represent the intensity of the red, green and blue colors. Each channel is represented by 8 bits, and thus, values from 0 to 255 are possibles for each channel, being the value 0 for all channels supplying the black color while the value 255 for all channels the white color [26].

The use of digital images represents a current opportunity for the rapid and direct development of quantitative determinations, particularly when combined with colorimetric or fluorescence methods for a wide variability of applications [28,30–32]. For applications involving DIB and FDIB methods, it is necessary to use support platforms. Among the materials commonly used for the manufacture of these platforms are paper [12], ceramic plates [33], polystyrene microplates [28], polylactic acid [32] among others. For the process of obtaining the concentration of the analyte, some care must be taken into account regarding the control of the luminosity of the platform of analysis [15]. In fact, the excess of shadows and brightness can compromise the results of the analysis leading to a change in the values of the RGB, and, consequently, modify the analyte concentrations [34]. Therefore, it is necessary to use closed chambers during the analyses in order to avoid this inconvenience [12,28,32,33].

Thus, there is a demand for simple, fast, and low-cost analytical methodologies to evaluate the chemical compounds present in the cachaça to verify the conformity with the legislation. In this sense, in situations in which the determination of a chemical substance is difficult, due to a lack of instruments, costs, use of solvents, or due to the presence of interferents, the use of smartphone and digital image together multivariate calibration has the potential to solve this demand. Multivariate calibration, such as partial least squares (PLS), consider the presence of interferents when modeling the analyte of interest. The Multivariate calibration is used to avoid the physical separation of species and use of expensive and complex analysis. In this way, two or more analytes can be determined simultaneously without compromising the data, increasing the analysis speed and analytical frequency with deduced uses of harmful compounds to the environment and health person [35,36].

Thus, in this work an analytical methodology based on digital image analysis for the simultaneous determination of furfural and $Cu^{2+}$ in Brazilian cachaça samples using a two-phase system was developed. Partial least squares (PLS) regression was used to build the prediction models for copper and furfural contents in alcoholic beverages. To the best of our knowledge, no analytical methodology based on digital image analysis has been proposed for the simultaneous determination of two analytes in cachaça samples.

## 2. Materials and methods

### *2.1.Chemicals and samples*

The solutions were prepared with ultrapure water (resistivity > 18.0 MΩ cm) obtained from a Millipore Milli-Q system (USA) and all chemical reagents were of analytical grade. Cuprizone (bis (cyclohexanone) oxaldihydrazone, CPZ), copper sulphate pentahydrate, aniline, furfural, sodium hydroxide, ethylenediaminetetraacetic acid (EDTA) and ethanol were purchased from Sigma-Aldrich. Acetic acid was purchased from Merck. The 500 mg/L $Cu^{2+}$ stock solution was prepared by dissolving 0.196 g of $CuSO_4 \cdot 5H_2O$ in 100 mL purified water, and then standardized by complexometric titration using EDTA [12,37].

The 2500 mg/L CPZ stock solution was prepared in a 60% (v/v) ethanol – ultrapure water mixture and stored at 4º C. The other solutions in different concentrations were obtained by diluting the stock solution in ethanol – purified water 60% (v/v). The 0.2 mol/L borate buffer solution at pH 9.0 was prepared by dissolving $Na_2B_4O_7 \cdot 10H_2O$ in ultrapure water with the addition of NaOH 0.2 mol/L. The pH was measured on a benchtop pH meter (Mettler Toledo, USA).

A stock solution of furfural $1.0 \times 10^{-2}$ mol/L was prepared in 40% (ethanol/water) and stored in a suitable storage container away from sunlight and heat. The aniline solution in concentrated acetic acid was prepared daily. Forty-three samples were used in this work. Thirty-four samples were made using standard solutions of $Cu^{+2}$ and furfural, and the other nine samples were from alcoholic beverages. All samples of cachaça used for our studies were obtained from supermarkets in Viçosa city, state of Minas Gerais, Brazil.

*2.2. Apparatus and Instrumentation*

A closed chamber used to obtain digital images was built in order to employ apparatus as simple as possible, in such a way as to make its operation more accessible and corroborate with some principles of green chemistry. In this sense, a chamber of recycled paper with dimensions of 20 × 10 × 6 cm was used as an apparatus of image capture. On the top of the box an opening was made to capture the digital image of a Xiaomi redmi note 8 smartphone. Moreover another opening was performed to allow the illumination by the LED of the smartphone, **Fig.1.**

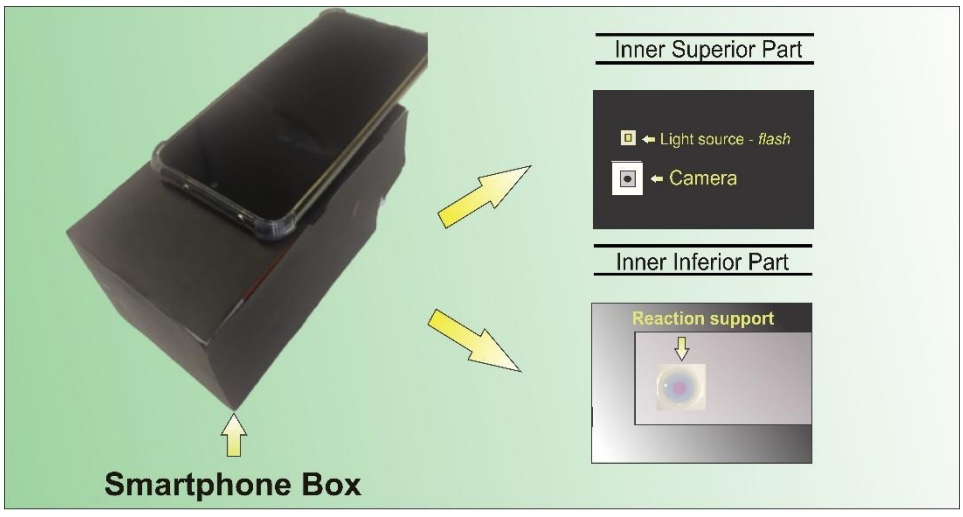

**Fig.1.** Closed chamber used to obtain digital images for determination of $Cu^{2+}$ and furfural in cachaça using a smartphone. At the bottom, a porcelain plate was used to accommodate the chemical reactions.

One of the main advantages of the apparatus presented in Fig. 1 is that it does not require external lighting sources, such as lamps and LEDs, normally used in this type of analysis to obtain a homogenization of the light to capture the digital images with adequate precision. In fact, the smartphone's built-in flash was used as a light source to capture digital images [6,38,39]. The reactions were conducted in a porcelain plaque containing nine reaction vessels, with a maximum volume of 1 mL. Eppendorf (Germany) automatic pipettes were used to transfer precise volumes of reagents and/or samples to the porcelain plate, which was placed inside the chamber to capture the images. In addition, only the central cavity of the porcelain plate was used for analysis, since it offered a homogeneous illumination, i.e., absence of excess brightness or shadows [40].

*2.3. Two-Phase System Optimization*

Furfural reacts with aniline in acidic medium forming furfulidenanelline, which presents a pink color. On the other hand, $Cu^{2+}$ reacts with CPZ in a basic medium to form a blue complex. Due to the low solubility of the anilinium ion in a hydroalcoholic system, a biphasic system of pink and blue solutions is formed, composed of $Cu^{2+}$/CPZ and furfural/anilinium ion in the center of the reaction module.

Therefore, standard solutions of different concentrations of furfural and $Cu^{2+}$ were placed on the porcelain plate, totaling 150 µL. Then 100 µL borate buffer (pH 9) and then 100 µL CPZ were added. Then, 20 µL of aniline ion (aniline in acetic acid) was added, totaling 370 µL of total volume in the solution. The final solution was adjusted to 40% alcohol/water, as this is the concentration normally found in cachaças. **Table S1** shows the volumes of all reagents used in the work to set up the partial least squares (PLS) regression. In the case of cachaça samples, the volumes of $Cu^{2+}$, furfural and 40% alcohol were substituted by the samples.

Studies were carried out to find the best reaction conditions for both reactions, in order to mitigate possible influences of some reaction component of one reaction

on the other. The pH of the solution was maintained at 9, using a borate buffer as discussed in previous work [41]. The ideal concentration of cuprizone used in the complexation of $Cu^{2+}$ was studied individually from 50 to 160 mg/L. In addition, different aniline ion solutions were prepared, varying different proportions of aniline and acetic acid volumes. All tests aimed to obtain the highest possible analytical response. In all these studies, the concentration of $Cu^{2+}$ was kept fixed at 5 mg/L and furfural fixed at 5 mg/100 mL of anhydrous alcohol.

As both reactions are carried out at different concentrations of $H^+$ ions, the optimal reaction time had to be optimized, as the complex will dissolve with time, due to the increase in acidity of the reaction medium, as acetic acid will naturally migrate to the aqueous phase, and impairing the formation of the Cu/CPZ complex. Therefore, a kinetic study aiming to obtain the highest analytical signal for both reactions as well as a time in which the two reactions were separated by a two-phase system was carried out.

For the analytical response, the mean value of the R, G or B channel measured by sample or standard solution was used and subtracted from the mean value of the $R_0$, $G_0$ or $B_0$ acquired from the analytical blank. As the complementary color of the pink is green, the G channel will be used to measure the Furfural. Similarly, the R channel will be used to measure the $Cu^{2+}$ with cuprizone. Sometimes, the analytical curves with R, G or B data vs. concentration are reported in the literature [42]. The concept of complementary color is used for colorimetry and/or spectrophotometry [43–46]. However, the captured signal from a digital camera is due to reflection, and thus, the reflected signal based on R, G or B value is correlated with the absorbance, and this reflected signal has been used in the literature. Thus, the analytical signal is a decrease in the RGB signal, i.e. the greater the signal drop, the greater is the analytical response [28,33,41,47].

*2.4 Image processing*

The images were imported to MATLAB 2019a (MathWorks, Natick, USA). Each image is composed by 2448 x 3264 pixels. Therefore, the image dimension was reduced, cutting the image around the area where the sample was placed. After that the image was rotated from 0 to 342 degrees with steps of 18 degrees, 20

different images were generated, and then, the median of each pixel for all imagens were used to acquire a corrected image. Then, each image was decomposed in its red, green, and blue data. The values of the middle horizontal pixels for each image were used. The matrices of independent variables (X), that were used for modeling, were built, where each line represents an image, and the columns the pixels of the image, ranging from 1 to 600. Four different X matrices were built, considering the histograms for each color (XR, XG, XB) and the histograms of all three colors concatenated (XRGB) [29,48].]

*2.5 Multivariate Regression*

Partial least squares (PLS) regression was used to build the prediction models for $Cu^{2+}$ and furfural contents in alcoholic beverages. The X matrices were divided into a calibration set, comprising 70% of the standard solution samples, and a prediction set, comprising the remaining 30% of the real samples, using the Kennard-Stone algorithm. The calibration step and therefore the model is made using only the calibration set, whereas the prediction set is used to validate the model, using standards that were not used to create the model. As a means to find the best model, ten-fold random cross-validation were used, and 1 to 10 latent variables evaluated. The best PLS models that returned the lowest root mean squared error of cross-validation (RMSECV) were chosen. After finding the best PLS models, the ordered predictors selection (OPS) was performed to select the most predictive variables (available at www.deq.ufv.br/chemometrics). The OPS is performed sorting the variables according to an informative vector, and then searching for the best combination of variables. All OPS methods and informative vectors were studied using a size 50 window and increments of 20 variables [49,50].

## 3. Results and Discussion

### *3.1. Optimization of reaction conditions.*

The reactions of $Cu^{2+}$ with cuprizone and furfural with aniline were optimized to obtain the best analytical responses. Initially, the more adequate concentration of cuprizone was evaluated. As the product of the $Cu^{2+}$-cuprizone complexation is blue,

the channel that presented the high analytical signal was the R channel, as previously discussed due to the to be the complementary color, and therefore, it was used as an analytical response. As can be seen in **Fig. 2**, starting from the cuprizone concentration equivalent to 70 mg/L,there is a signal drop, and thus, the greater the analytical response. Moreover, the analytical signal is very stable leading to obtain precise data to quantify $Cu^{2+}$ ions, and therefore, this concentration was used for further studies.

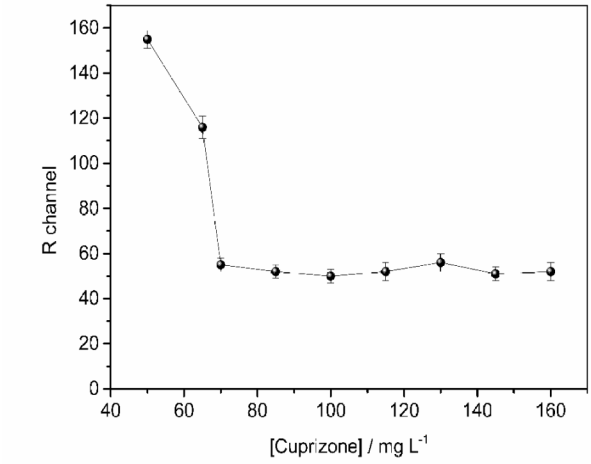


**Fig 2.** Effect of increasing cuprizone concentration on the formation of the $Cu^{2+}$-cuprizone complex as a function of the R channel. The concentration of $Cu^{2+}$ was kept fixed at 5 mg $L^{-1}$.

The appropriate concentration of the aniline ion for the furfural reaction was also studied. Therefore, several concentrations of the aniline were evaluated in order to obtain a satisfactory analytical signal. As the reaction between the aniline ion and the furfural generates a chromophore with a pinkish color, the complementary G channel presented the best analytical response as expected. In fact, there is a high signal drop of the G channel when the aniline ion concentration was equivalent to 1.2 mol $L^{-1}$. After this concentration, the signal goes up again indicating that the solution is getting less intense, **Fig. 3**.

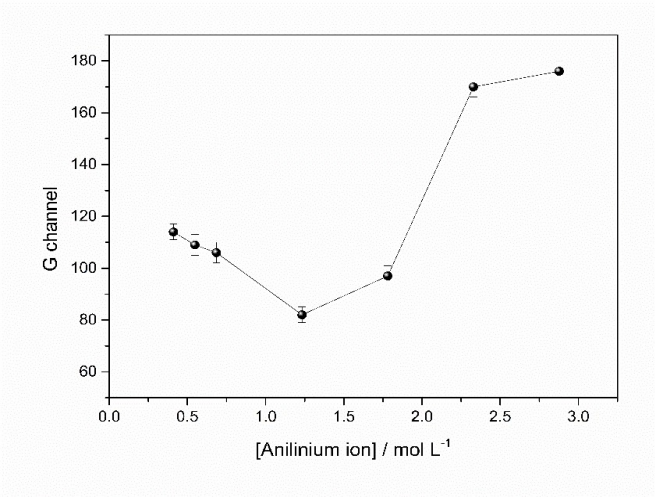


.

**Fig 3.** Different concentrations of anilinium ion and the response given in the green (G) channel.

Finally, the kinetics of both reactions were evaluated concomitantly, to verify the level of stability of the reactions, since both are carried out amid different concentrations of pH. Thus, as can be seen in **Fig. 4**, the R channel for $Cu^{2+}$-cuprizone reaction remained stable up to 4 minutes of reaction, after which time, an increase in the values of the respective channel was observed, which was caused by the acidification of the reaction medium, since the $H^+$ ions naturally migrated through the two-phase system, thus, the complex was falling with the time. On the other hand, for the reaction of furfural with the aniline ion, a maximum analytical response was obtained after 1.5 minutes, and the signal remained constant until approximately 5 minutes.

From the data obtained in this experiment, it was decided to choose the reaction time of 1.5 minutes as appropriate, since both reactions remained stable with maximum analytical responses. In addition, the use of a reduced reaction time increases the analytical frequency of the analysis.

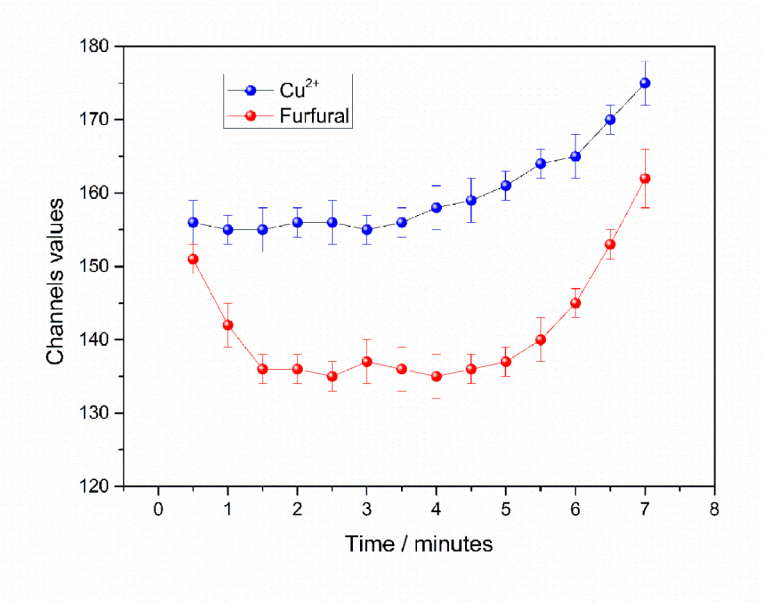


**Fig. 4.** Effect of time on analytical response in the reactions of (i) $Cu^{2+}$-cuprizone, and (ii) furfural-aniline ion. In reaction (i) the R channel was used, and in reaction (ii) the G channel was used.

### *3.2. Model validation and analysis of real samples*

**Fig. 5** shows the concentration of $Cu^{+2}$ and furfural for each standard solution sample and cachaça sample used in this work. Samples from 1 to 34 represent the standard solutions and among 35 to 43 the cachaça samples. The standard solution samples cover a wider range of concentration, and the inclusion of cachaça samples brings variation related to the possible matrix effect to the model, therefore making it possible to use the model to predict the concentration of $Cu^{+2}$ and furfural in real cachaça samples.

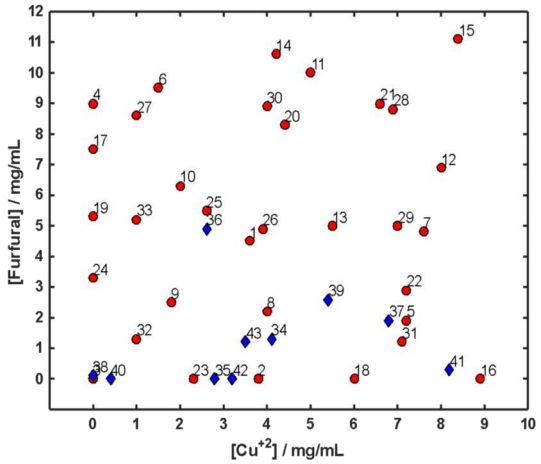


**Fig. 5.** Concentration of $Cu^{+2}$ versus furfural of the standard solution samples (red circles) and cachaça samples (blue diamonds).

**Fig. 6** shows the digital images acquired for each sample. It can be observed a wide variation in the blue and pink color due to the presence of $Cu^{+2}$ and furfural in the samples. A white region is observed due to the camera flash. In addition, some variations in the shape of the pink region are observed. This region of the digital image should be not used to avoid spurious signals as reported by Benedetti et al. [51]. Thus, the analyst cannot control these factors, therefore an image preprocessing step was put in place to correct them.

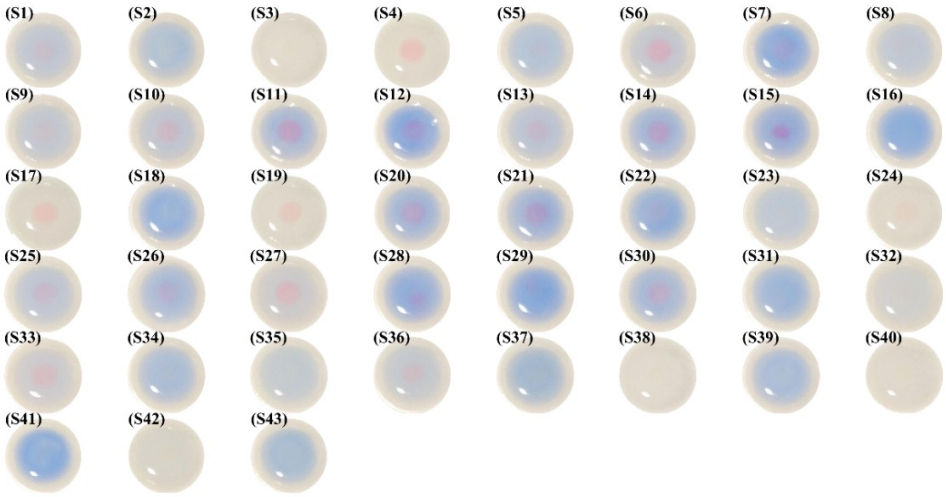


**Fig. 6**. Digital images captured from each sample of cachaça to copper and furfural analysis. Samples (S).

A univariate calibration was tested for the calibration of both analytes, however, the overlapping of concomitant colors of the two reactions made an adequate analysis impossible in this way. Therefore, the multivariate model was necessary. **Fig. 7** shows the image preprocessing process. The white regions were removed and some variations in the shape of the pink region were corrected. The best PLS models to predict the $Cu^{+2}$ and furfural contents were acquired using middle horizontal pixels of the green channel. **Fig. S1** presents the intensity of the middle horizontal line of the green channel for each sample. The middle horizontal pixel is representative of the whole sample as it was acquired by rotating the image and calculating an average pixel of the rotated figures. Figure 7 shows the middle horizontal pixels for each sample.

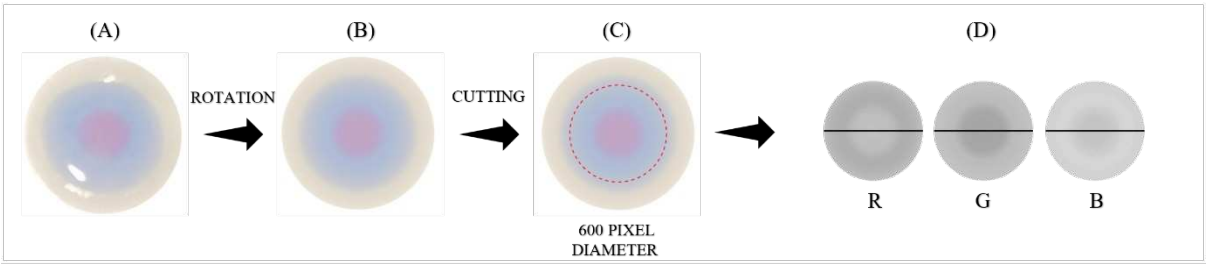


**Fig. 7.** Image preprocessing steps. Original image (A), corrected image after rotation (B), selected region where the dotted red line represents the 600-pixel circle (C), and the RGB images where the black line represents the middle horizontal pixels used to build the models (D).

Table 1 shows the PLS model parameters for $Cu^{+2}$ and furfural models. The models presented a high correlation coefficient of calibration and prediction. Although the method using all variables (PLS) generated a good model, the application of OPS (PLS-OPS) reduced the error of the models selecting more predictive variables. **Fig. 8** shows the reference values versus the values predicted for the calibration and prediction set using the method performed to determine $Cu^{+2}$ and furfural. It can be observed a good fit between the reference, i.e., value of the concentration used to perform the calibration set, and the predicted values, which corroborated with the results presented in Table 1.

**Table 1.** Modeling parameters for $Cu^{+2}$ and furfural determination.

| Analyte | Method | Variables | RMSEC | Rc | RMSECV | Rcv | RMSEP | Rp | LV |
|---|---|---|---|---|---|---|---|---|---|
| $Cu^{+2}$ | PLS | 600 | 0.38 | 0.99 | 1.39 | 0.88 | 1.42 | 0.83 | 6 |
| | PLS-OPS | 50 | 0.20 | 1.00 | 0.56 | 0.98 | 0.49 | 0.98 | 6 |
| Furfural | PLS | 600 | 0.54 | 0.99 | 1.08 | 0.95 | 1.86 | 0.90 | 5 |
| | PLS-OPS | 49 | 0.33 | 1.00 | 0.76 | 0.98 | 0.82 | 0.99 | 5 |

RMSEC: root mean square error of calibration; Rc: correlation coefficient of calibration; RMSECV: root mean square error of cross-validation; Rcv: correlation coefficient of cross-validation; RMSEP: root mean square error of prediction; Rp: correlation coefficient of prediction; LV: latent variables. RMSEC, RMSECV, RMSEP are in mg/mL.

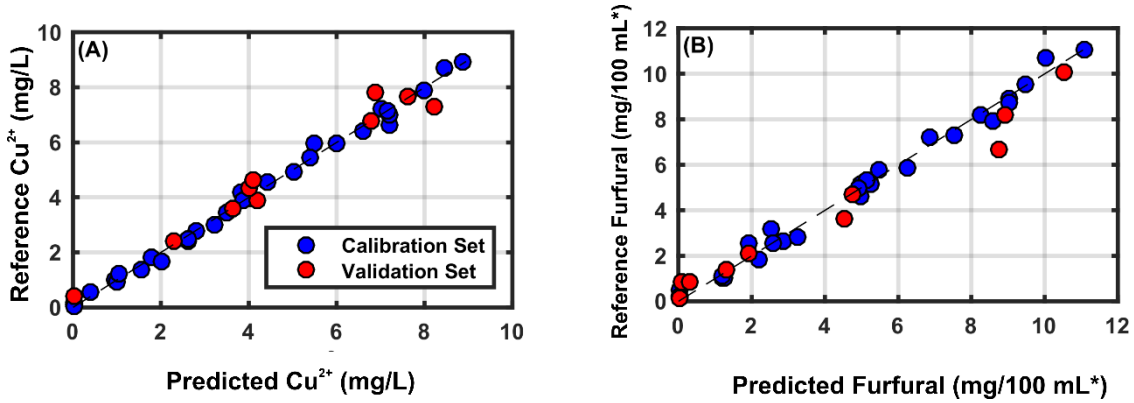


*Concentration expressed in mg per 100 mL of anhydrous alcohol

**Fig. 8.** Reference versus predicted values for $Cu^{+2}$ (A) and furfural (B). The blue filled circles represent the calibration samples and the red filled circles the validation samples.

Table 2 presents the comparison among the concentration of the calibration set and the values obtained by using the prediction set for both $Cu^{+2}$ and furfural determinations. The models presented a satisfactory capacity to predict $Cu^{+2}$ and furfural for both samples using standard solution and samples of cachaça, presenting an average absolute error of 0.2 mg/L for $Cu^{2+}$ model, and 0.3 mg/100 mL of anhydrous alcohol for the furfural model.

Table 2. Concentration of the calibration set (Standard) and the values obtained by using the prediction set for the samples used for model validation.

| | Sample | | $Cu^{2+}$ (mg/L) | | | Furfural (mg/100mL[a]) | | |
|---|---|---|---|---|---|---|---|---|
| | | | Calibration value | Predicted value | R.E% | Calibration value | Predicted value | AE |
| **01** | Standard | Validation | 3.6 | 3.6 ± 0.2 | 0.0 | 4.6 | 3.6 ± 0.4 | 21.7 |
| **02** | Standard | Calibration | 3.8 | 4.2 ± 0.3 | 10.5 | 0.0 | 0.5 ± 0.3 | - |
| **03** | Standard | Calibration | 0.0 | 0.2 ± 0.1 | - | 0.0 | 0.2 ± 0.2 | - |
| **04** | Standard | Calibration | 0.0 | 0.12 ± 0.1 | - | 9.0 | 8.9 ± 0.2 | 1.1 |
| **05** | Standard | Calibration | 7.2 | 6.72 ± 0.2 | -6.9 | 1.9 | 2.6 ± 0.3 | -36.8 |
| **06** | Standard | Calibration | 1.5 | 1.42 ± 0.2 | -6.7 | 9.5 | 9.6 ± 0.1 | -1.1 |
| **07** | Standard | Validation | 7.6 | 7.72 ± 0.3 | 1.3 | 4.8 | 4.7 ± 0.2 | 2.1 |
| **08** | Standard | Calibration | 4.0 | 4.02 ± 0.2 | 0.0 | 2.2 | 1.9 ± 0.1 | 13.6 |
| **09** | Standard | Calibration | 1.8 | 1.82 ± 0.1 | 0.0 | 2.5 | 3.2 ± 0.3 | -28.0 |
| **10** | Standard | Calibration | 2.0 | 1.72 ± 0.2 | -15.0 | 6.3 | 5.8 ± 0.2 | 7.9 |
| **11** | Standard | Calibration | 5.0 | 4.92 ± 0.2 | -2.0 | 10.0 | 10.7 ± 0.4 | -7.0 |
| **12** | Standard | Calibration | 8.0 | 7.92 ± 0.3 | -1.3 | 6.9 | 7.2 ± 0.3 | -4.3 |
| **13** | Standard | Calibration | 5.5 | 6.02 ± 0.3 | 9.1 | 5.0 | 5.1 ± 0.1 | -2.0 |
| **14** | Standard | Validation | 4.2 | 3.9 ± 0.2 | -7.1 | 10.6 | 10.0 ± 0.4 | 5.7 |
| **15** | Standard | Calibration | 8.4 | 8.7 ± 0.4 | 3.6 | 11.1 | 11.1 ± 0.2 | 0.0 |
| **16** | Standard | Calibration | 8.9 | 8.9 ± 0.3 | 0.0 | 0.0 | -0.2 ± 0.2 | - |
| **17** | Standard | Calibration | 0.0 | 0.1 ± 0.1 | - | 7.5 | 7.3 ± 0.1 | 2.7 |
| **18** | Standard | Calibration | 6.0 | 6.0 ± 0.2 | 0.0 | 0.0 | -0.1 ± 0.1 | - |
| **19** | Standard | Calibration | 0.0 | 0.0 ± 0.1 | - | 5.3 | 5.2 ± 0.2 | 1.9 |
| **20** | Standard | Calibration | 4.4 | 4.5 ± 0.1 | 2.3 | 8.3 | 8.2 ± 0.2 | 1.2 |
| **21** | Standard | Calibration | 6.6 | 6.4 ± 0.3 | -3.0 | 9.0 | 8.8 ± 0.3 | 2.2 |
| **22** | Standard | Calibration | 7.2 | 7.0 ± 0.2 | -2.8 | 2.9 | 2.6 ± 0.3 | 10.3 |
| **23** | Standard | Validation | 2.3 | 2.4 ± 0.2 | 4.3 | 0.0 | 0.1 ± 0.1 | - |
| **24** | Standard | Calibration | 0.0 | -0.1 ± 0.1 | - | 3.3 | 2.8 ± 0.1 | 15.2 |
| **25** | Standard | Calibration | 2.6 | 2.4 ± 0.2 | -7.7 | 5.5 | 5.7 ± 0.2 | -3.6 |
| **26** | Standard | Calibration | 3.9 | 3.9 ± 0.2 | 0.0 | 4.9 | 4.7 ± 0.2 | 4.1 |
| **27** | Standard | Calibration | 1.0 | 1.0 ± 0.2 | 0.0 | 8.6 | 7.9 ± 0.4 | 8.1 |
| **28** | Standard | Validation | 6.9 | 7.8 ± 0.4 | 13.0 | 8.8 | 6.7 ± 0.2 | 23.9 |
| **29** | Standard | Calibration | 7.0 | 7.2 ± 0.3 | 2.9 | 5.0 | 4.6 ± 0.3 | 8.0 |
| **30** | Standard | Validation | 4.0 | 4.4 ± 0.2 | 10.0 | 8.9 | 8.2 ± 0.4 | 7.9 |
| **31** | Standard | Calibration | 7.1 | 7.1 ± 0.1 | 0.0 | 1.2 | 1.0 ± 0.2 | 16.7 |
| **32** | Standard | Calibration | 1.0 | 0.9 ± 0.3 | -10.0 | 1.3 | 1.0 ± 0.2 | 23.1 |
| **33** | Standard | Calibration | 1.0 | 1.2 ± 0.2 | 20.0 | 5.2 | 5.3 ± 0.1 | -1.9 |
| **34** | Standard | Validation | 4.1 | 4.6 ± 0.2 | 12.2 | 1.3 | 1.4 ± 0.2 | -7.7 |
| **35** | Cachaça | Calibration | 2.8 | 2.8 ± 0.1 | 0.0 | 0.0 | -0.2 ± 0.2 | - |
| **36** | Cachaça | Calibration | 2.6 | 2.5 ± 0.1 | -3.8 | 4.9 | 5.0 ± 0.2 | -2.0 |

**continua...**

| | Sample | | $Cu^{2+}$ (mg/L) | | | | | |
|---|---|---|---|---|---|---|---|---|
| | | | Calibration value | Predicted value | R.E% | Calibration value | Predicted value | AE |
| **37** | Cachaça | Validation | 6.8 | 6.7 ± 0.1 | -1.5 | 1.9 | 2.1 ± 0.1 | -10.5 |
| **38** | Cachaça | Validation | 0.0 | 0.4 ± 0.2 | - | 0.1 | 0.8 ± 0.4 | -700.0 |
| **39** | Cachaça | Calibration | 5.4 | 5.4 ± 0.1 | 0.0 | 2.6 | 2.5 ± 0.2 | 3.8 |
| **40** | Cachaça | Calibration | 0.4 | 0.6 ± 0.2 | 50.0 | 0.0 | 0.2 ± 0.2 | - |
| **41** | Cachaça | Validation | 8.2 | 7.3 ± 0.3 | -11.0 | 0.3 | 0.9 ± 0.2 | -200.0 |
| **42** | Cachaça | Calibration | 3.2 | 3.0 ± 0.2 | -6.3 | 0.0 | 0.2 ± 0.3 | - |
| **43** | Cachaça | Calibration | 3.5 | 3.4 ± 0.2 | -2.9 | 1.2 | 1.2 ± 0.1 | 0.0 |

RE: Relative error (%)

**[a]Concentration in mg/100 mL of anhydrous ethanol**

As can be seen from the table above, the multivariate calibration was adequate to predict most standard solutions and real samples. Samples 38 and 41 showed an above-average experimental error, although the predicted values are still far from the maximum allowed by legislation, and therefore cannot generate inconsistencies in the sample's compliance with the standards established by MAPA.

Furthermore, the results obtained through both methods were statistically comparable using the paired t-test with 95% confidence in a bilateral test. The t value (0.57) for $Cu^{2+}$ and t value (1.03) for furfural calculated was lower than the critical t (2.018). In that sense, no statistically significant differences in the results were generate by either method.

Moreover no sample analyzed had furfural concentration above the maximum allowed by MAPA, which is 5 mg/100 mL of anhydrous alcohol. On the other hand, three of the analyzed samples (37, 39 and 41) were in disagreement with the maximum concentration of $Cu^{2+}$ allowed by Brazilian legislation, which is 5 mg/L, indicating that 33% of the analyzed samples are in disagreement with the standards established by MAPA. In addition, only two samples (38 and 40) had concentrations of $Cu^{2+}$ accepted by European legislation, i.e., concentration lower than 2 mg/ L, which reaffirms that high concentrations of this metal are the main obstacle to the export of Brazilian cachaça [12].

In this way, the proposed based method can be a very useful alternative in the quality control of beverages, in which the technical manager of the alembic can carry

out the analyzes in a simple and practical way to certify that the cachaças manufactured are in accordance with the norms established by the legislation. Brazilian market, guaranteeing the manufacture of a product with superior sensorial quality, which is also safe for human consumption.

## 4. Conclusions

An analytical methodology based on digital image analysis was carried out to determine $Cu^{2+}$ and furfural simultaneously using a two-phase system. Furfural reacts with aniline in acidic medium forming furfulidenanelline, which presents a pink color. On the other hand, $Cu^{2+}$ reacts with CPZ in a basic medium to form a blue complex. Partial least squares (PLS) regression was used to build the prediction models for $Cu^{2+}$ and furfural contents in alcoholic beverages. After finding the best PLS models, the ordered predictors selection (OPS) was performed to select the most predictive variables. The proposed method was effective to estimate the values of $Cu^{2+}$ and furfural in cachaças, with a mean absolute error of 0.2 mg/L for $Cu^{2+}$ model, and 0.3 mg/100 mL of anhydrous alcohol for the furfural model. None of the cachaça samples had furfural levels above those allowed by Brazilian legislation. However, 33% of the samples had $Cu^{2+}$ levels above the permitted level. The developed method presents a highly promising alternative for carrying out in situ analysis of $Cu^{2+}$ and furfural in cachaças. Due to its low cost (in the order of a few cents), portability, simplicity, and speed (2 minutes per analysis), the present proposal has countless advantages in relation to the methods previously described with regard to its applicability *in situ* analyzes.

## References

[1] W.T. Suarez, O.D. Pessoa-Neto, V.B. dos Santos, A.R. de A. Nogueira, R.C. Faria, O. Fatibello-Filho, M. Puyol, J. Alonso, A compact miniaturized continuous flow system for the determination of urea content in milk, Anal. Bioanal. Chem. 398 (2010) 1525–1533. https://doi.org/10.1007/s00216-010-4052-6.

[2] M.D.K. Franco, G.D.A. Castro, C. Vilanculo, S.A. Fernandes, W.T. Suarez, A

color reaction for the determination of Cu2 + in distilled beverages employing digital imaging Analytica Chimica Acta A color reaction for the determination of Cu 2 þ in distilled beverages employing digital imaging, Anal. Chim. Acta. 1177 (2021) 338844. https://doi.org/10.1016/j.aca.2021.338844.

[3] M. Vidal, R. Garcia-Arrona, A. Bordagaray, M. Ostra, G. Albizu, Simultaneous determination of color additives tartrazine and allura red in food products by digital image analysis, Talanta. 184 (2018) 58–64. https://doi.org/10.1016/J.TALANTA.2018.02.111.

[4] M.H. Sorouraddin, M. Saadati, F. Mirabi, Simultaneous determination of some common food dyes in commercial products by digital image analysis, J. Food Drug Anal. 23 (2015) 447–452. https://doi.org/10.1016/J.JFDA.2014.10.007.

[5] K.K. Beltrame, T.R. Gonçalves, S.T.M. Gomes, M. Matsushita, D.N. Rutledge, P.H. Março, P. Valderrama, Digital images and independent components analysis in the determination of bioactive compounds from grape juice, LWT. 152 (2021) 112308. https://doi.org/10.1016/J.LWT.2021.112308.

[6] J. Caleb, U. Alshana, Supramolecular solvent-liquid-liquid microextraction followed by smartphone digital image colorimetry for the determination of curcumin in food samples, Sustain. Chem. Pharm. 21 (2021) 100424. https://doi.org/10.1016/J.SCP.2021.100424.

[7] MAPA, Instrução normativa no. 24, de 08 de setembro de 2005. Manual operacional de bebidas e vinagres, (2005).

[8] L.M. De Souza, A.R. Alcarde, F.V. De Lima, A.M. Bortoletto, Produção de Cachaça de Qualidade, ESALQ, Piracicaba, 2013.

[9] MAPA, Instrução Normativa no. 13, de 30 de junho de 2005. Aprova o Regulamento Técnico para Fixação dos Padrões de Identidade e Qualidade para Aguardente de Cana e para Cachaça, (2005).

[10] M. de O.K. Franco, W.T. Suarez, V.B. dos Santos, Digital Image Method Smartphone-Based for Furfural Determination in Sugarcane Spirits, Food Anal. Methods. 10 (2017) 508–515. https://doi.org/10.1007/s12161-016-0605-4.

[11] A.M. Bortoletto, A.R. Alcarde, Assessment of chemical quality of Brazilian sugar cane spirits and cachaças, Food Control. 54 (2015) 1–6. https://doi.org/10.1016/j.foodcont.2015.01.030.

[12] M. de O.K. Franco, W.T. Suarez, V.B. dos Santos, I.S. Resque, M.H. dos Santos, L.F. Capitán-Vallvey, Microanalysis based on paper device functionalized with cuprizone to determine Cu2+ in sugar cane spirits using a smartphone, Spectrochim. Acta - Part A Mol. Biomol. Spectrosc. 253 (2021) 119580. https://doi.org/10.1016/j.saa.2021.119580.

[13] R.J. Ferreira, T.R. Rosa, J. Ribeiro, R.C. Barthus, Simultaneous metal determination in artisanal cachaça by using voltammetry and multivariate calibration, Food Chem. 314 (2020). https://doi.org/10.1016/J.FOODCHEM.2019.126126.

[14] A.F. Vilela, L. de S.C. Oliveira, M.B. Muniz, B.C.A. de MÉLO, M.J. de FIGUEIREDO, J. de M. Vieira Neto, Assessment of sensory and physical-chemical quality, and potential for certification of cachaças from the state of Paraíba, Brazil, Food Sci. Technol. 41 (2021) 661–668. https://doi.org/10.1590/FST.13520.

[15] M. de O.K. Franco, W.T. Suarez, M.V. Maia, V.B. dos Santos, Smartphone Application for Methanol Determination in Sugar Cane Spirits Employing Digital Image-Based Method, Food Anal. Methods. 10 (2017) 2102–2109. https://doi.org/10.1007/s12161-016-0777-y.

[16] M. de O.K. Franco, W.T. Suarez, V.B. dos Santos, I.S. Resque, A novel digital image method for determination of reducing sugars in aged and non-aged cachaças employing a smartphone, Food Chem. 338 (2021) 127800. https://doi.org/10.1016/j.foodchem.2020.127800.

[17] L.M. Zacaroni, M.D.G. Cardoso, A.A. Saczk, W.D. Santiago, J.P. Dos Anjos, J. Masson, F.C. Duarte, D.L. Nelson, Caracterização e quantificação de contaminantes em aguardentes de cana, Quim. Nova. 34 (2011) 320–324. https://doi.org/10.1590/S0100-40422011000200026.

[18] J. Masson, M. das G. Cardoso, L.M. Zacaroni, J.P. dos Anjos, A.A. Sackz, A.M. de R. Machado, D.L. Nelson, Determination of acrolein, ethanol, volatile acidity, and copper in different samples of sugarcane spirits, Food Sci. Technol. 32 (2012) 568–572. https://doi.org/10.1590/S0101-20612012005000075.

[19] J. Masson, M. das G. Cardoso, F.J. Vilela, F.A. Pimentel, A.R. de Morais, J.P.

dos Anjos, Parâmetros físico-químicos e cromatográficos em aguardentes de cana queimada e não queimada, Ciência e Agrotecnologia. 31 (2007) 1805–1810. https://doi.org/10.1590/S1413-70542007000600030.

[20] N.R. Reed, E.S.C. Kwok, Furfural, Encycl. Toxicol. Third Ed. (2014) 685–688. https://doi.org/10.1016/B978-0-12-386454-3.00147-0.

[21] R.A. Labanca, M. Beatriz, A. Glória, V. José, P. Gouveia, Determinação dos teores de cobre e grau alcoólico em aguardentes de cana produzidas no estado de Minas Gerais, Quim. Nov. 29 (2006) 1110–1113.

[22] G. Loudianos, J.D. Gitlin, Wilson's Disease, Semin. Liver Dis. 20 (2000) 353–364. https://doi.org/10.1055/s-2000-9389.

[23] European Copper Institute, Technical guide on metals and alloys used as food contact, (2011). http://copperalliance.eu/docs/default-source/resources/cu-risk-assessment_coe-food-contact-materials---eci-comments-20110627.pdf?sfvrsn=0 (accessed March 19, 2017).

[24] R.C. de Sena, M. Soares, M.L.O. Pereira, R. Cruz Domingues da Silva, F. Ferreira do Rosário, J.F. Cajaiba da Silva, A Simple Method Based on the Application of a CCD Camera as a Sensor to Detect Low Concentrations of Barium Sulfate in Suspension, Sensors. 11 (2011) 864–875. https://doi.org/10.3390/s110100864.

[25] A. Lopez-Molinero, D. Liñan, D. Sipiera, R. Falcon, Chemometric interpretation of digital image colorimetry. Application for titanium determination in plastics, Microchem. J. 96 (2010) 380–385. https://doi.org/10.1016/j.microc.2010.06.013.

[26] L.F. Capitán-Vallvey, N. López-Ruiz, A. Martínez-Olmos, M.M. Erenas, A.J. Palma, Recent developments in computer vision-based analytical chemistry: A tutorial review, Anal. Chim. Acta. 899 (2015) 23–56. https://doi.org/10.1016/J.ACA.2015.10.009.

[27] X. Liu, C. Xu, S. Xie, L. Zhu, X. Wang, Evaluating TiO2 photocatalysis performance in microtubes on paper background by smartphone: Principles and application examples, Chemosensors. 9 (2021). https://doi.org/10.3390/CHEMOSENSORS9080235.

[28] L.M.A. de Oliveira, V.B. dos Santos, E.K.N. da Silva, A.S. Lopes, H.A. Dantas-

Filho, An environment-friendly spot test method with digital imaging for the micro-titration of citric fruits, Talanta. 206 (2020) 120219. https://doi.org/10.1016/J.TALANTA.2019.120219.

[29] R.C. Gonzalez, R.E. Woods, Digital Image Processing, 2008.

[30] Y. Sun, M. Wei, R. Liu, H. Wang, H. Li, Q. Kang, D. Shen, A smartphone-based ratiometric fluorescent device for field analysis of soluble copper in river water using carbon quantum dots as luminophore, Talanta. 194 (2019) 452–460. https://doi.org/10.1016/J.TALANTA.2018.10.019.

[31] Z. Zhao, L. Wei, M. Cao, M. Lu, A smartphone-based system for fluorescence polarization assays, Biosens. Bioelectron. 128 (2019) 91–96. https://doi.org/10.1016/J.BIOS.2018.12.031.

[32] J.P.B. de Almeida, V.B. dos Santos, G.A. do Nascimento, W.T. Suarez, W.M. de Azevedo, A.F. Ferreira, M.V. Maia, A fluorescence digital image-based method using carbon quantum dots to evaluate the compliance of a biocidal agent, Anal. Methods. 14 (2022) 2631–2641. https://doi.org/10.1039/D2AY00678B.

[33] I.S. Resque, V.B. dos Santos, W.T. Suarez, An environmentally friendly analytical approach based on spot test and digital image to evaluate the conformity of bleaching products, Chem. Pap. 2019 737. 73 (2019) 1659–1668. https://doi.org/10.1007/S11696-019-00717-W.

[34] S. Paciornik, A. V. Yallouz, R.C. Campos, D. Gannerman, Scanner image analysis in the quantification of mercury using spot-tests, J. Braz. Chem. Soc. 17 (2006) 156–161. https://doi.org/10.1590/S0103-50532006000100022.

[35] M. Forina, S. Lanteri, M. Casale, Multivariate calibration, J. Chromatogr. A. 1158 (2007) 61–93. https://doi.org/10.1016/J.CHROMA.2007.03.082.

[36] J. Sanchez, Multivariate Calibration. John, Biometrical J. 33 (1991) 418–418. https://doi.org/10.1002/BIMJ.4710330407.

[37] M. de O.K. Franco, G.A. Dias Castro, C. Vilanculo, S.A. Fernandes, W.T. Suarez, A color reaction for the determination of Cu2+ in distilled beverages employing digital imaging, Anal. Chim. Acta. 1177 (2021) 338844. https://doi.org/10.1016/j.aca.2021.338844.

[38] A.P. Holkem, M. Voss, S.K. Schlesner, G.A. Helfer, A.B. Costa, J.S. Barin, E.I.

Müller, P.A. Mello, A green and high throughput method for salt determination in crude oil using digital image-based colorimetry in a portable device, Fuel. 289 (2021) 119941. https://doi.org/10.1016/J.FUEL.2020.119941.

[39] S. Soares, F.R.P. Rocha, Spot test for determination of uric acid in saliva by smartphone-based digital images: A new proposal for detecting kidney dysfunctions, Microchem. J. 162 (2021) 105862. https://doi.org/10.1016/J.MICROC.2020.105862.

[40] V.B. dos Santos, E.K.N. da Silva, L.M.A. de Oliveira, W.T. Suarez, Low cost in situ digital image method, based on spot testing and smartphone images, for determination of ascorbic acid in Brazilian Amazon native and exotic fruits, Food Chem. 285 (2019) 340–346. https://doi.org/10.1016/J.FOODCHEM.2019.01.167.

[41] K.D. Pessoa, W.T. Suarez, M.F. dos Reis, M. de Oliveira Krambeck Franco, R.P.L. Moreira, V.B. dos Santos, A digital image method of spot tests for determination of copper in sugar cane spirits, Spectrochim. Acta - Part A Mol. Biomol. Spectrosc. 185 (2017) 310–316. https://doi.org/10.1016/j.saa.2017.05.072.

[42] V.H.M. Luiz, L.S. Lima, E.L. Rossini, L. Pezza, H.R. Pezza, Paper platform for determination of bumetanide in human urine samples to detect doping in sports using digital image analysis, Microchem. J. 147 (2019) 43–48. https://doi.org/10.1016/j.microc.2019.03.006.

[43] W.T. Suarez, O.D. Pessoa-Neto, V.B. Dos Santos, A.R. De Araujo Nogueira, R.C. Faria, O. Fatibello-Filho, M. Puyol, J. Alonso, A compact miniaturized continuous flow system for the determination of urea content in milk, Anal. Bioanal. Chem. 2010 3983. 398 (2010) 1525–1533. https://doi.org/10.1007/S00216-010-4052-6.

[44] S.K. Kohl, J.D. Landmark, D.F. Stickle, Demonstration of Absorbance Using Digital Color Image Analysis and Colored Solutions, J. Chem. Educ. 83 (2006) 644. https://doi.org/10.1021/ed083p644.

[45] K. Cantrell, M.M. Erenas, I. de Orbe-Payá, L.F. Capitán-Vallvey, Use of the hue parameter of the hue, saturation, value color space as a quantitative analytical parameter for bitonal optical sensors., Anal. Chem. 82 (2010) 531–42.

https://doi.org/10.1021/ac901753c.

[46] L. Byrne, J. Barker, G. Pennarun-Thomas, D. Diamond, S. Edwards, Digital imaging as a detector for generic analytical measurements, Trends Anal. Chem. 19 (2000) 517–522. https://doi.org/10.1016/S0165-9936(00)00019-4.

[47] T.A. Catelani, D.B. Bittar, L. Pezza, H.R. Pezza, Determination of amino acids in gym supplements using digital images and paper platform coupled to diffuse reflectance spectroscopy and USB device., Talanta. 196 (2018) 523–529. https://doi.org/10.1016/J.TALANTA.2018.12.052.

[48] D. Douglas, S. Fernandes, F. Romeo, G. Krepper, S. Di Nezio, M. Fabián Pistonesi, M.E. Centurión, M. César, U. De Araújo, P. Henrique, G. Dias Diniz, Quantification and identification of adulteration in the fat content of chicken hamburgers using digital images and chemometric tools, (2018). https://doi.org/10.1016/j.lwt.2018.10.034.

[49] J. V. Roque, W. Cardoso, L.A. Peternelli, R.F. Teófilo, Comprehensive new approaches for variable selection using ordered predictors selection, Anal. Chim. Acta. 1075 (2019) 57–70. https://doi.org/10.1016/J.ACA.2019.05.039.

[50] R.F. Teófilo, J.P.A. Martins, M.M.C. Ferreira, Sorting variables by using informative vectors as a strategy for feature selection in multivariate regression, J. Chemom. 23 (2009) 32–48. https://doi.org/10.1002/CEM.1192.

[51] L.P. Dos Santos Benedetti, V.B. Dos Santos, T.A. Silva, E.B. Filho, V.L. Martins, O. Fatibello-Filho, A digital image-based method employing a spot-test for quantification of ethanol in drinks, Anal. Methods. 7 (2015) 4138–4144. https://doi.org/10.1039/C5AY00529A.

## SUPPLEMENTARY MATERIAL

**Table S1:** Volumes of all reagents used in the work to set up the partial least squares (PLS) regression

| Sample | $Cu^{+2}$ (µL) | Furfural (µL) | 40% Alcohol (µL) | Borate buffer (µL) | CPZ (µL) | Aniline ion (µL) |
|---|---|---|---|---|---|---|
| 1 | 34 | 43 | 113 | 100 | 100 | 20 |
| 2 | 36 | 0 | 154 | 100 | 100 | 20 |
| 3 | 0 | 0 | 190 | 100 | 100 | 20 |
| 4 | 0 | 86 | 104 | 100 | 100 | 20 |
| 5 | 68 | 18 | 104 | 100 | 100 | 20 |
| 6 | 15 | 90 | 85 | 100 | 100 | 20 |
| 7 | 72 | 45 | 73 | 100 | 100 | 20 |
| 8 | 38 | 21 | 131 | 100 | 100 | 20 |
| 9 | 17 | 24 | 149 | 100 | 100 | 20 |
| 10 | 19 | 59 | 112 | 100 | 100 | 20 |
| 11 | 48 | 95 | 47 | 100 | 100 | 20 |
| 12 | 76 | 65 | 49 | 100 | 100 | 20 |
| 13 | 52 | 48 | 90 | 100 | 100 | 20 |
| 14 | 40 | 100 | 49 | 100 | 100 | 20 |
| 15 | 80 | 105 | 4 | 100 | 100 | 20 |
| 16 | 85 | 0 | 105 | 100 | 100 | 20 |
| 17 | 0 | 71 | 118 | 100 | 100 | 20 |
| 18 | 57 | 0 | 133 | 100 | 100 | 20 |
| 19 | 0 | 50 | 140 | 100 | 100 | 20 |
| 20 | 42 | 78 | 70 | 100 | 100 | 20 |
| 21 | 63 | 86 | 42 | 100 | 100 | 20 |
| 22 | 68 | 27 | 95 | 100 | 100 | 20 |
| 23 | 22 | 0 | 168 | 100 | 100 | 20 |
| 24 | 0 | 31 | 159 | 100 | 100 | 20 |
| 25 | 25 | 52 | 113 | 100 | 100 | 20 |
| 26 | 37 | 46 | 107 | 100 | 100 | 20 |
| 27 | 9 | 82 | 99 | 100 | 100 | 20 |
| 28 | 65 | 83 | 42 | 100 | 100 | 20 |

(continua...)

| Sample | $Cu^{+2}$ (µL) | Furfural (µL) | 40% Alcohol (µL) | Borate buffer (µL) | CPZ (µL) | Aniline ion (µL) |
|---|---|---|---|---|---|---|
| 29 | 66 | 47 | 77 | 100 | 100 | 20 |
| 30 | 38 | 85 | 67 | 100 | 100 | 20 |
| 31 | 68 | 11 | 111 | 100 | 100 | 20 |
| 32 | 10 | 12 | 168 | 100 | 100 | 20 |
| 33 | 10 | 49 | 131 | 100 | 100 | 20 |
| 34 | 39 | 12 | 139 | 100 | 100 | 20 |

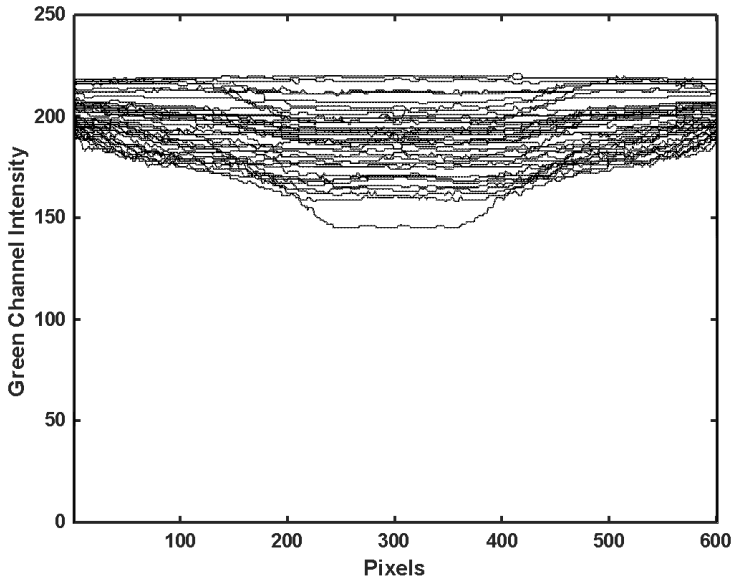


**Fig. S1.** Intensity of the middle horizontal line of the green channel for each sample.

# CAPÍTULO 6 - CONCLUSÃO

Quatro métodos baseados em análises digitais foram propostos para determinação de alguns analitos importantes para o monitoramento da qualidade química e sensorial de cachaças, tais como: açúcares redutores, acidez volátil, furfural e cobre, sendo que esta última análise também foi estendida para amostras de Tequila e Whiskey.

Os métodos utilizam baixa quantidade de reagentes e, portanto, corrobora os preceitos da Química Verde. Além disso, pode ser facilmente utilizado por produtores de cachaça com reduzido acesso a infraestrutura para avaliação da qualidade fermentativa, bem como para verificar se os teores das substâncias estão dentro dos limites aceitáveis, pela legislação brasileira, permitindo mais espaço para os produtores fazer ajustes em seu sistema de produção com baixo custo e alta portabilidade.

Os métodos apresentaram ser eficientes, eficazes, além de apresentar boas faixas de recuperação, indicando ausências de efeitos de matriz. Por fim, os resultados de todas as análises foram comparadas com os métodos oficiais e notou-se que não houveram diferenças estatisticamente significativas entre os resultados obtidos à 95% de confiança.

Além disso, os métodos se destacam pela portabilidade, pois as análises podem ser feitas com o próprio smartphone em aplicativos integrados, tudo isso torna o método uma alternativa altamente promissora para controle de qualidade de cachaças e outras bebidas destiladas.